Title
Investigations Into Human Lipoxygenase Biosynthesis of Oxylipins, Their Roles in Inflammation, and Drug Discovery

Permalink
https://escholarship.org/uc/item/3rv3813m

Author
Freedman, John Cody

Publication Date
2019

Peer reviewed|Thesis/dissertation

UNIVERSITY OF CALIFORNIA

SANTA CRUZ

INVESTIGATIONS INTO HUMAN LIPOXYGENASE BIOSYNTHESIS OF OXYLIPINS, THEIR ROLES IN INFLAMMATION, AND DRUG DISCOVERY

A dissertation submitted in partial satisfaction
of the requirement for the degree of

DOCTOR OF PHILOSOPHY

In

CHEMISTRY

By

John "Cody" Freedman

December 2019

The Dissertation of Cody Freedman
is approved by:

_____
Professor Michael Stone, Chair

_____
Professor Theodore R. Holman

_____
Professor Seth Rubin

_____
Quentin Williams
Vice Provost and Dean of Graduate Studies

Table of Contents

List of Figures

List of Tables

List of Schemes

Abstract

Investigations Into Human Lipoxygenase Biosynthesis of Oxylipins, Their Roles in Inflammation, and Drug Discovery

Cody Freedman

The research in this dissertation explores the bioactivity and biosynthesis of lipoxygenase-derived products from polyunsaturated fatty acids as well as drug discovery. The diseases that cause most of the mortality today are due to chronic inflammation, which is caused by the lack of a proper resolution phase. The pro-resolution molecules are oxylipins catalyzed by oxygenases and derived from fish oil. Dietary, genetic, and environmental effects have a role in altering these lipid signaling pathways and causing inflammation. This thesis examines how these molecules are made, their effects on resolving inflammation, and possible relations to disease. The first chapter investigates human 12-lipoxygenase metabolites from omega-6 docosapentaenoic acid as a promising novel anti-platelet for the treatment of the life-threatening complications of cardiovascular diseases. The second chapter quantifies oxyipins and cytokines in human blood as possible biomarkers for heart failure. The next chapter characterizes the Pseudomonas Aeruginosa lipoxygenase, reveals possible roles in biofilm formation and manipulation of host immune response, and discovers first in class selective inhibitors. Finally, the last chapter describes the resolution of inflammation and the biosynthesis of a class of specialized proresolving mediators, the maresins.

Acknowledgements

Foremost, I would like to express how grateful I am to have gotten to work under Ted Holman. He is an absolute amazing mentor, scientist, role model and person that is continuously supportive, knowledgeable, and enthusiastic. He has taught me how to think and communicate scientifically and become a personable and respectable leader. I cannot believe how far I have come under his guidance and can't thank Ted enough for everything he has done for me.

Next, thank you to one of my best friends, mentors, and biggest role models, Josh Deschamps. He was a previous graduate student in Ted's lab, went to industry, and came back for a postdoc, in which I was lucky enough to be a part of. Josh is an incredible scientist and awesome person, whose combination of intelligence, personality, humbleness, work ethic, and curiosity for all aspects of life is remarkable and admirable. Josh made my graduate work infinitely fun and I appreciate every minute we worked together.

Thank you to my committee, Seth Rubin and Michael Stone, I appreciate all of your incredibly insightful questions and help. You are both inspirational scientists and thoughtful people that I look up to immensely.

I would also like to thank the entire Holman lab and other members in the UCSC Chemistry Department including especially my best friend and coworker Carissa Tsai and my incredibly intelligent undergraduate Adrianne Tran along with Michelle Armstrong, Aby Green, Chris Smyrniotis, Steve Perry, Chris Van Hoorebeke, Mikey Dang, Melissa Stanley, Anh McClean, Caitlin Clausen, Scott,

Yomi, James, Graham Roseman, Valerie Chen, Kevin Schilling, Tillini Wijeratne, Terrin Chang, Caileen Brison, Eifie Chen, Quiangli Zhang, Josh and Cam, and Keelan Guiley.

Next I would like to thank collaborators I worked with at the University of Michigan and UCSF. At Michigan, I had the pleasure to work with the incredible platelet master Michael Holinstat and his lab workers, Jen Yeung, Ben tourdot, and Adrianne. At UCSF, I was lucky enough to be able to collaborate with the master molecular modelers Matt Jacobson and CK for molecular modeling help.

Last, but not least, I would like to thank my family for the support through everything. I could not have done this without the incredible love from Patty Freedman, Rick Freedman, Astra Freedman, and Daniel Freedman. You are the best family anyone could ask for and I love you all more than anything. I also cannot forget Rocky, Phoebe, and Birdy Freedman for being the best animals friends anyone could ask for.

Chapter 1

INTRODUCTION

1.1 Polyunsaturated Fatty Acids

Western diets have been to blame for many of the diseases that plague the country and create a high burden on society. A red meat based diet contains high levels of arachidonic acid (AA), a 20-carbon 4 double bond (C20:4) omega-6 fatty acid (**Figure 1**).
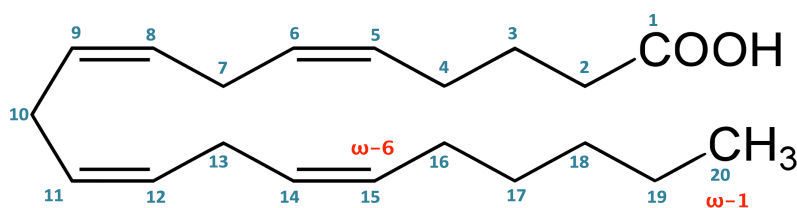
Figure 1.1-The structure of cis-5,8,11,14-eicosatetraenoic acid (arachidonic acid, AA).

This is the major polyunsaturated fatty acids (PUFA) substrate in humans, and it is found esterified in phospholipids of cellular membranes or in the free form most abundantly in the brain, muscles (10-20%), and liver [1]. PUFAs are carboxylic acid containing hydrocarbons with more than one double bond. Omega-6 represents the double bond position closest to the methyl end of the fatty acid, with arachidonic acid and other important PUFA's containing all cis/Z configured double bonds. The simplest omega-6 polyunsaturated fatty acid, which is found in vegetable and safflower oils, is linoleic acid (LA, C18:2). LA along with a plant desaturase product of LA, alpha linolenic acid (ALA, C18:3), found in canola and soybean oil as well as flax and chia seeds, are essential fatty acids [2]. From these two plant-derived fatty

acids, all of the other needed PUFAs can be formed through the actions of human desaturase and elongase enzymes (desaturation being the rate limiting step) [3]. Desaturation and elongation is performed prior to carbon 9 from the carboxylate side, highlighting the necessity of these omega-6 and 3 double bond locations to form other PUFAs. Through these enzymes, LA is desaturated to gamma-linoleic acid (GLA, C18:3) and then elongated to dihomo-gamma-linoleic acid (DGLA, C20:3) or omega-6 docosapentaenoic acid (DPA$_{\omega-6}$, C22:5), key fatty acids involved in blood thinning (*vida infra*). In a similar matter, ALA is converted to omega-3 fatty acids such as eicosapentaenoic acid (EPA, C20:5), omega-3 docosapentaenoic acid (DPA$_{\omega-3}$), and docosahexaenoic acid (DHA), key PUFAs found in fish oil and involved in creating extremely potent anti-inflammatory and pro resolving compounds (*vida infra*).

1.2 Enzymes in Lipid Metabolism

PUFAs become specifically oxidized by multiple enzymes, such as isozymes of cyclooxygenase (COX), lipoxygenase (LOX), cytochrome P450 (CYP450), and soluble epoxide hydrolase (sEH), which convert the PUFA substrates to the powerful oxylipin mediators of inflammation (**Scheme 1.1**). When PUFA is consumed or enzymatically produced, cells esterify them in the phospholipid bilayer through the actions of transferases, such as glycerol-3-phosphate acyltransferase [4]. PUFA such as those mentioned earlier are most commonly placed in the 2nd position of glycerol and cleaved by phospholipase A2 after cellular activation [5]. The fatty acids are

enzymatically oxidize in the bilayer or as the free form and bind various cellular G-protein coupled receptors (GPCRs) to elicit different responses. Any PUFA containing a 1,4 penta-diene structural motif can be a substrate for oxidation by the above enzymes. Cyclooxygenase is a heme-containing enzyme that catalyzes the formation of prostaglandins (PG) from AA, a pro-inflammatory compound that is inhibited by aspirin to reduce pain and swelling [6]. Lipoxygenase is a non-heme iron-containing enzyme that participates in the pro and anti-inflammatory cascades through hydrogen abstraction and oxidation of PUFA. Important AA derived pro-inflammatory products of lipoxygenases are the human 5-lipoxygenase (5h-LOX) derived leukotrienes (LT's), such as leukotriene A_4 (LTA$_4$), which cause mucous secretion and broncoconstriction and are inhibited by FDA approved drugs such as zileuton for the treatment of asthma [7]. Anti-inflammatory compounds produced by a second enzyme, human reticulocyte 15-lipoxygenase-1 (h15-LOX-1) or human platelet 12-lipoxygenase (h12-LOX), in concert with h5-LOX, are called the lipoxins (**Scheme 1.2**). Lipoxins promote resolution of inflammation through reducing neutrophil chemotaxis and promoting macrophage phagocytosis [8]. Another enzyme that is involved in forming epoxides is cytochrome P450, in which the epoxide product is subjected to hydrolysis by a hydrolase to create doubly oxygenated stereochemically defined products that also modulate inflammation (diHETEs) [9].

Arachidonic Acid

Lipoxygenases

Cyclooxygenases

Cytochrome P450s

Hydroperoxyeicosatetraenoic Acids

Thromboxanes

Prostaglandins

Epoxyeicosatetraenoic Acids

5-HpETE
12-HpETE
15-HpETE

TXB_2
TXA_2

PGE_2
PGD_2
PGI_2
PGF_{2a}

5,6-EET
8,9-EET
11,12-EET
14,15-EET

Hydolase

diHETEs

5,6-epoxy-ETE (LTA_4)
14,15-epoxy-ETE
HETEs
diHETEs

5,12diHETE (LTB_4)

LTC_4
LTD_4
LTE_4

LXA_4
LXB_4
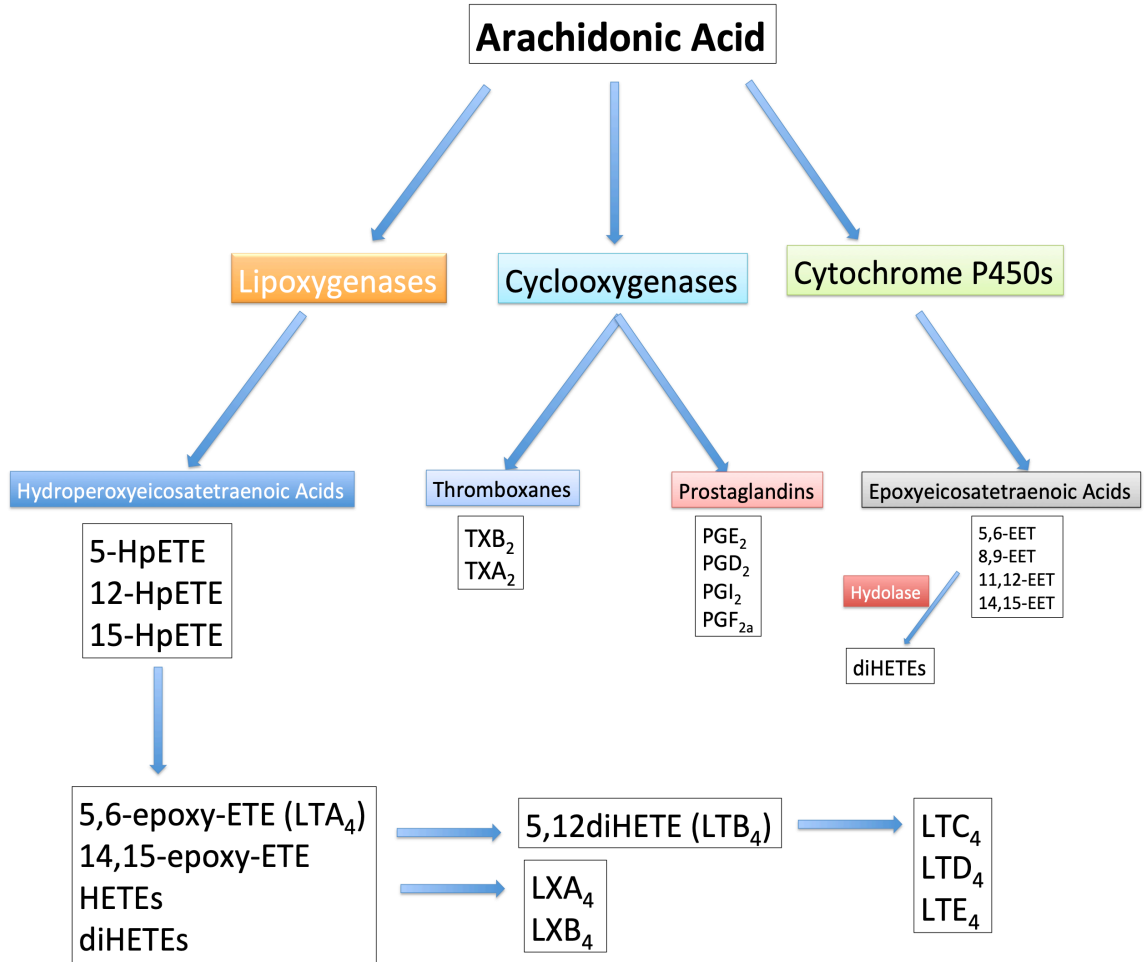
Scheme 1.1- AA metabolism by LOX, COX, and CYP450.
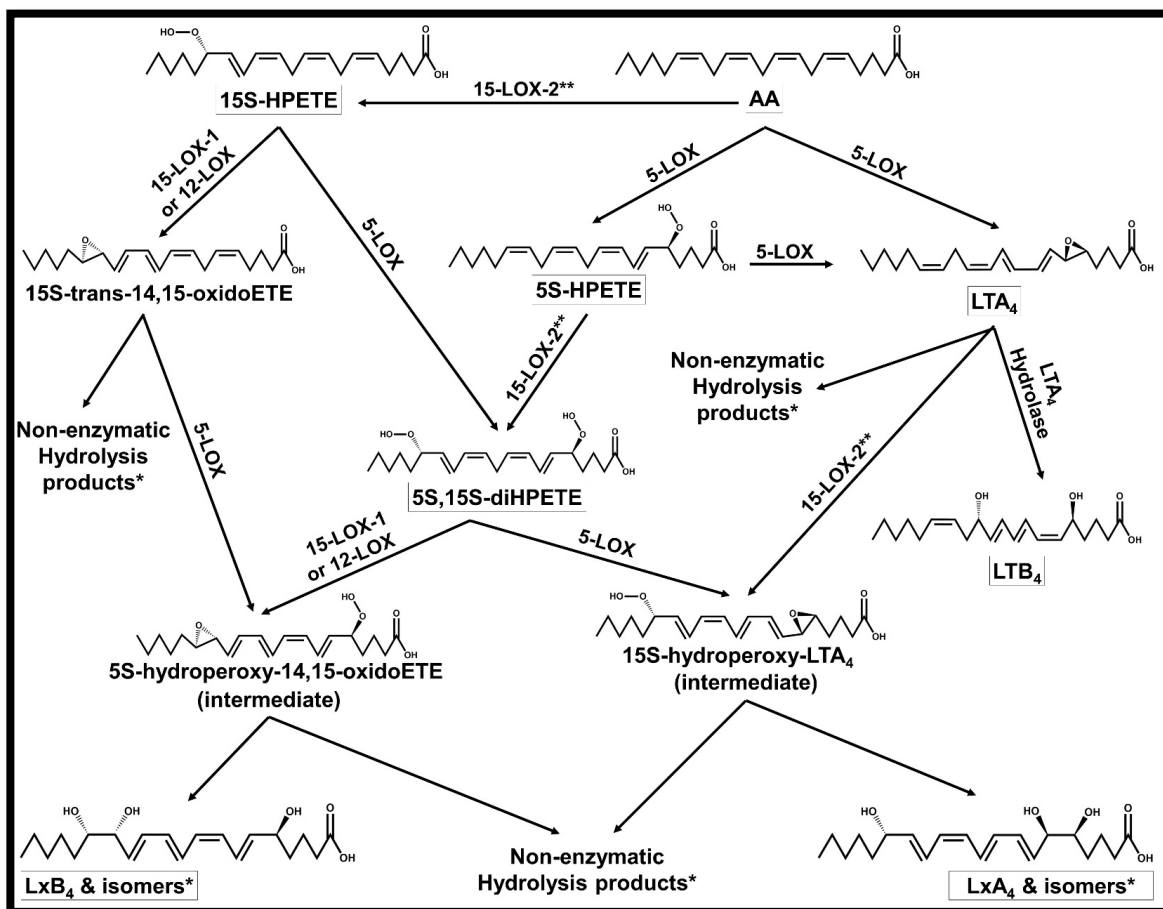
Scheme 1.2- AA metabolism by LOXs to proinflammatory molecules 5S-HpETE and LTA$_4$, and further metabolism to anti-inflammatory molecules lipoxins.

1.3 Lipoxygenase

Lipoxygenase is the main focus of this thesis and are found abundantly in many tissues of the plant and animal kingdoms and rarely in some bacteria [10]. There are six human LOX isozymes which all contain catalytic irons chelated by 3 histidines and a C-terminal isoleucine. Their primary reactivity is to abstract a hydrogen atom from a bis-allylic methylene on a polyunsaturated fatty acid and insert molecular oxygen, generating a hydroperoxide product. This hydroperoxide is

primarily produced specifically in the S chirality by 5 lipoxygenase's including h15-LOX-1, h15-LOX-2, h12-LOX, h5-LOX, and eLOX3 while one isozyme 12R-LOX, oxygenates in the R chirality [11] (**Figure 1.2**).

Gene	Enzyme	Major Expression Site
ALOX5	**h5-LOX**	**Neutrophils/dendritic cells**
ALOX15	**h15-LOX-1**	**Eosinophils/macrophages**
ALOX15B	**h15-LOX-2**	**Skin/hair roots**
ALOX12	**h12-LOX**	**Platelets**
ALOX12B	**h12R-LOX**	**Skin**
ALOXE3	**eLOX3**	**Skin**

Figure 1.2- LOX isozyme Genes, common name, and major expression site [11].

The naming of specific LOX isozymes is dependent on the carbon number of arachidonic acid (AA) that becomes oxidized. For example, (h12-LOX) produces 95% (12S-HpETE) from AA, and (h15-LOX-1) produces 10% (15S-HpETE). However, if DHA is the substrate then the numbering of the oxygenated carbon changes. This is due to the fact that the fatty acid substrate enters into the active site methyl-end first, and therefore the oxygenation nomenclature starts from the omega end of the molecule. h12-LOX principally oxygenates on the w-9 carbon (i.e. 95% 12-HpETE or 81% (14S-HpDHA)), while h15-LOX-1 principally oxygenates at w-6 (i.e. 90% 15-HpETE or 46% (17S-HpDHA)). This oxygenation percentage is the case for humans, yet lower primates and mammals make less 15 products from their 15-

LOX, thus murine 15-LOX-1 makes 80% 12-HpETE, confusing research as well as complicating drug design [12]. It is proposed that this shift in reactivity has led to human's ability to create more of the pro-resolving molecules that will be discussed later [13]. The second catalysis LOX isozymes can perform, is to react with a hydrogen peroxide oxylipin product and abstract a second hydrogen atom from a bis-allylic methylene carbon, generating a septadienyl radical. However, instead of oxygen attacking this septadienyl radical intermediate, the hydroperoxide moiety dehydrates to form an epoxide. The most characterized example of this mechanism is the reaction of 5S-HpETE and h5-LOX, to generate the 5,6-epoxide LTA_4, described earlier and with a reaction diagram later in **Scheme 1.3**. An epoxide formed from DHA reacting with h15-LOX-1 and h12-LOX will be described later and in its own chapter of this thesis, the 13,14-epoxy-DHA, a key intermediate to potent resolvers of inflammation, the maresins. In addition to the promiscuity of this class of enzymes, is the addition of allosteric sites, which regulate oxylipin formation and substrate preference and is another key aspect of the last chapter of this thesis. The full spectrum of fatty acids available through diet may have an impact on which specific signaling pathways are preferred, resulting in more pro-inflammation or pro-resolution. The information on this vast network of chemical mediators made from sequential enzymatic actions on PUFA substrates is scant to say the least, which highlights the need to define their biosynthesis and biological response in order to define effective drug development for treating disease.
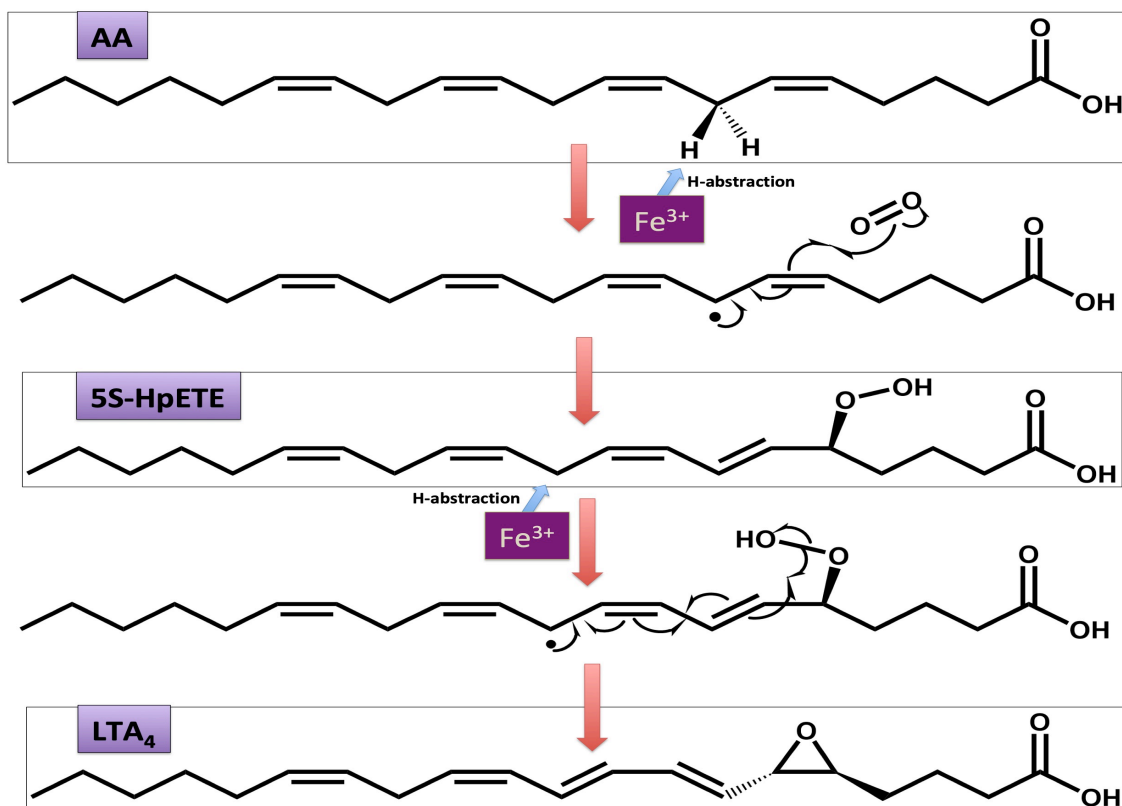
Scheme 1.3- h5-LOX catalysis of AA to LTA$_4$.

1.4 Oxylipins and inflammation

As was briefed on earlier, PUFAs are critical elements in an effective inflammatory response. Acute inflammation is a necessity in response to injury and infection but can lead to chronic inflammation and disease if not properly regulated [14]. Resident immune cells initiate the proper pro-inflammatory response, which is amplified by neutrophils, eosinophils, M1 polarized macrophages by producing AA derived LTs and PGs [15]. Most inflammatory therapeutics have so far focused on

inhibiting the formation of these pro-inflammatory molecules, such as the non-steroidal anti-inflammatory drugs (NSAIDS), subsequently, this pro-inflammatory defensive process eventually transitions to the pro-resolution phase by M2 polarized macrophages, producing the conversion of LTs to lipoxins as well as EPA/DPA/DHA derived potent oxy-lipin molecules such as maresins, resolvins, and neuroprotectins, otherwise know as specialized pro-resolving mediators (SPMs) (**Scheme 1.3**) [16,17]. This shift in cellular phenotype resulting in new oxylipins products with different activities is called lipid mediator class switching (**Figure 1.3**). It is now recognized that if this switch to pro-resolution does not occur then over time inflammation builds upon itself and chronic inflammatory diseases, such as cardiovascular disease, stroke, Alzheimer's disease, atherosclerosis, and cancer occur [18]. The challenge is that the biocatalysts that produce the pro-inflammatory molecules, such as lipoxygenase (LOX) and cyclooxygenase (COX) isozymes, are the same biocatalysts that produce the pro-resolution molecules [19,20]. Revealing the power of these oxylipin mediators, along with elucidation of their biosynthetic pathways will surely allow for better therapeutic intervention into a number of diseases. This thesis is divided into different diseases and their relation to LOXs metabolites, in hopes of creating a better picture of lipid metabolism and its effect on health.
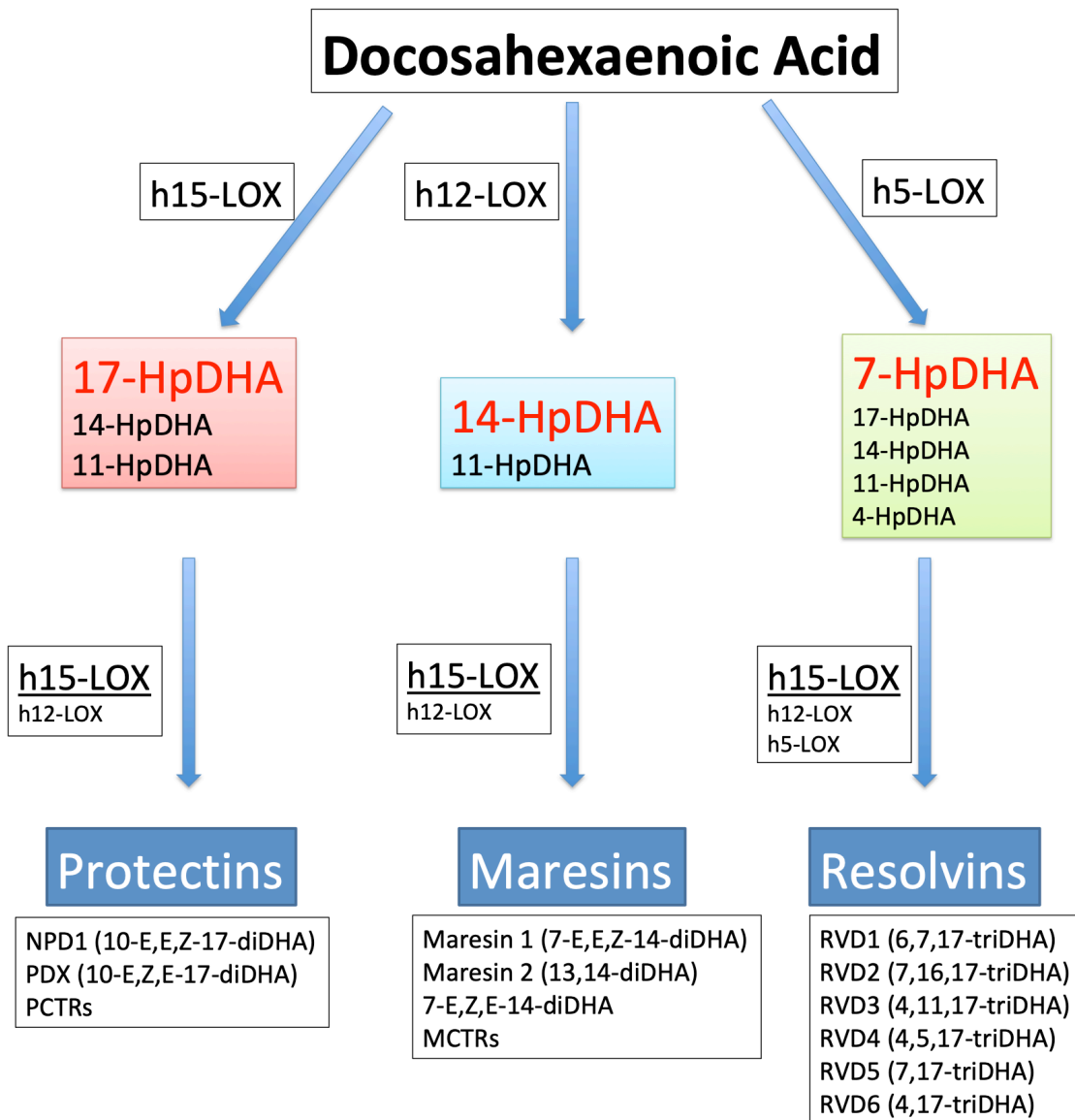
Scheme 1.4- DHA metabolism by LOX isozymes to specialized pro-resolving mediators, i.e. protectins, maresins, and resolvins.
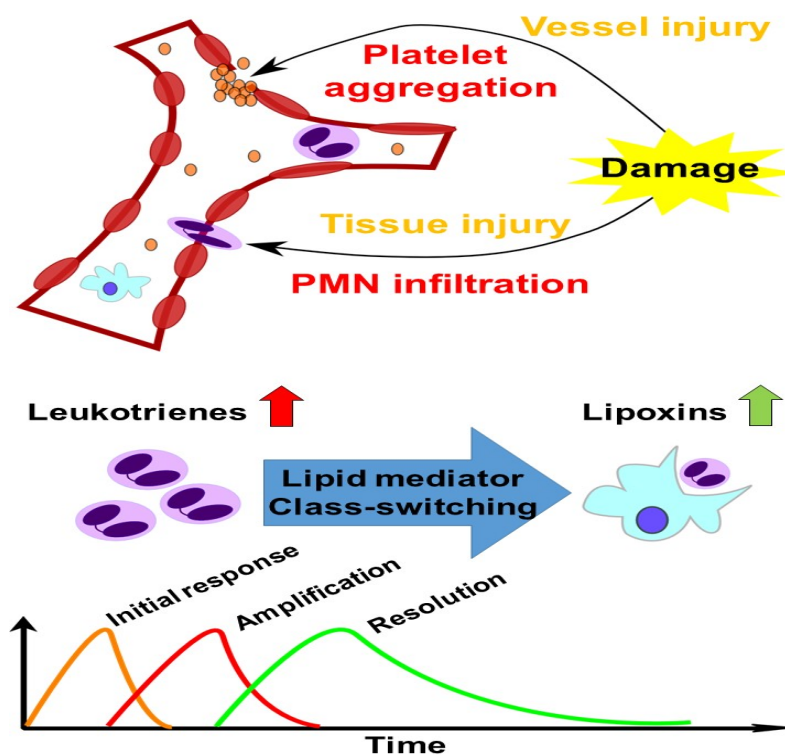
Figure 13- Inflammation diagram displaying the proper response involving lipid mediator class-switching.

1.5 Oxylpins as Antiplatelets

A major burden on society is cardiovascular disease, which is the leading cause of death in the US, accounting for a third of all deaths annually at about 1 death every 40 seconds [21]. In addition to these statistics, the population average age continues to rise which is a direct risk factor for CVDs. Platelets hold a key role in regulating vascular thrombosis and homeostasis, directly effecting cardiovascular health [22]. Hyper platelet activation is a large contributor to these diseases. In light of this detriment, current antiplatelet drugs have significantly decreased risks of occlusive clotting events (**Figure 1.4**). However, some anti-platelets, as mentioned

earlier, such as heparin cause excessive bleeding while others such as aspirin can cause stomach ulcers [23,24]. Some new anti-platelets have shown improvements in reducing thrombotic events, yet they still persist and continue to be the leading cause of mortality and morbidity in industrialized countries including the US [21]. Therefore, it is critical to fine tune intracellular signaling processes to regulate platelet activation, creating a balance between hemostasis and normal vascular flow. And again, diet has been shown decrease the risk of clot associated cardiovascular events [25]. This has led to the need of clear links between dietary supplementation of PUFAs, biochemical effects, and well-designed clinical trial data showing CVD risk reduction. Unfortunately, the knowledge on dietary PUFA and their actions on clot protection is limiting due to the complexity of the pathways, the high impact of diet, and the low levels of metabolites. Both omega-3 and omega-6 fatty acids have been recently screened for anti-platelet showing some potent modulators of platelet reactivity [26]. Previously in the Holman and Holinstat lab, we had identified dihomo-gamma-linolenic acid (DGLA), an omega-6 PUFA, is converted by 12-lipoxygenase (h12-LOX) in human platelets to 12S-hydroxyeicosatetraenoic acid (12S-HETrE). 12S-HETrE was found to exert its anti-thrombotic effects partly through the prostacyclin (IP) receptor, a G protein-coupled receptor (GPCR), on platelets [27,28]. These studies provided insight on the efficacy of exogenous DGLA, which is also a predominant PUFA found on the lipid bilayer, on regulating platelet function.
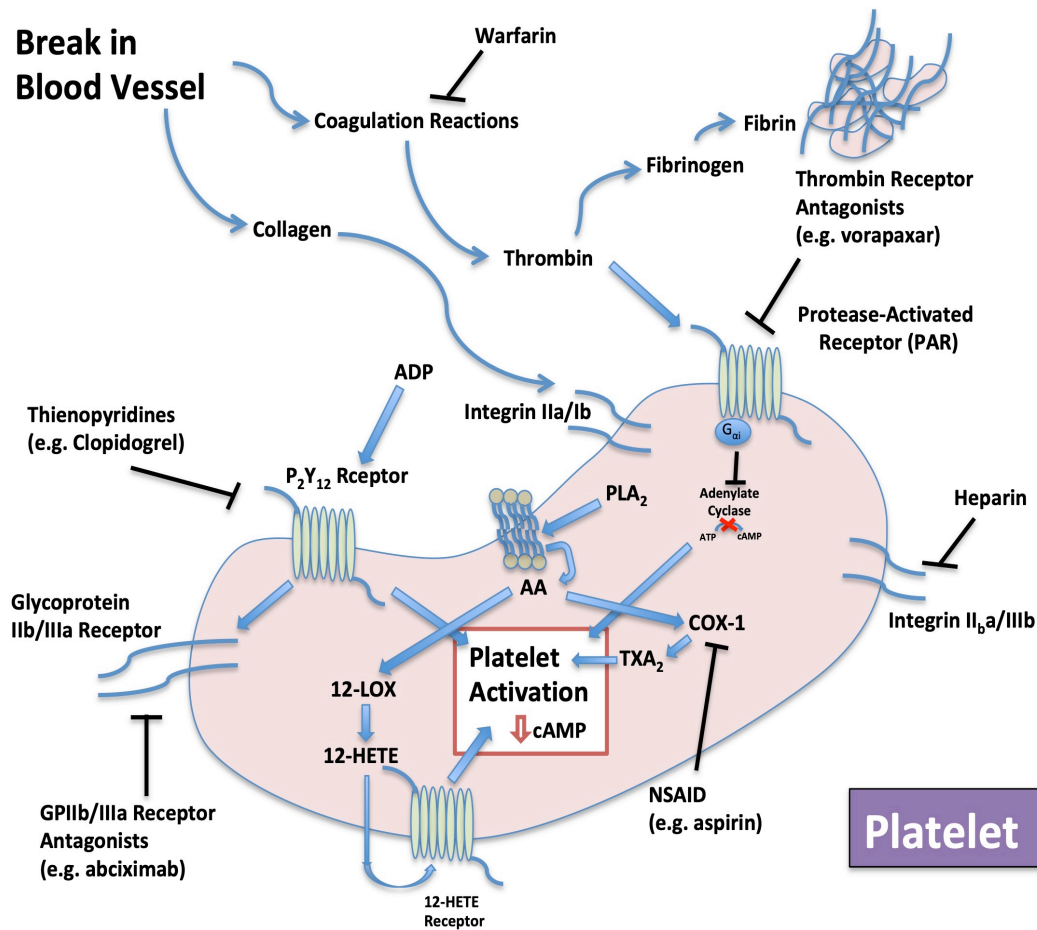
Figure 1.4- Diagram showing mechanisms of platelet activation and common   FDA approved anti-platelets in the clinic.

Focus has been examining major PUFAs in the regulation of platelet function; however, the minor PUFAs found in diet, such as docosapentaenoic acid (DPA), has not been well characterized or investigated in regulating platelet function. DPA can be either omega-3 or omega-6 and until recently the omega-6 configuration has been largely unavailable in the pure form. Cis-7,10,13,16,19-docosapentaenoic acid (DPA, ω-3) and cis-4,7,10,13,16-docosapentaenoic acid (DPA, ω-6) has been shown to be metabolized by lipoxygenase into 11S-hydroperoxy-docosapentaenoic acid (11S-

HpDPA$_{\omega-6}$) and 14S-hydoperoxy-docosapentaenoic acid (14S-HpDPA$_{\omega-6}$) in human platelets, with the omega-6 isomer having mostly the 14th carbon oxygenated. Lipoxygenase displayed slightly lower catalytic efficiency for these substrates and the amount of the substrates found in blood is low with the omega-6 being especially scant (*vida infra*). A previous study pointed to the anti-aggregation properties of the omega-3 isomer of DPA being through inhibition of collagen or U46619-mediated platelet aggregation by directly inhibiting the cyclooxygenase (COX-1) activity [29]. Work in our lab demonstrated that these anti-platelet effects of PUFAs are mediated by their oxylipins generated by lipoxygenases [26]. The h12-LOX activity found in platelets is a main focus of this chapter, and characterization of DPA isomers and their derived oxylipins as well as platelet reactivity effects and mechanism of action elucidation. We show for the first time that DPA, omega-6 and their h12-LOX derived oxylipins, 11S-HpDPA$_{\omega-6}$ and 14S-HpDPA$_{\omega-6}$, strongly inhibited platelet activation compared to DHA and DPA omega-3 (**Figure 1.5**). Interestingly, the derived oxylipins of DPA$_{\omega-6}$, did not directly induce G$_{as}$ signaling effector, such as protein kinase A (PKA) activation. Instead, these oxylipins mediated their inhibitory effect on platelet function through peroxisome proliferator-activator receptor-alpha (PPARAα), a member of the nuclear receptor superfamily with involvement in lipid uptake. Backed up with mouse studies these claims are substantially supported and give insight to a potent form of natural anti-platelets as well as implications of lipoxygenase and cyclooxygenase inhibition.
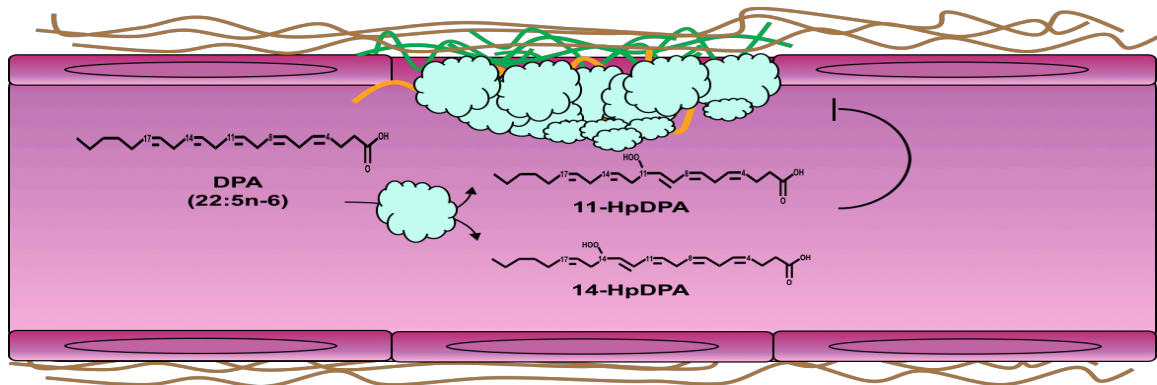
Figure 1.5- DPA$_{\omega-6}$ being metabolized by human platelets to 11 and 14-HpDPA$_{\omega-6}$ and inhibiting platelet activation and thus occlusive thrombus growth through receptor binding.

1.6 Heart Failure Biomarker Discovery

Heart failure (HF) is another major health problem causing mortality and morbidity in the world that is built from hypertension and ischemia. This leads to complications such as heart attacks; however the lipid signaling underlying the physical symptoms is largely unknown. HF is directly related to lipoxygenase expression and PUFA metabolism. Increased expression of h15-LOX-1 and its metabolites 15S-HETE has been seen in hypoxic heart tissue [36]. However, the exact role h15-LOX-1 is playing in heart disease is unknown. Specific lipid mediators could be key chemical signals relaying information about the dying heart. Identifying the pathological processes involved along with the biochemistry behind it could reveal new biomarkers that would enable therapeutic intervention before a heart fails. Some currently used biomarkers are heart muscle deterioration proteins such as troponin T, oxidative molecules like oxidized low-density lipoproteins, and hormones

16

such as norepinephrine and angiotensin II [37]. However, these biomarkers are ridden with false positives and negatives, highlighting the need for more indicators that can be added together to insure proper diagnosis of future HF. This has called for large clinical trials, like the one in this chapter, relating current biomarkers with lipids, enabling more personalized medicine to treat the individual cause of the complex disease process and improve patient care.

1.7 Cystic Fibrosis: Investigations of Pseudomona's Lipoxygenase

Cystic fibrosis is a genetic disease effecting 30,000 people in the US that causes increased likelihood of lung infections and causes difficulty of breathing [38]. Pseudomonas Aeruginosa (P. aeruginosa) is one of the main bacteria responsible for death in cystic fibrosis (CF) patients, and has recently been discovered to secrete a 15-LOX (LOXA). LOXA is a highly active lipoxygenase relative to humans and this particular LOX has a 200-fold increase in expression during biofilm formation. We have shown that the secreted lipoxygenase and its products may be necessary for the survival and proliferation of the bacteria in human airway cells through reduction of biofilms and production of SPM precursors. Production of 15-HpETE, a precursor to LXB_4, can turn off host pro-inflammatory response, also through its high activity the LOX can reduce the remove substrate from h5-LOX resulting in less LTA_4 reducing the inflammatory response and thus inhibiting the clearance of the bacteria. In addition, P.aeruginosa is resistant to most antibiotics due to genetic variance and

17

biofilm protection. We characterized the bacterial enzyme and screened for first in class LOXA inhibitors, which can be used to help treat nosocomial pneumonia infections in CF patients through possibly reducing biofilm formation (*vida infra*).

1.8 Maresins and The Resolution of Inflammation

Acute inflammation is a beneficial response to injury, but if left unresolved, can lead to chronic inflammation causing many of the diseases previously mentioned as well as others that create a burden on society [39]. The focus of drug targeting for inflammation has been on anti-inflammation, or the inhibition of pro-inflammatory molecules. This has led to remarkable advancements in medicine; however, lots of diseases have still prevailed. The recent shift in understanding is that stopping inflammation is not as beneficial as once thought, being that, as mentioned earlier, many of the pro-inflammatory molecules are used as substrates to create the pro-resolving mediators that return tissue to a healthy state [40]. The resolution phase of inflammation is active and a delicate orchestration of molecule transformation and cell differentiation. The power of the aforementioned fish oil derived PUFA, especially DHA, DPA, and EPA is that they result in the SPMs created through the lipoxygenase pathway [41]. Examples of these molecules are the previously mentioned D-series resolvins, neuroprotectins, and maresins created from DHA and DPA as well as the E-series resolvins made from EPA. The SPM's are extremely potent molecules that dismantle the inflammatory response and promote wound

18

healing and tissue regeneration. Without these molecules, inflammatory responses build upon each other destroying tissue and cells leading to disease. Delineating the biochemical pathways and biological responses of these molecules will enable better drug development and supplementation efforts to combat disease.

In summary, with proper dietary intake of PUFAs, it is not a stretch, to say that enabling a strong resolution response could substantially reduce the previously mentioned diseases. However, genetics and environmental effects will still cause disease through unregulated inflammatory responses. This thesis will cover some advances in the understanding of PUFA metabolism by lipoxygenase and the effects of the derived oxylipins on health and disease.

Published paper:

Deschamps JD, *et al.* (2016) Biochemical and cellular characterization and inhibitor discovery of *Pseudomonas aeruginosa* 15-lipoxygenase. Biochemistry 55(23):3329–3340.

References

[1]   Smith, GI; Atherton, P; Reeds, DN; Mohammed, BS; Rankin, D; Rennie, MJ; Mittendorfer, B (2011). "Omega-3 polyunsaturated fatty acids augment the muscle protein anabolic response to hyperinsulinaemia-hyperaminoacidaemia in healthy young and middle-aged men and women". *Clinical Science*. 121 (6): 267–78. doi:10.1042/cs20100597

[2]   Das UN. (2013). Autism as a disorder of deficiency of brain-derived neurotrophic factor and altered metabolism of polyunsaturated fatty acids. Nutrition.;29(10):1175-1185

[3]   Calder PC. (2013). Omega-3 polyunsaturated fatty acids and inflammatory processes: nutrition or pharmacology? Br J Clin Pharmacol. 75(3):645–662. 10.1111/j.1365-2125.2012.04374.x

[4]   Yu J, Loh K, Song Z, Yang H, Lin S. (2018). Update on glycerol-3-phosphate acyltransferases: the roles in the development of insulin resistance. *Nutr Diabetes*. 8:34. doi: 10.1038/s41387-018-0045-x

[5]   Decker, E. A. (1996). The role of stereospecific saturated fatty acid position on lipid nutrition. *Nutrition Reviews.*, 54: 108–110.

[6]   R. Flower (2003). What are all the things that aspirin does?
        BMJ, 327, pp. 572-573

[7]   Liu MC, Dube LM, Lancaster J. (1996) Acute and chronic effects of a 5-liopxygenase inhibitor in asthma: a 6-month randomized multicenter trial. J Allergy Clin Immunol; 98:859-871

[8]   J.A. Chandrasekharan, N. Sharma-Walia. (2015). Lipoxins: nature's way to resolve inflammation. J. Inflamm. Res., 8 pp. 181-192

[9]   McDonnell AM, Dang CH. (2013). Basic review of the cytochrome p450 system. J Adv Pract Oncol.;4(4):263–8.

[10]   Baysal, T. and Demirdöven, A. (2007) Lipoxygenase in fruits and vegetables: a review. Enzyme Microb. Technol. 40, 491– 496.

[11]   H. Kuhn, S. Banthiya, K. van Leyen (2015). Mammalian lipoxygenases and their biological relevance. Biochim. Biophys. Acta, 1851, pp. 308-330

[12]   L. Kutzner, K. Goloshchapova, D. Heydeck, S. Stehling, H. Kuhn, N.H. Schebb (2017). Mammalian ALOX15 orthologs exhibit pronounced dual positional specificity with docosahexaenoic acid Biochim Biophys Acta, 1862, pp. 666-675.

[13]   S. Adel, F. Karst, A. Gonzalez, Lafont, M. Pekarova, P. Saura, L. Masgrau, J. M. Lluch, S. Stehling, T. Horn, H. Kuhn, D. Heydeck (2016). Evolutionary alteration of ALOX15 specificity optimizes the biosynthesis of antiinflammatory and proresolving lipoxins Proc. Natl. Acad. Sci. U. S. A., 113, pp. E4266-E4275

[14]   Tabas I, Glass CK (2013) Anti-inflammatory therapy in chronic disease: challenges and opportunities. *Science* 339: 166–172.

[15]   Chen, L.; Deng, H.; Cui, H.; Fang, J.; Zuo, Z.; Deng, J.; Li, Y.; Wang, X.; Zhao, L. (2018). Inflammatory responses and inflammation-associated diseases in organs. *Oncotarget*, *9*, 7204–7218

[16]   Serhan, C. N., Chiang, N., and Van Dyke, T. E. (2008) Resolving 646 inflammation: dual anti-inflammatory and pro-resolution lipid 647 mediators. *Nat. Rev. Immunol.* 8, 349−361.

[17]   Wongrakpanich, S.; Wongrakpanich, A.; Melhado, K.; Rangaswami, J. A (2018). comprehensive review of non-steroidal anti-inflammatory drug use in the elderly. *Aging Dis. 9*, 143–150.

[18]   Su Sugimoto MA, Sousa LP, Pinho V, Perretti M, Teixeira MM. (2016) Resolution of Inflammation: What Controls Its Onset? *Front Immunol. 7*:160. doi: 10.3389/fimmu.2016.00160.

[19]   R. Wisastra, F.J. Dekker (2014). Inflammation, cancer and oxidative lipoxygenase activity are intimately linked Cancers. *Basel.* 6 (3), pp. 1500-1521

[20]   Serhan, C. N., Chiang, N. & Van Dyke, T. E. (2008).Resolving inflammation: dual anti-inflammatory and pro-resolution lipid mediators. *Nature Rev. Immunol.* 8, 349–361.

[21]   CDC, NCHS. Underlying Cause of Death 1999-2013 on CDC WONDER Online Database, (2015). Data are from the Multiple Cause of Death Files, 1999-2013, as compiled from data provided by the 57 vital statistics jurisdictions through the Vital Statistics Cooperative Program. Accessed Feb. 3.

[22]   Koupenova M, Kehrel BE, Corkrey HA, Freedman JE. (2017). Thrombosis and platelets: an update.Eur Heart J. *38*:785–791. doi: 10.1093/eurheartj/ehw550.

[23]   Krishnamurthy M, Freedman ML. (2005) Complications of anticoagulation with heparin. *Virtual Mentor*; 7: 432- 435.

[24]   B. Cryer, K.W. Mahaffey (2014). Gastrointestinal ulcers, role of aspirin, and clinical outcomes: pathobiology, diagnosis, and treatment J Multidiscip Healthc, 7, pp. 137-146.

[25]   SS, Hawkes C, de Souza RJ, Mente A, Dehghan M, Nugent R, Zulyniak MA, Weis T, Bernstein AM, Krauss RM, Kromhout D, Jenkins DJ, Malik V, Martinez-Gonzalez MA, Mozaffarian D, Yusuf S, Willett WC, Popkin BM. (2015). Food consumption and its impact on cardiovascular disease:

importance of solutions focused on the globalized food system: a report from the Workshop Convened by the World Heart Federation.J Am Coll Cardiol. *66*:1590–1614. doi: 10.1016/j.jacc.2015.07.050.

[26]   Ikei KN, Yeung J, Apopa PL, Ceja J, Vesci J, Holman TR, et al. (2012). Investigations of human platelet-type 12-lipoxygenase: role of lipoxygenase products in platelet activation. *J Lipid Res.* 53(12):2546-59.

[27]   Tourdot BE, Adili R, Isingizwe ZR, Ebrahem M, Freedman JC, Holman TR, et al. (2017) 12-HETrE inhibits platelet reactivity and thrombosis in part through the prostacyclin receptor. *Blood Adv.* 1(15):1124-31.

[28]   Yeung J, Tourdot BE, Adili R, Green AR, Freedman CJ, Fernandez-Perez P, et al. (2016). 12(S)-HETrE, a 12-lipoxygenase oxylipin of dihomo-gammalinolenic acid, inhibits thrombosis via Galphas signaling in platelets. *Arterioscler Thromb Vasc Biol*; 36:2068-77.

[29]   Akiba S, Murata T, Kitatani K, and Sato T. (2000). Involvement of lipoxygenase pathway in docosapentaenoic acid-induced inhibition of platelet aggregation. *Biol Pharm Bull.* 23(11):1293-7.

[30]   Iso H, Rexrode KM, Stampfer MJ, et al. (2001) Intake of fish and omega-3 fatty acids and risk of stroke in women. JAMA. *285*: 304–312.

[31]   Grenon SM, Owens CD, Nosova EV, Hughes-Fulford M, Alley HF, Chong K, et al. (2013) Short-Term, High-Dose Fish Oil Supplementation Increases the Production of Omega-3 Fatty Acid-Derived Mediators in Patients With Peripheral Artery Disease (the OMEGA-PAD I Trial). J Am Heart Assoc. 4(8):e002034.

[32]   Risk, Prevention Study Collaborative G, Roncaglioni MC, Tombesi M, Avanzini F, Barlera S, et al. (2013) ω-3 fatty acids in patients with multiple cardiovascular risk factors. N Engl J Med. 368(19):1800-8.

[33]   Mozaffarian D, Marchioli R, Macchia A, Silletta MG, Ferrazzi P, Gardner TJ, et al. (2012) Fish oil and postoperative atrial fibrillation: the Omega-3 Fatty Acids for Prevention of Post-operative Atrial Fibrillation (OPERA) randomized trial. *JAMA.* 308(19):2001-11.

[34]   Mozaffarian D, and Wu JH. (2011) Omega-3 fatty acids and cardiovascular disease: effects on risk factors, molecular pathways, and clinical events. *J Am Coll Cardiol.* 58(20):2047-67.

[35] Kromhout D, Giltay EJ, Geleijnse JM (2010). Alpha Omega Trial G. ω-3 fatty acids and cardiovascular events after myocardial infarction. *N Engl J Med.*;363(21):2015-26.

[36] Magnusson LU, Lundqvist A, Asp J, Synnergren J, Johansson CT, Palmqvist L, et al. (2012). High expression of arachidonate 15-lipoxygenase and proinflammatory markers in human ischemic heart tissue. Bio-chem Biophys Res Commun; 424(2):327–30. https://doi.org/10.1016/j.bbrc.2012.06.117 PMID:22750246.

[37] Ibrahim NE, Januzzi JL., Jr. (2018) Established and emerging roles of biomarkers in heart failure. Circ Res. ;123:614–629.

[38] Mirtajani SB, Farnia P, Hassanzad M, Ghanavi J, Farnia P, Velayati AA. (2017) Geographical distribution of cystic fibrosis; the past 70 years of data analyzis. Biotechnol Res J;1:105-12.

[39] Pahwa, R.; Jialal, I. (2018). StatPearls: *Chronic Inflammation* Treasure Island, FL, USA.

[40] Serhan, C. N. & Savill, J. (2005). Resolution of inflammation: the beginning programs the end. *Nature Immunol.* 6, 1191–1197.

[41] Serhan, C. N. (2014). Pro-resolving lipid mediators are leads for resolution physiology. *Nature* 510, 92–101.

Chapter 2

PLATELET AGGREGATION EFFECTS OF H12-LIPOXYGENASE

METABOLITES OF OMEGA-6 DOCOSAPENTAENOIC ACID

2.1 Abstract

Platelet-mediated thrombosis is the primary underlying mechanism leading to life-threatening cardiovascular events. Regulating excessive platelet reactivity is an essential aspect of antithrombotic therapy. A number of anti-platelet drugs have been developed to target specific signaling pathways or endpoints involved in platelet activation. Despite the effectiveness of current anti-platelet therapies, uncontrolled thrombosis or bleeding complications still persist, warranting the development of novel anti-thrombotic strategies. Previously, we had presented that 12-HETrE, an oxylipin generated by human 12-lipoxygenase (h12-LOX) oxidation of omega-6 polyunsaturated fatty acid (PUFA), dihomo-g-linolenic acid (DGLA), could be an approach to modulate platelet reactivity through the prostacyclin receptor [9]. Here, we demonstrate that the elongated form of DGLA, docosapentaenoic acid (DPA; 22:5 ω-6) can also be endogenously oxidized by platelet h12-LOX to generate two distinct oxylipins, 11-HpDPA$_{\omega\text{-}6}$ and 14-HpDPA$_{\omega\text{-}6}$ to regulate platelet reactivity. Both 11- and 14-HpDPA$_{\omega\text{-}6}$ potently inhibited platelet aggregation as well as adhesion on collagen-coated flow chamber under venous and arterial shear. In support of the ex vivo findings, laser-induced thrombus formation (platelet and fibrin) in the cremaster vessel of wild-type mice intravenously administered with either 11- and 14-HpDPA$_{\omega\text{-}6}$ were attenuated compared to vehicle control. Interestingly, both 11-and 14-HpDPA$_{\omega\text{-}6}$ inhibited platelet activation in a G$_{as}$ independent manner. Instead, 11-HpDPA$_{\omega\text{-}6}$ and 14-HpDPA$_{\omega\text{-}6}$ exerted their anti-platelet effects through the peroxisome proliferated-

25

activated receptor (PPAR), by which pharmacological antagonism of the PPARs reversed the ability of the metabolites to inhibit platelet aggregation. This is the first study to demonstrate the novel metabolites of omega-6 DPA generated by h12-LOX to also have a role in regulating platelet activation through the PPAR pathway.

2.2 Introduction

Cardiovascular disease is the leading cause of death in the US resulting in nearly 1 in 3 deaths annually [1]. Platelets play an essential role in cardiovascular health through regulation of clot formation in the vessel mediating both the hemostatic and thrombotic responses to vascular insult [2]. Aberrant platelet activation is a major contributor to thrombotic-related diseases, such as stroke or myocardial ischemia and FDA-approved antiplatelet drugs have significantly decreased mortality due to occlusive thrombotic events. However, despite remarkable improvements in anti-platelet agents, thrombotic-associated events still persist and continue to be the leading cause of mortality and morbidity in industrialized countries including the US. In an effort to further decrease the risk of cardiovascular events resulting from unwanted clot formation, a number of clinical studies have tested the hypothesis that dietary supplementation of polyunsaturated fatty acids (PUFAs) may significantly reduce cardiovascular-related diseases due to thrombotic complications. Unfortunately, due to the confounding biological properties of PUFAs and the scant mechanistic insight as to how they elicit protection in the vessel, the results of these

studies remain inconclusive as to their role in cardiovascular protection from platelet activation and thrombosis (3-5) 6, 7).

Many of these clinical trial studies have focused on fish oils which are comprised primarily of ω-3 PUFAs showing inconsistency in the effectiveness of the PUFAs in reducing mortality associated with cardiovascular-related complications or rate of major cardiovascular events, the cardioprotective role of ω-6 PUFAs still remains unclear and understudied. Previous prospective cohort studies have focused primarily on linoleic acid (LA) as the predominant of ω-6 PUFA, which have generated mixed results on the relationship between LA intake and coronary heart disease (CHD) risk. Furthermore, there are concerns for high intake of LA based on the assumption that LA is converted to the pro-inflammatory and thrombotic substrate, arachidonic acid (AA), which may increase risk for CHD. Because of rate-limiting conversions of PUFAs from their precursors, these studies have masked what precise PUFAs provide cardioprotection, indirectly through reducing thrombotic risks. Thus to delineate PUFAs having potential potent anti-platelet properties, we had screened both ω-3 and ω-6 PUFAs on platelet function, as previously reported (8). We had identified that dihomo-γ-linolenic acid (DGLA), an ω-6 PUFA, is enzymatically converted to 12(S)-hydroxyeicosatetrienoic acid (12-HETrE) by 12-lipoxygenase (h12-LOX) in platelets. 12-HETrE was found to exert its anti-thrombotic effects partly through the prostacyclin (IP) receptor, a G protein-coupled receptor (GPCR), on platelets (9, 10). These studies provided insight on the efficacy of exogenous DGLA, which is also a predominant PUFA found on the lipid bilayer,

27

on regulating platelet function. Despite the effort to investigate the major PUFAs in the regulation of platelet function, the minor constituent of PUFAs found in diet, such as docosapentaenoic acid (DPA), has not been well characterized or investigated in regulating platelet function.

Unlike DGLA, there are two isomers of DPA, which can have either ω-3 or ω-6 unsaturation. All-cis-7,10,13,16,19-docosapentaenoic acid (DPA, ω-3) (DPA$_{\omega\text{-}3}$) had been briefly characterized to be metabolized in a lipoxygenase-dependent manner into 11-hydroxy-docosapentaenoic acid (11-HDPA$_{\omega\text{-}3}$) and 14-hydoxy-docosapentaenoic acid (14-HDPA$_{\omega\text{-}3}$) in human platelets(9). Subsequently, all-cis-4,7,10,13,16-docosapentaenoic acid (DPA, ω-6) was also demonstrated to be metabolized to 14-HDPA, ω-6(10-12). The earlier study reported DPA, ω-3, inhibited collagen or U46619-mediated platelet aggregation by directly inhibiting the cyclooxygenase (COX-1) activity (15) and by accelerating their isomer product formation. In contrast to the previous studies, we report that the anti-platelet effects of PUFAs are mediated by their oxylipins generated by oxygenases.

The objectives of this study were to characterize DPA isomers and their derived oxylipins from h12-LOX in platelet function and elucidate their mechanism of action in inhibiting platelet reactivity. We show for the first time that DPA, ω-6 and their h12-LOX derived oxylipins, 11-HpDPA$_{\omega\text{-}6}$ and 14-HpDPA$_{\omega\text{-}6}$, strongly inhibits platelet activation compared to DPA, ω-3. Interestingly, the derived oxylipins of DPA, ω-6, did not directly induce $G\alpha_s$ signaling effector, such as protein kinase A (PKA) activation. Instead, these oxylipins mediated their inhibitory effect on platelet

function through peroxisome proliferator-activator receptor-α (PPARα), a member of the nuclear receptor superfamily. Platelets from PPARα deficient mice (PPAR$\alpha^{-/-}$) were unable to respond sufficiently to DPA, ω-6, derived oxylipins compared to the wild-type (WT) platelets. Additionally, thrombus formation was not attenuated in PPAR$\alpha^{-/-}$ administered with DPA ω-6, and its h12-LOX oxylipins compared to WT. In support, a PPAR transactivation assay was also performed, showing the robust activation of PPARα by the oxylipins, 11- and 14-HpDPA$_{\omega-6}$. Altogether, this demonstrates that targeting PPARA may be an attractive therapeutic strategy, especially in the context of prevention of thrombosis.

2.3 Methods

Chemicals: Docosapentaenoic acid (DPA$_{\omega-6}$) was purchased from Nu Chek Prep, Inc. at +99% purity. Reagent and HPLC grade chemicals were used (Fisher Scientific, Pittsburgh, PA, USA).

Expression and Purification of h15-LOX-1 and h12-LOX: Recombinant expression and purification of wild-type h12-LOX was performed in a baculovirus SF9 cell system. The purities of the enzymes were assessed with a sodium dodecyl sulfate polyacrylamide gel to be >95%. The metal content was assessed on a Finnigan inductively coupled plasma mass spectrometer (ICP-MS), using an iron standard solution and curve along with Cobalt-EDTA as an internal standard.

Synthesis and Purification of Oxylipins: 14S-hydrperoxy-4Z,7Z,10Z,12E,16Z-docosapentaenoic acid (14S-HpDPA$_{\omega-6}$) and 11S-hydrperoxy-4Z,7Z,10E,12Z,16Z-docosapentaenoic acid (11S-HpDPA$_{\omega-6}$), were synthesized in 200 mL 25 mM HEPES buffer at pH 8.0 for h12-LOX. Absorbance increase at 234 nm was monitored until it reached completion and quenched with 0.4% (v/v) glacial acetic acid. The solution was extracted 3 times with 100 mL Dichloromethane and evaporated to dryness. The docosanoid products were purified with a normal phase Phenomonex silica column (5 μm, 250 mm x 10 mm) and an isocratic mixture of 99% hexane, 1% isopropanol and 0.1% trifluoroacetic acid. The purity was checked by LC-MS/MS to be greater than 95%.

Human platelet preparation: University of Michigan Institutional Review Boards approved all protocols involving human subjects. In accordance with the Declaration of Helsinki, written informed consent was obtained from healthy donors prior to each blood draw. Blood was drawn into sodium citrate tubes and centrifuged at 200xg for 10 minutes, and platelet rich plasma
(PRP) was collected. PRP was subsequently spun with acid citrate dextrose solution and apyrase at 2000xg; and then adjusted to 3×10^8 platelets/mL in tyrodes buffer.

Effect of 14S-HpDPA$_{\omega-6}$ and 11S-HpDPA$_{\omega-6}$ on Human Platelet Aggregation and Lipidomics: For aggregation assays , 250 μL of washed human platelets (3 x 10^8 /mL) were incubated with 1-10 μM oxylipin 12S-HETrE for 10 minutes at 37 °C in a glass cuvette. The oxylipin metabolite treated platelets were stimulated with 0.25

µg/mL collagen while stirring at 1100 rpm in a Chrono-log model 700 aggregometer and aggregation was analyzed via a decrease in light transmittance. For lipidomics, 3×10^8 platelets resuspended in a mL of Tyrode's buffer were incubated with 10 µM DPA$_{\omega\text{-}6}$ for 10 minutes and stimulated with collagen. Supernatants from washed platelets were extracted by C18 cartridge using published methods [12]. The products were resuspended in 50/50 acetonitrile and 0.1% formic acid water and analyzed by LC/MS. The m/z transitions used for 14S-HDPA$_{\omega\text{-}6}$ was 345.2 $\rightarrow$ 205.2, 11S-HDPA$_{\omega\text{-}6}$ 345.2 $\rightarrow$ 165.2.

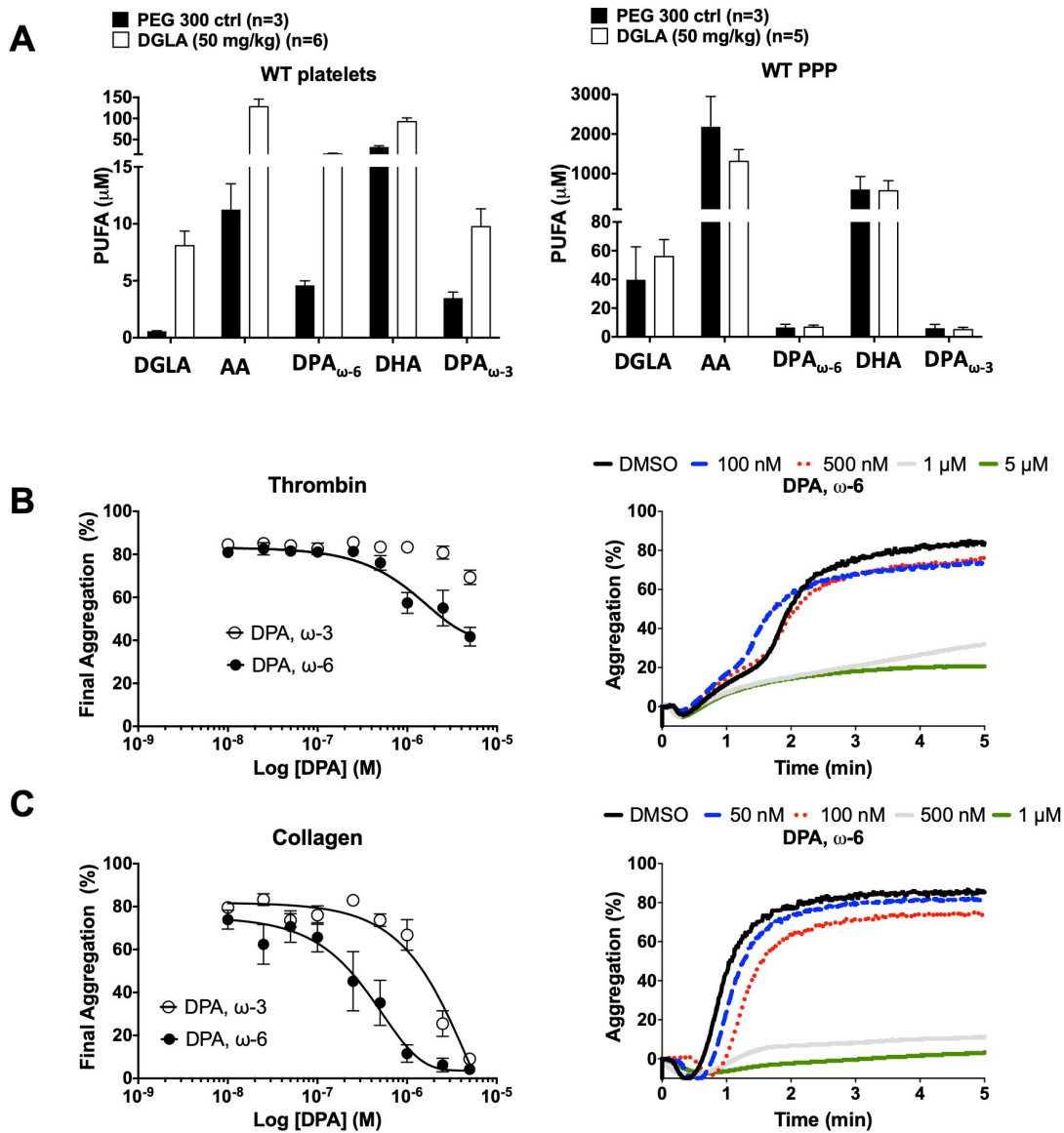**Polyunsaturated fatty acids (PUFAs) and h12-LOX oxylipins**: Omega-6 docopentaenoic acid (DPA) was purchased from NuChek. The h12-LOX derived oxylipins of DPA$_{\omega\text{-}6}$, 11-hydroperoxydocosapentaenoic acid (11-HpDPA$_{\omega\text{-}6}$), 14-hydroperoxydocosapentaenoic acid (14-HpDPA$_{\omega\text{-}6}$), were obtained by incubating DPA$_{\omega\text{-}6}$ with recombinant h12-LOX. Oxylipins were further purified by HPLC semiprep column following substrate reactions with platelet h12-LOX.

Arterial flow shear: DiOC6-labeled human citrated whole blood was pretreated with vehicle control (DMSO) or DPA, omega-6, metabolites for 5 minutes, and 2.5 mM CaCl2 was immediately added before perfusion through a collagen-°©coated (100 µg/mL) Ibidi Slide at 15 dyn/cm2.

2.4 Results and Discussion

Dietary supplementation of polyunsaturated fatty acids (PUFAs) enriched in DGLA affects platelet lipid content. We previously reported that acute intravenous (IV) administration of one of the ω-6 PUFAs, DGLA, resulted in reduced thrombi formation in wild-type (WT) mice *in vivo*; however, mice deficient in h12-LOX, were unable to form stable thrombi in the presence of DGLA (7, 14). To further support the observation that IV administration of DGLA results in reduction of thrombus formation and that this reduction is due to DGLA and not an artifact of IV injection, WT mice were orally gavaged with 50 mg/kg of DGLA for 30 days. Following the 30-day oral gavage regimen, platelet activation was similarly reduced and platelet clots that did form were observed to be unstable in vivo (data not shown). While it is presumed that the inhibition of platelet activation was due to effects of DGLA and its oxidized lipid metabolites (oxylipins) formed in the platelet, it is also recognized that PUFAs undergo elongation in the body by endogenous desaturates following dietary supplementation (15). To assess whether increased consumption of DGLA via oral gavage in WT mice resulted in altered lipid content and if potential alteration of content had an effect on platelet function fatty acid content of the platelet plasma membrane was measured. Following completion of the 30-day oral gavage treatment, washed platelets and platelet rich plasma (PPP) from WT mice fed with either PEG300 vehicle control or 50 mg/kg of DGLA were collected and measured for some of the ω-3 and -6 PUFAs (DGLA, arachidonic acid (AA), docosapentaenoic acid

(DPA), and docohexaenoic acid (DHA)). Both ω-3 and -6 forms of DPA, AA, and DGLA were found to be significantly increased in WT platelets, but not in PPP (Figure 1A), confirming previous reports that habitual feeding of PUFAs in WT mice lead to increased incorporation into membranes as components of phospholipids or conversion to other fatty acids (18, 19). Surprisingly, the largest increase in fatty acid in the membrane was from docosapentanoic acid (DPA). To determine if either or both of the DPA fatty acids (ω-3 and ω-6) play a regulatory role in platelet activation, each fatty acid was dose-dependently added to washed human platelets (10 nM to 5 μM) prior to EC_{80} concentrations of either thrombin (Figure 1B) or collagen (Figure 1C) were added to stimulate platelet aggregation. Human platelets pre-treated with ω-6 DPA showed markedly reduced platelet aggregation in response to thrombin or collagen compared to ω-3 suggesting the structure of the fatty acid plays a role in potency.

Figure 2.1- Dietary supplementation of DGLA enhances ω-3 and-6 DPA in platelets. **A)** Platelets and platelet rich plasma (PPP) from wild-type mice (WT) were measured for ω-3 or -6 polyunsaturated fatty acids (PUFAs) (DGLA, AA, DPA, and DHA) following 1 month of dietary supplementation of 50 mg/kg of DGLA (n=5) or PEG300 control (n=3). The potency of both ω-3 and-6 DPA were determined by human platelet aggregation in response to **B)** thrombin or **C)** collagen (n=10).

The anti-platelet effects of h12-LOX oxidized, DPA ω-6, 11- and 14-HpDPA$_{\omega-6}$. As previously described, the anti-thrombotic or anti-platelet effects of DGLA is partially due to its h12-LOX-oxylipin, 12-HETrE (16, 20) (6). To determine which oxygenase is responsible for the generation of oxylipins derived DPA$_{\omega-6}$, we treated platelets with COX-1 inhibitor, indomethacin, or h12-LOX inhibitor, ML-355. 14-HpDPA$_{\omega-6}$ was found to be the predominant oxylipin compared to 11-HpDPA$_{\omega-6}$ in platelets treated with DPA$_{\omega-6}$ (Figure 2A); however, the detection of these metabolites was reduced with ML-355 (Figure 2A). Interestingly, no COX-1 derived products were detected in the platelets when treated with excess DPA$_{\omega-6}$, suggesting DPA$_{\omega-6}$ is an inert substrate of COX-1 in platelets; whereas, h12-LOX- derived metabolites of DPA$_{\omega-6}$ are the major lipid mediators exerting their regulatory role on platelet function.

11- and 14-HpDPA$_{\omega-6}$ were directly assessed for their ability to regulate agonist-induced platelet aggregation (**Figure 2.2-C,D**). Both 11- and 14-HpDPA$_{\omega-6}$ dose dependently (10 nM to 5 μM) and potently inhibited platelet aggregation in response to EC$_{80}$ concentration of either thrombin (Figure 2C) or collagen (Figure 2D). This showed that the oxylipins inhibited platelet-mediated aggregation regardless of GPCR or non-GPCR activation. Additionally, we measured intracellular calcium mobilization, a precursor to integrin-mediated platelet aggregation, in the presence of DPA$_{\omega-6}$, 11- or 14-HpDPA$_{\omega-6}$ (Figure 2E). DPA$_{\omega-6}$, 11- or 14-HpDPA$_{\omega-6}$ dose dependently decreased calcium mobilization induced by EC$_{80}$ concentration of convulxin, a snake venom toxin that acts on the GPVI collagen receptor (Figure 2E).

Despite differences in the amount of 11- and 14-HpDPA generated by h12-LOX in the human platelets (Figure 2A) treated with ω-6 DPA, the maximal inhibition concentration achieved for both metabolites are observed below 1 μM for collagen and 5 μM for thrombin stimulation of platelet aggregation. These data indicate that the anti-platelet effects of DPA$_{\omega-6}$, is mediated at least in part by its h12-LOX derived oxylipins, 11-and 14-HpDPA$_{\omega-6}$. In comparison, previously reported anti-thrombotic oxylipins 12-HETrE and 12-HpETrE had maximum inhibitory effects above 10 μM with the peroxide being 5 fold more potent then the alcohol.
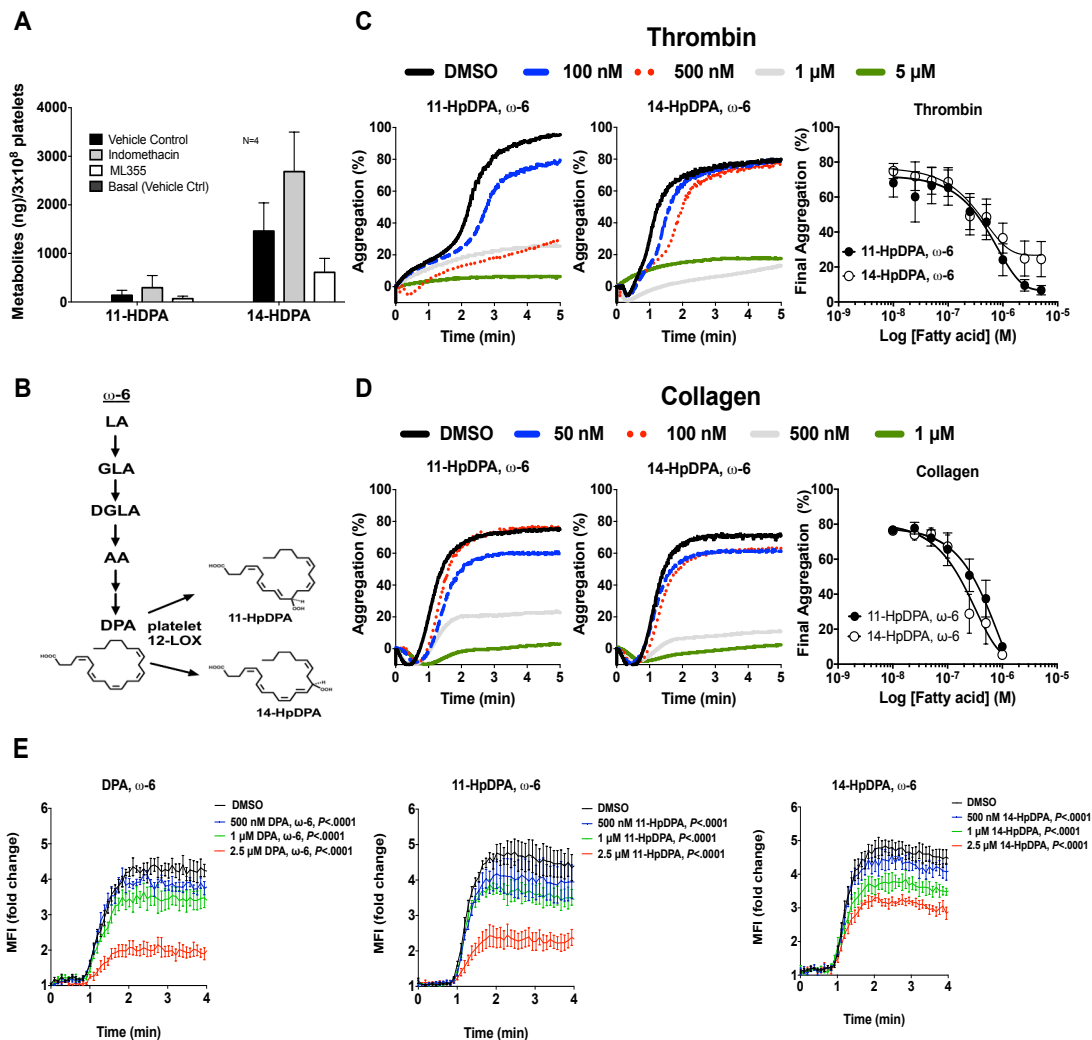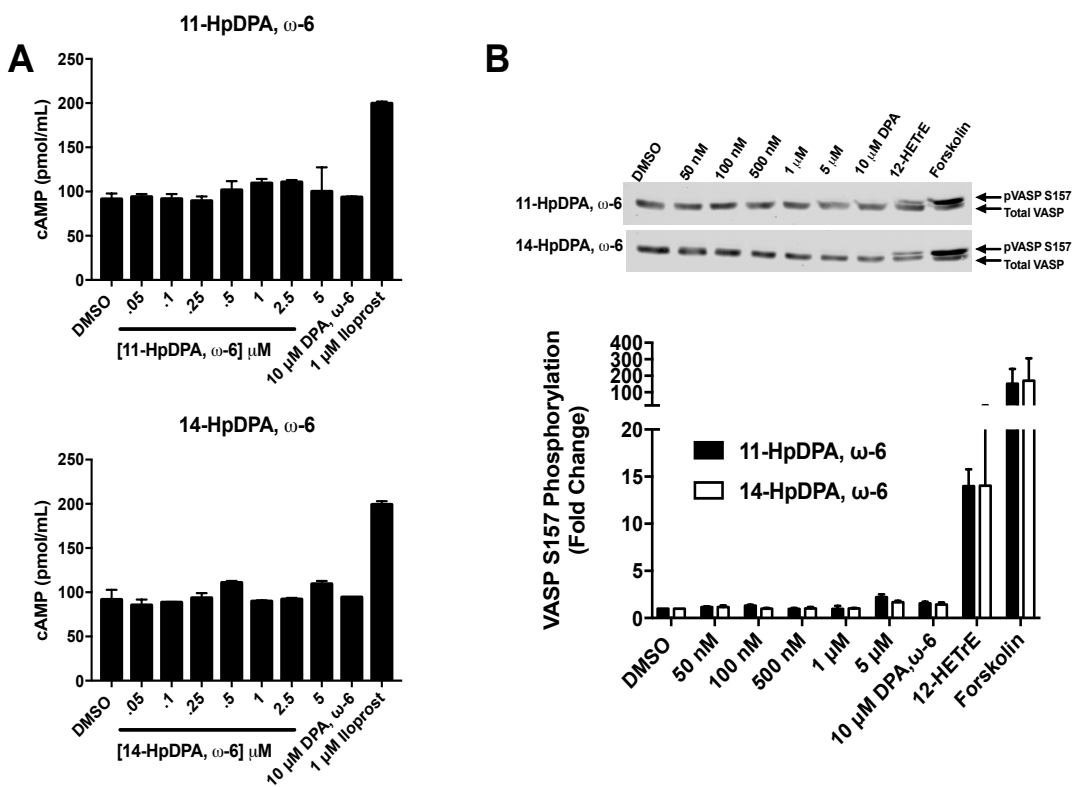
Figure 2.2- h12-LOX derived DPA$_{\omega\text{-}6}$, oxylipins 11- and 14-HpDPA$_{\omega\text{-}6}$, inhibit platelet activation. Oxylipins derived from platelets (n=4) were assessed by **A)** incubating human platelets with 10 μM DPA$_{\omega\text{-}6}$ in the presence of vehicle control (DMSO), h12-LOX inhibitor (ML355), or COX-1 antagonist (indomethacin) prior to mass spectrometry. **B)** The major metabolites produced from DPA$_{\omega\text{-}6}$ in platelets are h12-LOX derived, 11- and 14-HpDPA$_{\omega\text{-}6}$. The effects of 11- and 14-HpDPA$_{\omega\text{-}6}$ were assessed by incubation human platelets with varying concentration of DPA$_{\omega\text{-}6}$ metabolites for 5 minutes prior to **C)** thrombin (n=10), **D)** collagen-induced (n=10) platelet aggregation, and **E)** calcium mobilization mediation by convulxin (n=5).

h12-LOX derived oxylipins of DPA$_{\omega\text{-}6}$, 11- and 14-HpDPA$_{\omega\text{-}6}$, inhibit platelet function

in a $G_{\alpha S}$-independent signaling mechanism. The h12-LOX-derived oxylipin of DGLA,

12(S)-HETrE, was previously shown to signal its inhibitory effects on platelet activation and thrombosis through a Gαs-dependent mechanism, coupled to the prostacyclin receptor(9, 10). To determine if the h12-LOX-derived oxylipins of DPA$_{\omega-6}$ inhibit platelet activation in a similar mechanism to 12-HETrE, intracellular cyclic AMP (cAMP) was measured in washed human platelets incubated with 10 μM of a nonselective phosphodiesterase (PDE) inhibitor, 3-isobutyl-1-methylxanthine (IBMX), prior to treatment of increasing concentrations of either 11- or 14-HpDPA$_{\omega-6}$ and DPA$_{\omega-6}$ (Figure 3A). As expected, platelets treated with iloprost, a synthetic analogue of prostacyclin, enhanced cAMP generation; however, cAMP production was not found to be induced in either 11- or 14-HpDPA$_{\omega-6}$ and DPA treated platelets (Figure 3A).

In support of the cAMP observation, phosphorylation of vasodilator-stimulated phosphoprotein (VASP) at serine 157 (S157), a surrogate maker for active cAMP-activated protein kinase, PKA, was measured in the presence of DPA$_{\omega-6}$ or its h12-LOX metabolites (11- and 14-HpDPA$_{\omega-6}$) for 1 minute. As expected, platelets treated with 12-HETrE or forskolin, a direct activator of AC, showed enhanced S157 VASP phosphorylation. VASP phosphorylation was not enhanced in platelets treated with DPA$_{\omega-6}$ or its h12-LOX metabolites (Figure 3B), suggesting a G$_{\alpha s}$-coupled GPCR-independent mechanism of platelet inhibition.
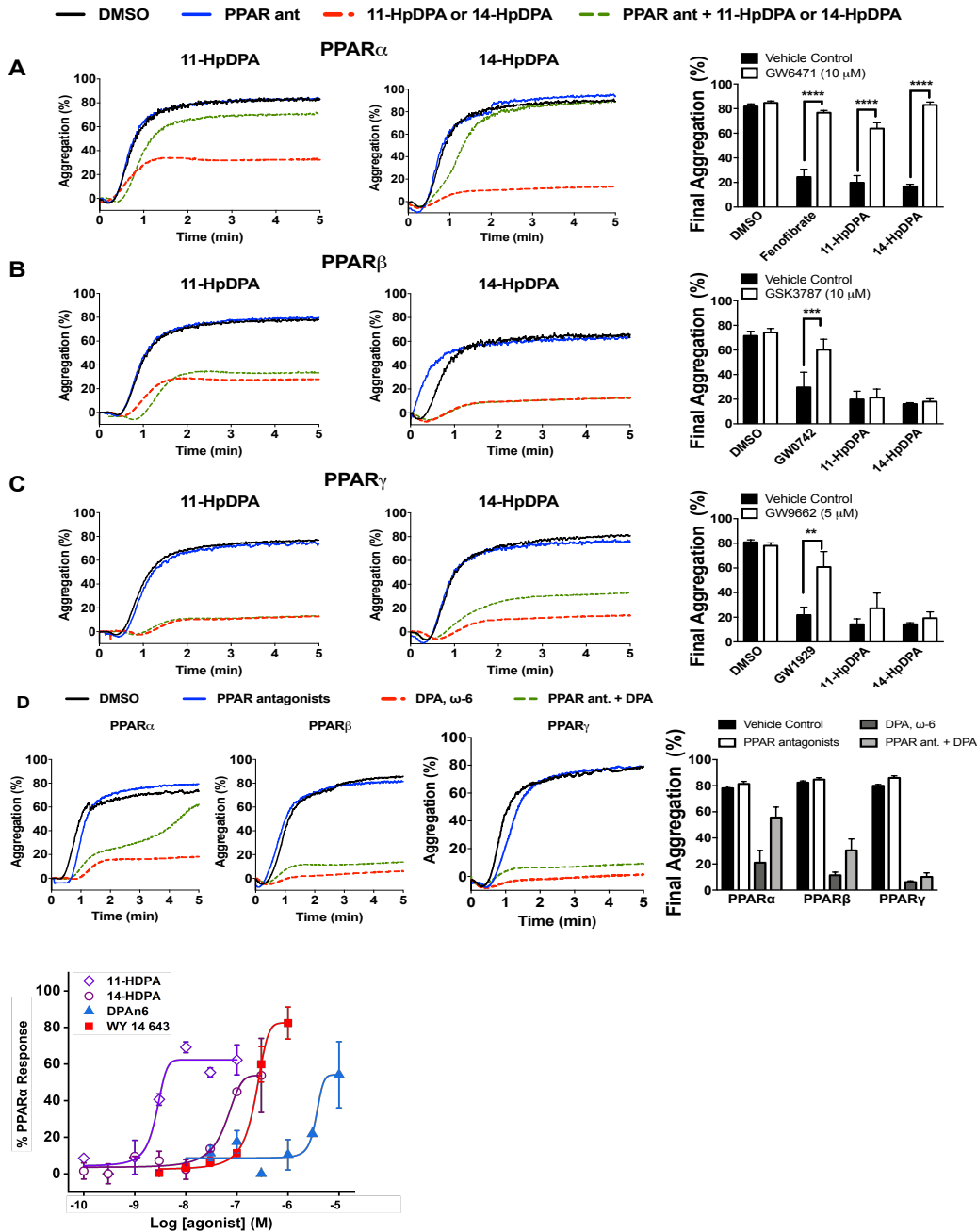
38

Figure 2.3- h12-LOX derived DPA$_{\omega\text{-}6}$, oxylipins 11- and 14-HpDPA$_{\omega\text{-}6}$, do not impinge on the Gas signaling pathway in platelets. Washed human platelets were treated with **A)** increasing concentrations of either 11-HpDPA$_{\omega\text{-}6}$ or 14-HpDPA$_{\omega\text{-}6}$, along with 10 μM DPA$_{\omega\text{-}6}$, and 1 μM of iloprost for 1 minute in the presence of 10 μM 3-isobutyl-1-methylxanthine (IBMX)   (n=2). **B)** Additionally, WASP S157 phosphorylation was not detected with the metabolites 11-HpDPA$_{\omega\text{-}6}$ or 14-HpDPA$_{\omega\text{-}6}$ confirming no cAMP increase.

h12-LOX-derived oxylipins of DPA modulate platelet activation through PPARA. While not being expressed on the surface of the platelet, Oxylipins have previously been shown to activate and intracellular receptor known as the peroxisome proliferator-activated receptor (PPARA), a subfamily of ligand-inducible transcription factors, following their diffusion through the plasma membrane (20-23). Since there is no nucleus in the platelet, PPAR activation would not be expected to

have any effect on platelet reactivity, however the reported nuclear-independent signaling effects of some of the members of the PPAR family in the platelet suggest that it is possible that DPA$_{\omega-6}$ oxylipins may regulate platelet reactivity in this manner(24, 25). Therefore, DPA$_{\omega-6}$ and its h12-LOX-derived oxylipins were assessed for their ability to directly activate PPARs in a non-genomic or transcriptional manner in platelets.

Mammals express three isoforms of PPAR, α, β/δ, and γ. To determine if DPA or its metabolites regulate platelet activation in a PPAR-dependent manner, selective antagonists for each PPAR isoform was tested to determine which PPAR isoform modulates platelet function in the presence of DPA and its metabolites (**Fig 2.4**). Washed human platelets were treated with or without the following antagonist, GW6471 for PPARα (**Fig 2.4A**), GSK3787 for PPARβ/δ (**Fig 2.4B**), or GW9662 for PPARγ (**Fig 2.4C**), prior to incubation with 11- or 14-HpDPA$_{\omega-6}$, or known PPAR agonists (Fenofibrate, GW0742, GW1929). Selective PPAR agonists, fenofibrate (PPARα), GW0742 (PPARβ/δ), and GW1929 (PPARγ) significantly inhibited collagen-stimulated platelet aggregation (**Figs 2.4A-C**) as previously reported (26-28); however, when pretreated with their respective PPAR antagonist, the PPAR agonists were unable to inhibit platelet aggregation. DPA and its h12-LOX metabolites (ranging from .5 to 1 μM that inhibited each donor's platelet at $\sim$ IC$_{20}$) (**Fig 2.4A-D**) were unable to inhibit collagen-mediated aggregation in platelets treated with fenofibrate. In contrast, platelets treated with GSK3787 or GW9662 were unable to rescue platelet aggregation inhibited by DPA, 11-, or 14-HpDPA$_{\omega-6}$.

To validate the PPARα antagonism observation in human platelets (**Fig 2.4A-D**), a cell-based PPAR transactivation reporter assay was conducted to determine the potency of PPARα binding to DPA and its h12-LOX metabolites in HEK293T cells transiently co-transfected with CMX-Gal4-PPARα, CMX-4-Gal4-β-galactosidase, and Tk-MH100x40luc (29, 30). 11- (EC_{50}=2.62 x 10^{-9} M) and 14-HpDPA (EC_{50}=5.58 x 10^{-8} M) dose dependently and potently induce PPARα activation (**Fig 2.4E**). As expected, WY 14 643, a known PPARα agonist, activated PPARα in HEK293T (EC_{50}=2.25 x 10^{-7} M). In contrast to 11- and 14-HpDPA$_{\omega-6}$ binding, DPA$_{\omega-6}$ did not exhibit a robust PPARα activation suggesting the fatty acid may partially regulate platelets in a PPARa-independent manner since DPA$_{\omega-6}$ activation of PPARα was observed at a significantly higher concentration (EC_{50}=3.55 x 10^{-6} M) than the metabolites or WY 14 643. Altogether, these data strongly implicate 11- and 14-HpDPA$_{\omega-6}$, derived from h12-LOX oxidation of DPA$_{\omega-6}$, modulate platelet function through their selective activation of PPARα in platelets at a nanomolar concentration range.

Figure 2.4- h12-LOX derived DPA, ω-6, oxylipins 11- and 14-HpDPA$_{ω-6}$, modulate platelet activation through PPAR . Washed human platelets were treated with **A)** 10 μM GW6471 (PPARα antagonist) (n=4), **B)** 10 μM GSK3787 (PPARb antagonist) (n=4), and **C)** 5 μM GW9962 (PPARg antagonist) (n=4) for 5 minutes prior to .5 to 1 μM incubation with 11- or 14-HpDPA$_{ω-6}$ and platelet aggregation stimulation with EC80 collagen. **D)** Similarly, platelets were treated with 1 to 2.5 μM of DPA$_{ω-6}$, in the presence of PPAR antagonists prior to collagen-induced aggregation (n=4). Representative of aggregation tracings for 11-, 14-HpDPA$_{ω-6}$, or DPA$_{ω-6}$ are shown on

the left. A cell-based PPAR transactivation reporter assay was performed in HEK293T cells that had been dose-dependently treated with DPA, 11- and 14-HpDPA$_{\omega-6}$, and PPARα agonist, WY 14643, for 8 hours prior to **E)** PPARα or **F)** PPARg luciferase assay.

To further assess the role of 11- and 14-HpDPA$_{\omega-6}$ as potential ligands for PPARα, platelets from PPARα deficient mice (PPARα$^{-/-}$), which were previously reported to be non-responsive to fenofibrate following collagen stimulation(26), were used for subsequent *ex vivo* and *in vivo* assays. Platelets from wild-type (WT) or PPARα$^{-/-}$ mice were treated with 0.5, 1, and 5 µM of DPA$_{\omega-6}$, 11-, or 14-HpDPA for 5 minutes prior to EC$_{80}$ collagen-induced aggregation. 0.5 and 1 µM of 11- and 14-HpDPA$_{\omega-6}$ failed to fully inhibit platelets from PPARα$^{-/-}$ mice in response to collagen compared to the WT mice treated with the same concentrations (Figure 5B,C); however, 5 µM of either metabolites fully inhibited platelet aggregation in platelets from both WT and PPARα$^{-/-}$ mice. There was also a difference in aggregation in response to DPA in platelets from WT and PPARα$^{-/-}$ mice in response to 0.5 µM of DPA as collagen-mediated platelet aggregation was not inhibited in platelets from PPARα$^{-/-}$ mice (**Fig 2.5A**). Altogether, the pharmacological and genetic inhibition and ablation as well as the cell-based assays demonstrate the selectivity of the 11- and 14-HpDPA$_{\omega-6}$ for PPARα activation over other isoforms of PPAR.

43
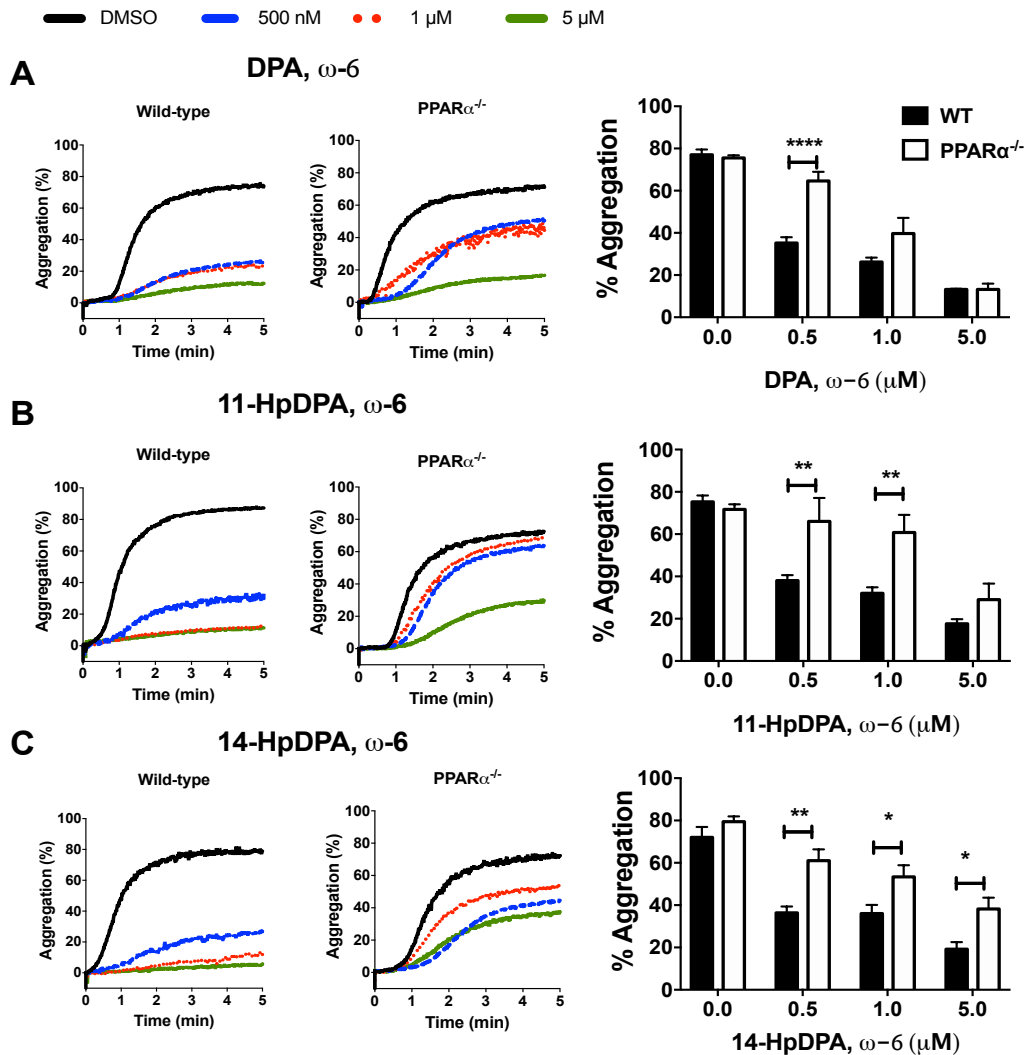
Figure 2.5- PPARα mediates the inhibitory effects of DPA metabolites on platelet aggregation. Washed platelets from wild-type and PPARα$^{-/-}$ were incubated with either **A)** DPA. 11-**B)** HpDPA$_{\omega-6}$, or **C)** 14-HpDPA$_{\omega-6}$, ranging from .5 to 5 μM, for 5 minutes prior to EC 80 collagen-induced aggregation.

h12-LOX derived oxylipins of DPA$_{\omega-6}$, 11- and 14-HpDPA$_{\omega-6}$, attenuates platelet adhesion under arterial shear condition. To determine whether the inhibitory effects of DPA$_{\omega-6}$ and its h12-LOX metabolites could be recapitulated in a more physiological setting, we assessed *ex vivo* platelet adhesion in whole blood under

arterial flow conditions in a collagen-coated microfluidic chamber. Sodium-citrated and recalcified whole blood was treated with varying concentrations of DPA$_{\omega-6}$, its h12-LOX metabolites, or an equivalent volume of DMSO for 5 minutes prior to perfusion over a collagen-coated surface at arterial shear rate (1800^{-1}S). DMSO treated platelets labeled with calcein-AM rapidly accumulated and adhered on the collagen-coated surface (**Fig 2.6A-C**). In contrast and consistent with ex vivo studies described in **Fig 2.5**, whole blood treated with DPA (**Fig 2.6A**) or its h12-LOX metabolites (**Fig 2.6 B-C**) exhibited significantly reduced platelet adherence.

45
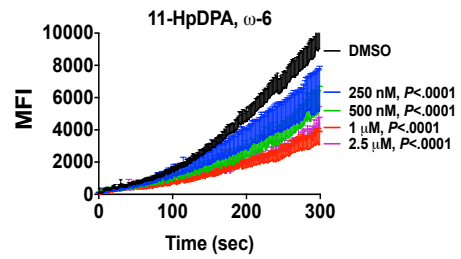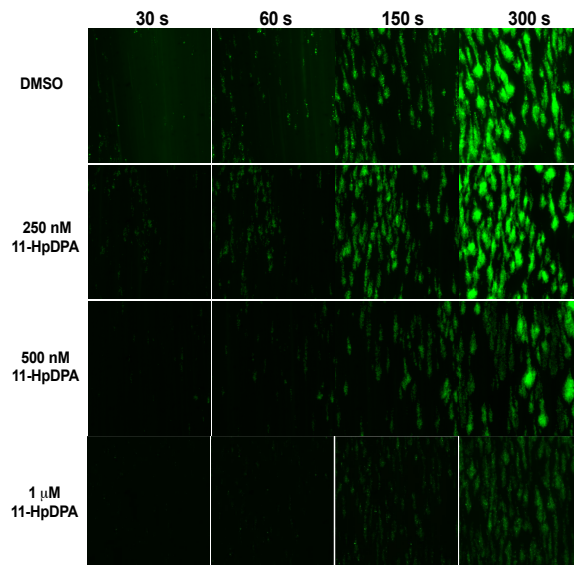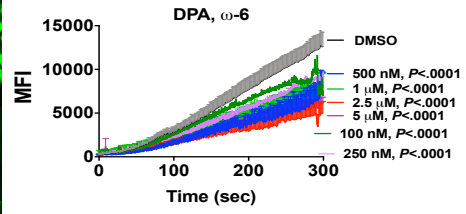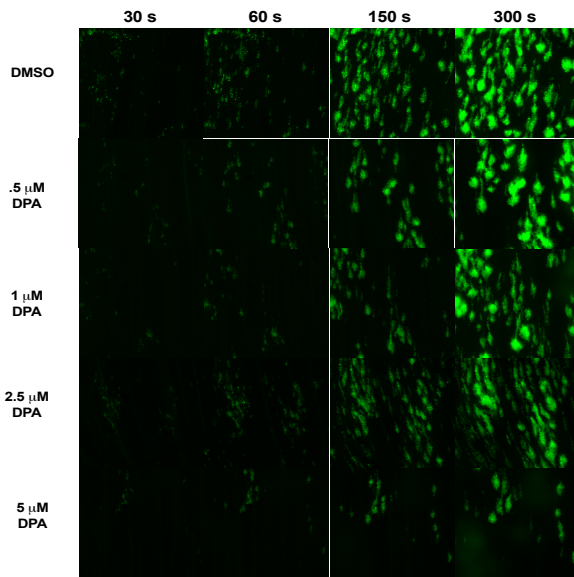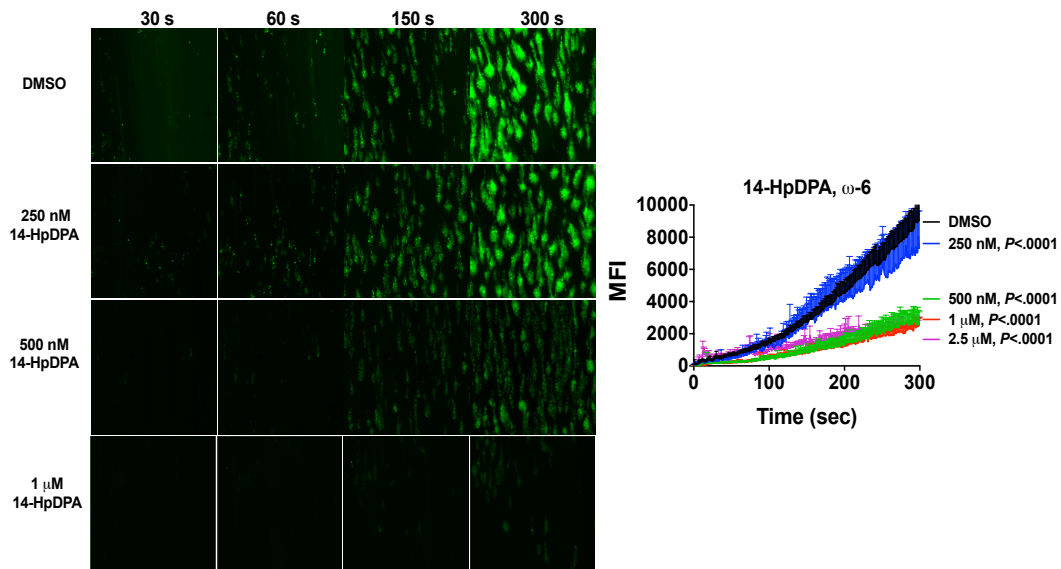
Figure 2.6. h12-LOX derived DPA$_{\omega-6}$, oxylipins 11- and 14-HpDPA$_{\omega-6}$, inhibit platelet accumulation on collagen-coated surface under arterial shear. Sodium-citrated whole blood were incubated with either DMSO, **A)** 100 nM to 5 µM of DPA$_{\omega-6}$, or 250 nM-2.5 µM (n=6) of **B)** 11- HpDPA$_{\omega-6}$ (n=5) or **C)** 14-HpDPA$_{\omega-6}$ (n=5) for 5 mins at 37C prior to perfusion over a collagen-coated surface at arterial shear rate (1800/s) for 5 minutes. Representative figures of each condition are shown on the left.

2.5 Conclusion

This study investigated a much-neglected polyunsaturated fatty acid, DPA omega-6, and its effects on platelets. In human platelets, h12-LOX was shown to generate more 14-HpDPA$_{\omega-6}$ than 11-HpDPA$_{\omega-6}$. Platelet aggregation in response to thrombin and collagen is potently inhibited by DPA$_{\omega-6}$ and its h12-LOX derived metabolites 14-HpDPA$_{\omega-6}$ and 11-HpDPA$_{\omega-6}$ around 250 nM. 14 and 11-HpDPA$_{\omega-6}$ inhibit thrombus formation in vitro and do not activate adenylate cyclase to generate cAMP. Finally platelet inhibition was shown to be mediated by 14 and 11-HpDPA$_{\omega-6}$ and to be dependent on PPARα activation. More mouse studies and even human vein

47

studies have also been investigated and will be reported later confirming the viability

of 14 and 11-HpDPA$_{\omega\text{-}6}$ as a novel anti-platelet.

*Unpublished as of now (Winter, 2019) But includes work by Michael Holinstat &

Jen Yeung.

References

[1]   CDC, NCHS. Underlying Cause of Death 1999-2013 on CDC WONDER Online Database, released 2015. Data are from the Multiple Cause of Death Files, 1999-2013, as compiled from data provided by the 57 vital statistics jurisdictions through the Vital Statistics Cooperative Program. Accessed Feb. 3, 2015.

[2]   Koupenova M, Kehrel BE, Corkrey HA, Freedman JE. Thrombosis and platelets: an update.Eur Heart J. 2017; *38*:785–791. doi: 10.1093/eurheartj/ehw550.

[3]   Grenon SM, Owens CD, Nosova EV, Hughes-Fulford M, Alley HF, Chong K, et al. Short-Term, High-Dose Fish Oil Supplementation Increases the Production of Omega-3 Fatty Acid-Derived Mediators in Patients With Peripheral Artery Disease (the OMEGA-PAD I Trial). *J Am Heart Assoc.* 2015;4(8):e002034.

[4]   Risk, Prevention Study Collaborative G, Roncaglioni MC, Tombesi M, Avanzini F, Barlera S, et al. n-3 fatty acids in patients with multiple cardiovascular risk factors. *N Engl J Med.* 2013;368(19):1800-8.

[5]   Mozaffarian D, Marchioli R, Macchia A, Silletta MG, Ferrazzi P, Gardner TJ, et al. Fish oil and postoperative atrial fibrillation: the Omega-3 Fatty Acids for Prevention of Post-operative Atrial Fibrillation (OPERA) randomized trial. *JAMA.* 2012;308(19):2001-11.

[6]   Mozaffarian D, and Wu JH. Omega-3 fatty acids and cardiovascular disease: effects on risk factors, molecular pathways, and clinical events. *J Am Coll Cardiol.* 2011;58(20):2047-67.

[7] Kromhout D, Giltay EJ, Geleijnse JM, and Alpha Omega Trial G. ω-3 fatty acids and cardiovascular events after myocardial infarction. *N Engl J Med.* 2010;363(21):2015-26.

[8] Ikei KN, Yeung J, Apopa PL, Ceja J, Vesci J, Holman TR, et al. Investigations of human platelet-type 12-lipoxygenase: role of lipoxygenase products in platelet activation. *J Lipid Res.* 2012;53(12):2546-59.

[9] Tourdot BE, Adili R, Isingizwe ZR, Ebrahem M, Freedman JC, Holman TR, et al. 12-HETrE inhibits platelet reactivity and thrombosis in part through the prostacyclin receptor. *Blood Adv.* 2017;1(15):1124-31.

[10] Yeung J, Tourdot BE, Adili R, Green AR, Freedman CJ, Fernandez-Perez P, et al. 12(S)-HETrE, a 12-lipoxygenase oxylipin of dihomo-gammalinolenic acid, inhibits thrombosis via Galphas signaling in platelets. *Arterioscler Thromb Vasc Biol* 2016;36:2068-77.

[11] Careaga MM, and Sprecher H. Synthesis of two hydroxy fatty acids from 7,10,13,16,19-docosapentaenoic acid by human platelets. *J Biol Chem.* 1984;259(23):14413-7.

[12] Milks MM, and Sprecher H. Metabolism of 4,7,10,13,16-docosapentaenoic acid by human platelet cyclooxygenase and lipoxygenase. *Biochim Biophys Acta.* 1985;835(1):29-35.

[13] Sprecher H, and Careaga MM. Metabolism of (ω-6) and (ω-3) polyunsaturated fatty acids by human platelets. *Prostaglandins Leukot Med.* 1986;23(2-3):129-34.

[14] Sprecher H. The metabolism of (ω-3) and (ω-6) fatty acids and their oxygenation by platelet cyclooxygenase and lipoxygenase. *Prog Lipid Res.* 1986;25(1-4):19-28.

[15] Akiba S, Murata T, Kitatani K, and Sato T. Involvement of lipoxygenase pathway in docosapentaenoic acid-induced inhibition of platelet aggregation. *Biol Pharm Bull.* 2000;23(11):1293-7.

[16] Yeung J, Tourdot BE, Adili R, Green AR, Freedman CJ, Fernandez-Perez P, et al. 12(S)-HETrE, a 12-Lipoxygenase Oxylipin of Dihomo-gamma-Linolenic Acid, Inhibits Thrombosis via Galphas Signaling in Platelets. *Arterioscler Thromb Vasc Biol.* 2016;36(10):2068-77.

[17] Nakamura MT, and Nara TY. Structure, function, and dietary regulation of delta6, delta5, and delta9 desaturases. *Annu Rev Nutr.* 2004;24:345-76.

[18]   Browning LM, Walker CG, Mander AP, West AL, Madden J, Gambell JM, et al. Incorporation of eicosapentaenoic and docosahexaenoic acids into lipid pools when given as supplements providing doses equivalent to typical intakes of oily fish. *Am J Clin Nutr.* 2012;96(4):748-58.

[19]   Balogun KA, Albert CJ, Ford DA, Brown RJ, and Cheema SK. Dietary omega-3 polyunsaturated fatty acids alter the fatty acid composition of hepatic and plasma bioactive lipids in C57BL/6 mice: a lipidomic approach. *PLoS One.* 2013;8(11):e82399.

[20]   Tourdot BE, Ahmed I, and Holinstat M. The emerging role of oxylipins in thrombosis and diabetes. *Front Pharmacol.* 2014;4:176.

[21]   Wahli W, and Michalik L. PPARs at the crossroads of lipid signaling and inflammation. *Trends Endocrinol Metab.* 2012;23(7):351-63.

[22]   Shearer GC, and Newman JW. Impact of circulating esterified eicosanoids and other oxylipins on endothelial function. *Curr Atheroscler Rep.* 2009;11(6):403-10.

[23]   Yeung J, Hawley M, and Holinstat M. The expansive role of oxylipins on platelet biology. *J Mol Med (Berl).* 2017;95(6):575-88.

[24]   Kliewer SA, Sundseth SS, Jones SA, Brown PJ, Wisely GB, Koble CS, et al. Fatty acids and eicosanoids regulate gene expression through direct interactions with peroxisome proliferator-activated receptors alpha and gamma. *Proc Natl Acad Sci U S A.* 1997;94(9):4318-23.

[25]   Forman BM, Tontonoz P, Chen J, Brun RP, Spiegelman BM, and Evans RM. 15-Deoxy-delta 12, 14-prostaglandin J2 is a ligand for the adipocyte determination factor PPAR gamma. *Cell.* 1995;83(5):803-12.

[26]   Ali FY, Armstrong PC, Dhanji AR, Tucker AT, Paul-Clark MJ, Mitchell JA, et al. Antiplatelet actions of statins and fibrates are mediated by PPARs. *Arterioscler Thromb Vasc Biol.* 2009;29(5):706-11.

[27]   Moraes LA, Spyridon M, Kaiser WJ, Jones CI, Sage T, Atherton RE, et al. Non-genomic effects of PPARgamma ligands: inhibition of GPVI-stimulated platelet activation. *J Thromb Haemost.* 2010;8(3):577-87.

[28]   Unsworth AJ, Flora GD, and Gibbins JM. Non-genomic effects of nuclear receptors: insights from the anucleate platelet. *Cardiovasc Res.* 2018;114(5):645-55.

[29]   Li H, Gomes PJ, and Chen JD. RAC3, a steroid/nuclear receptor-associated coactivator that is related to SRC-1 and TIF2. *Proc Natl Acad Sci U S A.* 1997;94(16):8479-84.

Chapter 3

HEART FAILURE BIOMARKER DISCOVERY

3.1 Abstract

Human serum samples were extracted and analyzed by LC/MS for oxylipin correlation to known biomarker for heart failure, Troponin T. Statistical analysis was performed in relation of oxylipins to inflammatory cytokines, calcium score, and other statistics gained from patient data. Oxylipins including 5-HETE, 12-HETE, 15-HETE, 14-HDHA, and 13-HODE were found to not correlate significantly with troponin T. This is possibly due to no temporal information, missing values due to limits of detection, or no ground truth for the target molecule, troponin T. This data possibly shows the variability in oxylipin markers due to diet and may not be a good indicator of heart failure probability. However, correlations were found between oxylipins of the same origin such as 14-HDHA and 12-HETE. This indicates that our analysis of oxylipins was precise and makes sense. These oxylipins could also be used together to correlate specific lipoxygenase activity to other disease.

3.2 Introduction

Heart failure (HF) is a major health problem in the world causing mortality and morbidity that is caused primarily from hypertension and ischemia. It is characterized as weakening of the heart from plaque build up or other stressors. HF leads to life threatening complications such as heart attacks and stroke. The lipid signaling underlying the physical symptoms is largely unknown. Some currently used

biomarkers are heart muscle deterioration proteins such as troponin T, oxidative molecules like oxidized low-density lipoproteins, and hormones such as norepinephrine and angiotensin II [37]. The current biomarkers result in many false positives and negatives, highlighting the need for more indicators that can be added together to insure proper diagnosis of future HF.HF has been shown to be related to lipoxygenase expression and PUFA metabolism with increased expression of h15-LOX-1 and its metabolites 15S-HETE in hypoxic heart tissue [36]. However, the exact role h15-LOX-1 is playing in HF is unknown. Specific lipid mediators produced by h15-LOX-1 could be key chemical signals relaying information about the heart damage or weakening. Identifying new pathological biomarkers supported by biochemical data could help increase the chance heart failure is caught before it is life-threatening. In this study, a large blood sampling was acquired from patients with troponin T levels and other clinical statistics. Using LC-MS/MS and ELISA, oxylipins and cytokines were quantified and statistically correlated, in hopes of a better biomarker enabling more personalized medicine to treat the and predict heart failure probability.

3.3 Methods and Materials

Human material Serum samples from a large cohort (1087 patients) of well-characterized individuals with troponin T levels were provided by the Hultén Lab (University of Götherburg, Sweden), as part of the 2015 pilot by The Swedish Cardio

Pulmonary BioImage Study (SCAPIS) (**Figure 3.1**). Serum was obtained from

patients at Sahlgrenska University Hospital, after ethical approval from the local

Ethical Committee at the University of Gothenburg. An informed consent was

obtained from each individual. Serum was snap frozen in liquid nitrogen and

preserved in -80º C until processed.
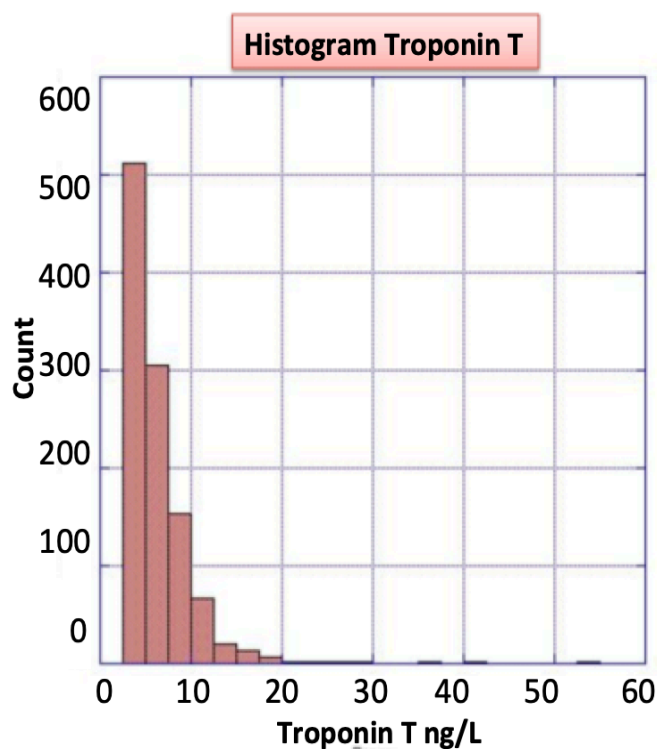
Figure 3.1- Histogram showing troponin levels for all 1087 patient serum samples.
Limit of detection 3 ng/L.

Standards: Deuterated oxylipins were purchased from Cayman Chemical (Ann

Arbor, MI) and used as quantitation standards for mass spectrometry. The following

compounds were included in the Internal Standard (IS) mixture: 12S-hydroxy-

5Z,8Z,10E,14Z-eicosatetraenoic-5,6,8,9,11,12,14,15-d8 acid (12(S)-HETE-d8); 9-

55

oxo-15S-hydroxy-prosta-5Z,8(12),13E-trien-1-oic-3,3,4,4-d4 acid (Prostaglandin B2-d4, PGB2-d4); 5S,12R-dihydroxy-6Z,8E,10E,14Z-eicosatetraenoic-6,7,14,15-d4 acid (Leukotriene B4-d4, LTB4-d4); (±)11,12-dihydroxy-5Z,11Z,14Z-eicosatrienoic-16,16,17,17,18,18,19,19,20,20,20-d11 acid ((±)11,12-DiHETrE-d_{11}); 9-oxo-11α,15S-dihydroxy-prosta-5Z,13E-dien-1-oic-3,3,4,4-d4 acid (Prostaglandin E2-d4, PGE2-d4); and 9α,11,15S-trihydroxy-thromba-5Z,13E-dien-1-oic-3,3,4,4-d4 acid (Thromboxane B2-d4, TxB2-d4). The mixture was designed to represent various classes of oxylipins that may be found in biological samples, to reflect the effects of solid phase extraction on their mass spectrometry response, and as quantitation standards for the non-deuterated analytes of the same class. 13S-hydroxy-9Z,11E-octadecadienoic-9,10,12,13-d4 acid (13(S)-HODE-d4) was used as Reconstitute Standard (RS), to account for changes in data acquisition conditions and instrument performance over time.

Biological sample preparation: Oasis HLB 30 mg SPE cartridges were purchased from Waters Co. (Milford, MA). LC-MS grade acetonitrile, methanol, ethyl acetate, formic acid, glyceroland glacial acetic acid were purchased from Fisher Scientific (Pittsburgh, PA). All other chemical reagents were purchase from Sigma (St. Louis, MO). Extraction was carried out using a 20-sample vacuum manifold, connected to an in-house vacuum line in a chemical fume hood. Prior to extraction, Waters Oasis HLB cartridges were washed with ethyl acetate (2 mL), methanol (2x 2 mL), and 95:5 v/v water/methanol with 0.1% acetic acid (2mL). Serum aliquots (170 μL) were then loaded onto the cartridges and spiked with 50 μL of the Internal Standard Solutions.

Cartridges were washed with 95:5 v/v water/methanol with 0.1% acetic acid (1.5 mL); the aqueous plug was pulled from the SPE cartridges with high vacuum, and SPE cartridges were further dried with low vacuum for about 20 minitues. SPE cartridges were eluted with 0.5 mL of methanol, followed by 2 mL of ethyl acetate into 7 mL glass scintillation vials containing 6 μL of 30% glycerol in MeOH as a trap solution. The volatile solvents were removed by evaporation under trap solution of 2 μL of glycerol remained. The residues were reconstituted in 50 μL of Reconstitute Standard in 0.1% Formic acid water and 50 μL of Acetonitrile. The samples were then mixed on a vortexer for 5 min, transferred to HPLC vials with low volume inserts, and analyzed on the same day.

LC-MS-MS analysis: The liquid chromatography system used for analysis was an ExionLC (Sciex, Framingham, MA). The autosampler was kept at 5 °C. Liquid chromatography was performed on a Synergi™ 4 μm Hydro-RP 80 Å, LC Column 150 x 2 mm purchased from Phenomenex (Torrance, CA). Chromatography method parameters were adapted from literature (Yang et al., 2009). Mobile phase A was water with 0.1% formic acid, mobile phase B was acetonitrile with 0.1% formic acid, purchased as premixed optima grade solvents from Fisher Scientific (Pittsburg, PA, USA). Gradient elution was performed at a flow rate of 400 μL/min for a total of 21 minutes run time. Injection volume was 90 μL. The gradient program is as follows:

| Time (mins)	Flow rate (mL)	Mobile hase A (%)	Mobile Phase B (%)
0.00	0.40	85	15
0.75	0.40	85	15
1.50	0.40	70	30
3.50	0.40	53	47
5.00	0.40	46	54
6.00	0.40	45	55
10.50	0.40	40	60
15.00	0.40	30	70
16.00	0.40	20	80
17.00	0.40	0	100
19.00	0.40	0	100
20.30	0.40	85	15
21.00	0.40	85	15

The column was connected to a Sciex X500B QTOF mass spectrometer equipped with an electrospray source and a quadrupole-time of flight (QTOF) mass analyzer. The instrument was operated in negative ionization and SWATH data acquisition mode. A mixed sample of IS and RS in acetonitrile at the same concentration was injected at the beginning of the sample sequence as reference standard for quantitation. Mass spec parameters were adapted from Yang et al (2009). Differences from Yang et al, were that ion sources gas 1 and 2 were set to 50 psi, CAD gas at 7 psi, and curtain gas was at 20 psi. Additionally, spray voltage was at -4500 V, DP at -60 V and CE at -15 V with a 5 V spread. Finally, TOF-MS and MS/MS start and stop masses were 50 Da to 800 Da.

Data Analysis: Identification of molecules was based on standard retention times and key diagnostic fragments. Analytes were measured using parent peak integration with baseline chromatographic separation. Quantification was performed by relating

analyte area to the area of a know amount of a deuterated internal standard with similar structure.

3.3 Results

Histogram of Oxylipins and Cytokines: Oxylipin and cytokine data was first examined for trends in the data through histogram plots (**Figure 3.2**). Data shows normal distribution of molecules with no statistical significance. 5-HETE shows a bimodal distribution, which could signify something of importance and should be treated as two separate data sets. Average ng/mL is reported showing 12-HETE and 13-HODE being the dominant oxylipins and INF-γ and IL-8 being the dominant cytokines found in the serum samples (**Figure 3.3**).
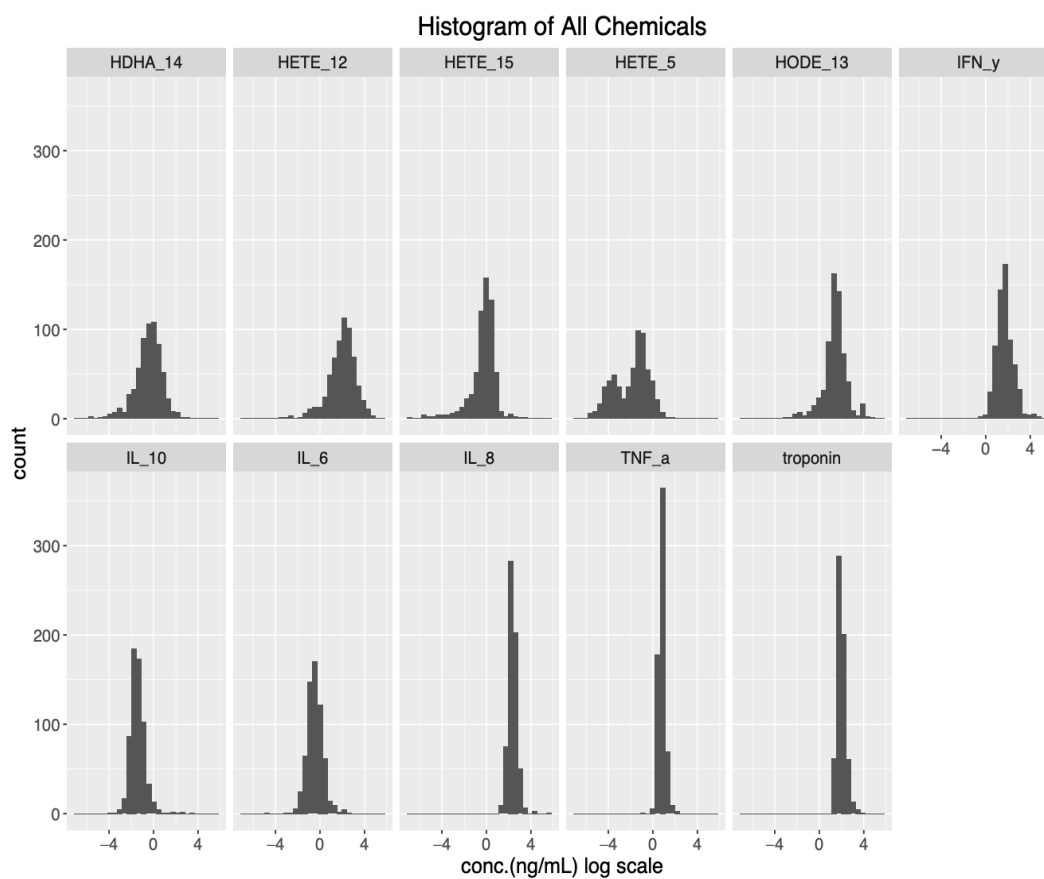
Figure 3.2- Histogram showing distribution of oxylipins and cytokines in patient serum samples.
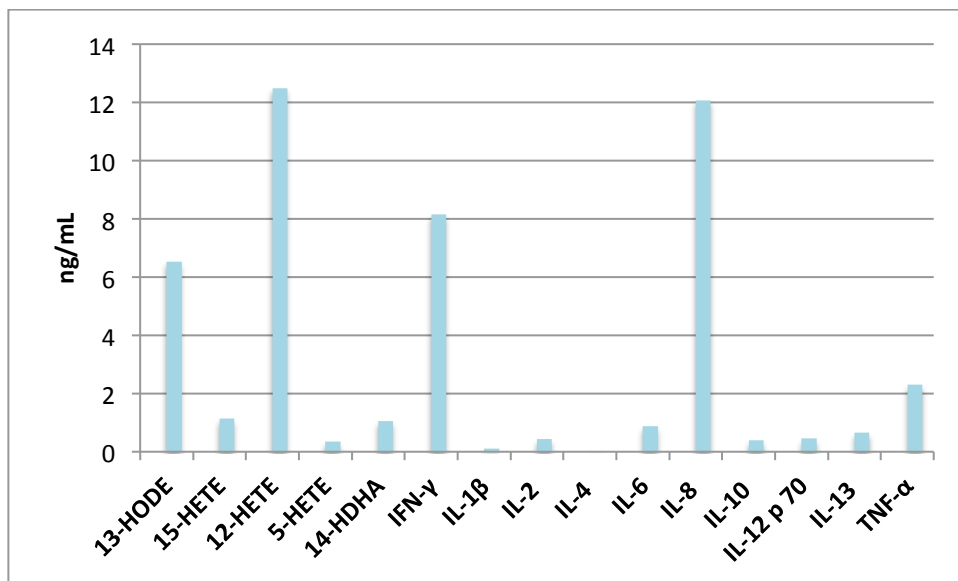
Figure 3.3- Average ng/mL of oxylipins and cytokines found in serum samples.

Relationships Among All Chemicals in Pairs Plots: Oxylipin and cytokine data was next related to each other and troponin T for possible correlations (**Figure 3.4**). Molecules show no statistically significant relationship to troponin T. However, molecules with known biological origin show strong correlations such as 12-HETE and 14-HDHA, both derived from the human 12-lipoxygenase pathway (**Figure 3.5**). Another molecule with strong correlation is 15-HETE and 13-HODE, both from 15-LOX-1. 15-LOX-1 can also catalyze 12-HETE and 15-HETE formation, which also correlate. One odd correlation is 5-HETE and 15-HETE, which could give some insight to biological specificity of 15-LOX-1 in vivo being different from in vitro.
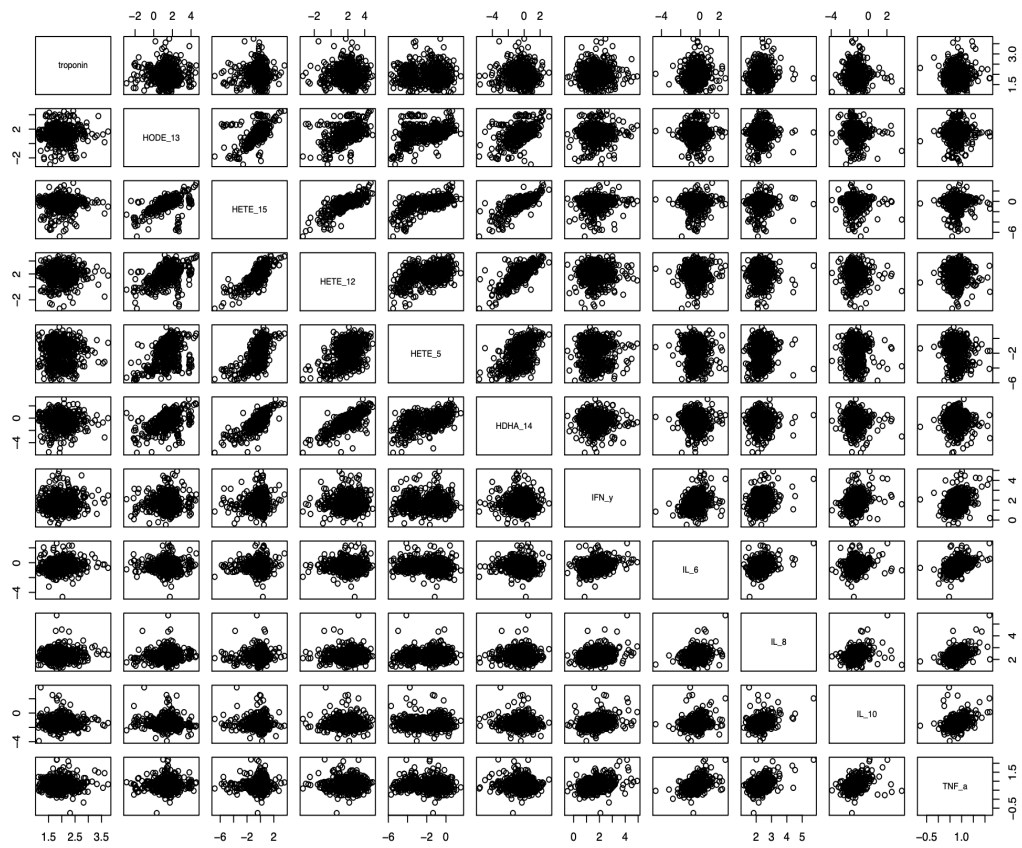
Figure 3.4- Pair plots showing correlation between oxylipins, cytokines, and troponin T within the selected population's serum.
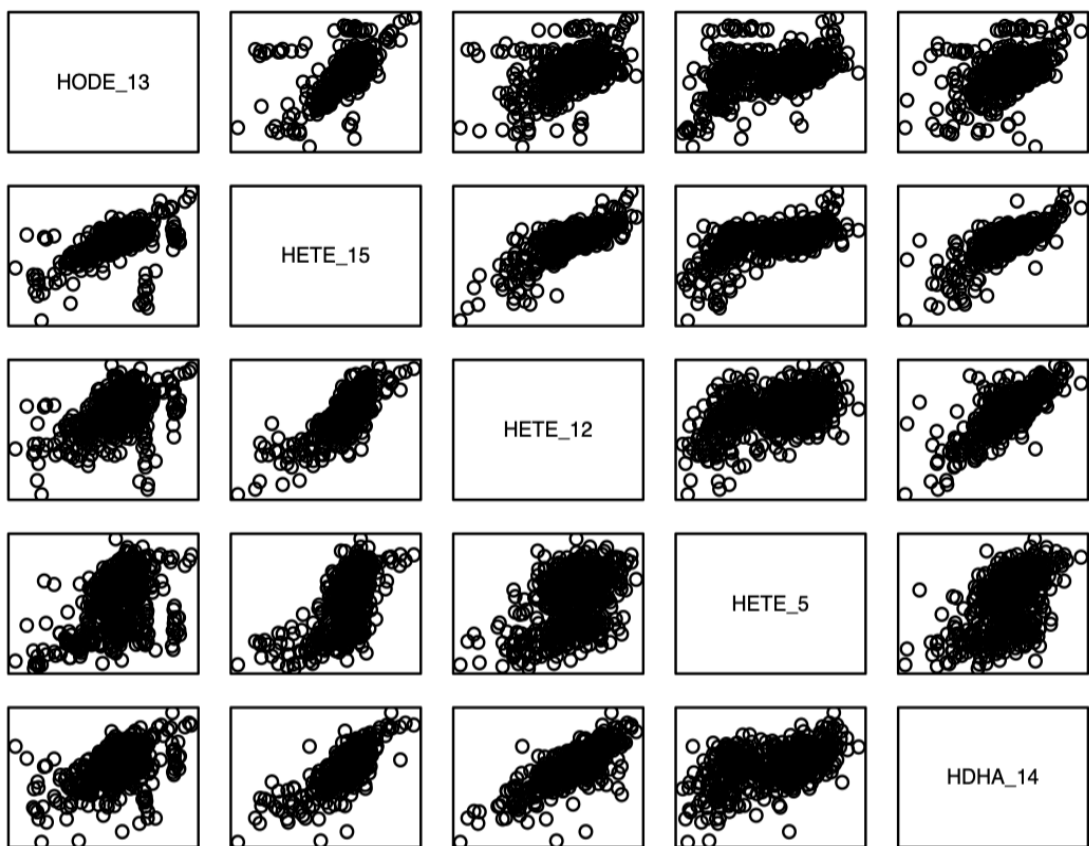
Figure 3.5- Close up of highly correlated oxylipins from pair plot that are derived from the same enzyme.

K-means clustering and visualization in PCA: A principal component analysis (PCA) was performed using K=2, which was used based on the best visualization (**Figure 3.6**). The goal was to attempt to separate original data into different meaningful groups to gain insight by analyzing each group separately. Both clusters are displayed as histogram plots in which no meaningful correlations were found for either cluster **(Figure 3.7).** Cluster 2 does contain high concentration for 12-HETE, 13-HODE, however, troponin levels were almost the same. A pair plot was made for both clusters showing no significant correlations for troponin T and molecules found in serum **(Figure 3.8)**.
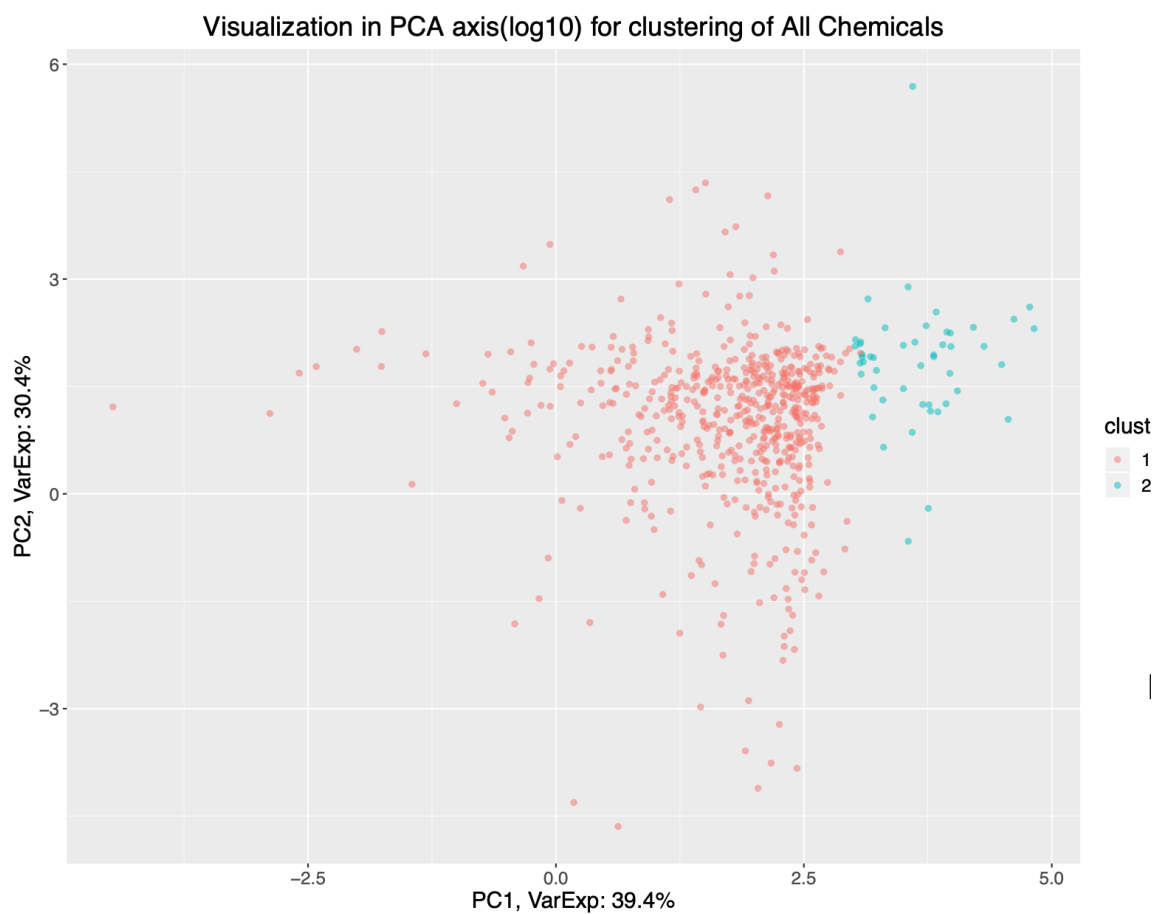
Figure 3.6- PCA plot- Using K=2 the above PCA plot was made which separated two groups of data into the two clusters.
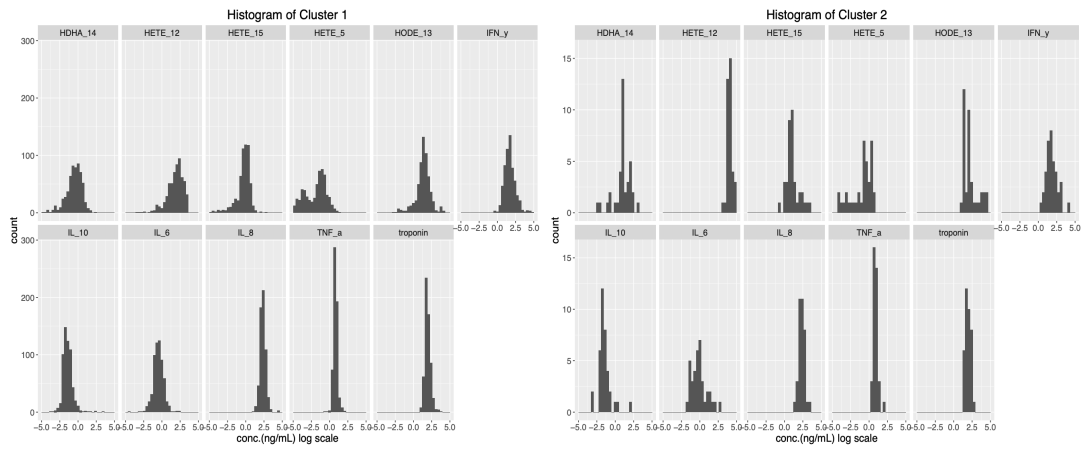
Figure 3.7- Histogram for each cluster.

(A)
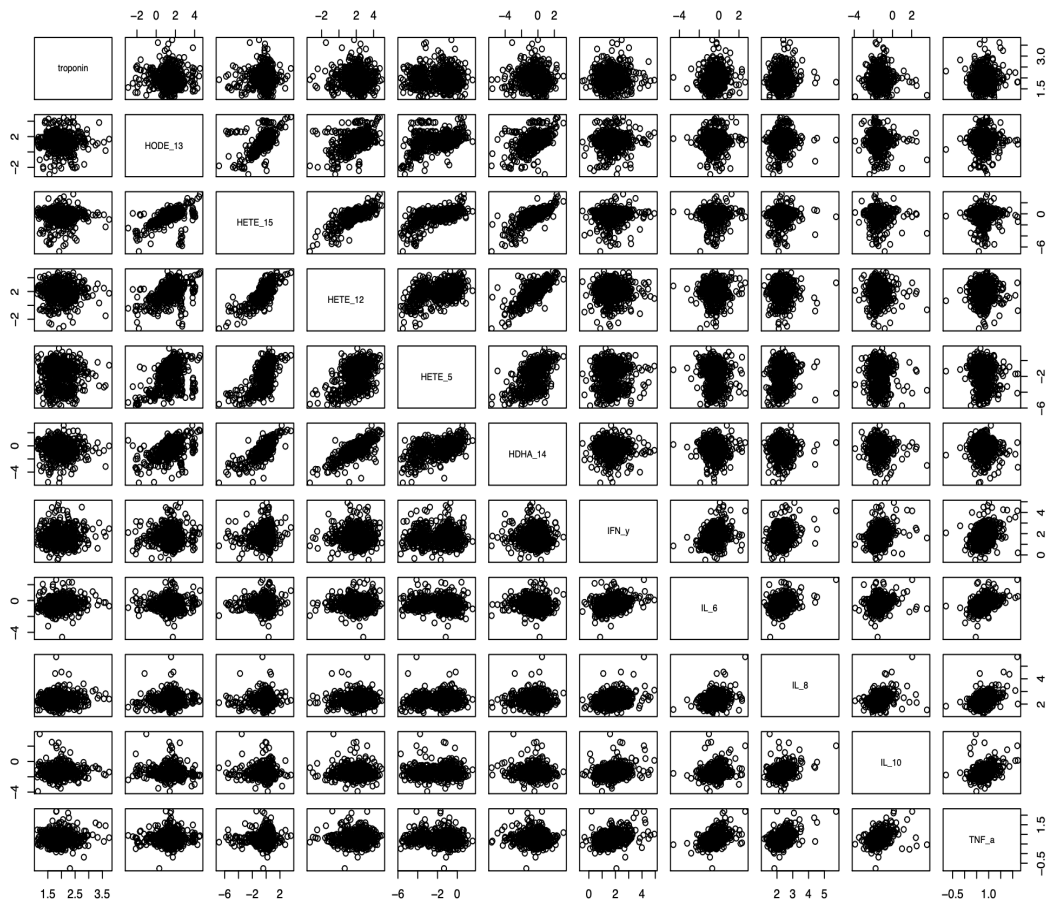
(B)
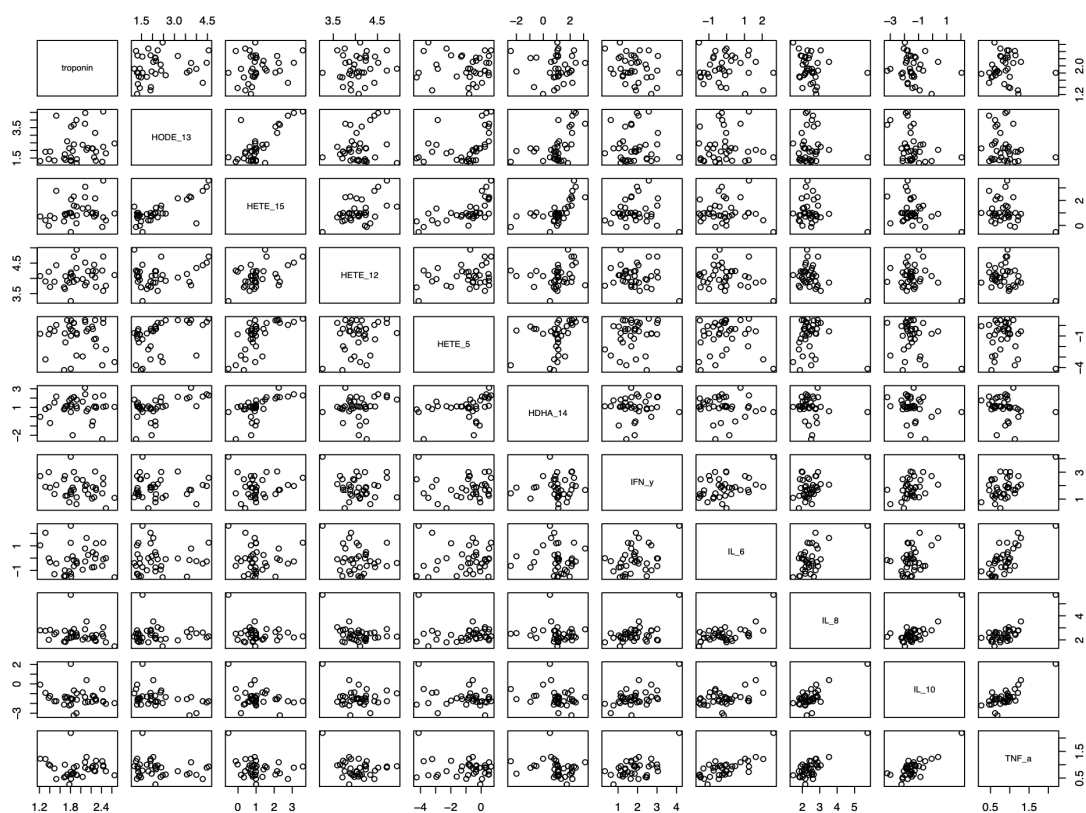
Figure 3.8- K-means pair plots for (A) cluster 1 and (B) cluster 2.

3.5 Discussion

In this study, a few results were found to be of some importance and requiring discussion. First, 12-HETE was found to be highly concentrated in the serum samples. This is likely due to high activation of 12-LOX in platelets during the blood clotting process in which serum is isolated. This could have implications in altering sample oxylipin data sets. Plasma is best used when analyzing oxylipins without known markers to correlate data to. Second, a normal gaussian distribution was found

for the analytes with no correlations to troponin T. This could be from no relation to oxylipins or cytokines due to variance in inflammation at the static time point of sample collection or not enough patients with known heart failure in the data set. Thirdly, oxylipins such as 12-HETE and 14-HDHA, correlate stongly together supporting the fact they have the same biological catalyst. This supports the validity of the data and could enable relation of the oxylipins to enzymatic activity. Finally, the PCA plots enabled a cluster of individuals to be found with high 12-HETE activity. This population will be used in the future to relate to other statistics acquired from the patients to see if any correlations are found to12-LOX activity.

3.6 Conclusion

No significant correlations were found for oxylipins and cytokines for troponin T in this study. Correlations were found for metabolites derived from the same lipoxygenase, which could help make sense or support future data and possibly allow *in vivo* lipoxygenase activity to be inferred through oxylipin correlations. This Future work will be relating these molecules to other statistics gathered from the study population.

*Unpublished as of now (Winter, 2019)

References

In Intro

Chapter 4

BIOCHEMICAL/CELLULAR CHARACTERIZATION AND INHIBITOR

DISCOVERY OF PSEUDOMONAS AERUGINOSA 15-LIPOXYGENASE

4.1 Abbreviations

AA, arachidonic acid; 5,12-DiHETE, 5,12-dihydroxy-6E,8E,10E,14Z-eicosatetraenoic acid; 5(S)-HETE, 5(S)-hydroxy-6E,8Z,11Z,14Z-eicosatetraenoic acid; 5(S)-HpETE, 5(S)-hydroperoxy-6E,8Z,11Z,14Z-eicosatetraenoic acid; 13(S)-HpODE, 13(S)-hydroperoxy-9Z,11E-octadecadienoic acid; k_{cat}, the rate constant for product release; k_{cat}/K_m, the rate constant for substrate capture; LOX, lipoxygenase; 5-LOX, human 5-lipoxygenase; h12-LOX, human platelet 12-lipoxygenase; 15-LOX-1, human reticulocyte 15-lipoxygenase-1; 15-LOX-2, human epithelial 15-lipoxygenase-2; soybean LOX-1, soybean lipoxygenase 1; LTA$_4$, leukotriene A$_4$; LTB$_4$, leukotriene B$_4$; LXA$_4$, lipoxin A$_4$; LXB$_4$, lipoxin B$_4$; PLAT, polycystin-1/lipoxygenase/alpha-toxin; PMNL, polymorphonuclear leukocyte; PUFA, polyunsaturated fatty acid; RvD1, resolvin D1; RvE1, resolvin E1; MEM, Minimal essential media; MOI, multiplicity of infection; CFU, colony forming units.

4.2 Abstract

Pseudomonas aeruginosa is an opportunistic pathogen which can causes nosocomial and chronic infections in immunocompromised patients. *P. aeruginosa* secretes a lipoxygenase, LoxA, but the biological role of this enzyme is currently unknown. LoxA has poor sequence similarity to both soybean LOX-1 (s15-LOX-1) and human

70

15-LOX-1, 37% and 39%, respectively and yet has comparably fast kinetics to s15-

LOX-1 ($k_{cat} = 181+/-6$ s^{-1} and $k_{cat}/K_M = 16+/-2$ mM^{-1}s^{-1} at pH 6.5). LoxA is capable

of efficiently catalyzing the peroxidation of a broad range of free fatty acid (FA)

substrates (e.g. AA and LA) with high positional specificity, indicating a 15-LOX.

Its mechanism is through a hydrogen-atom abstraction (kinetic isotope effect (KIE)

greater than 30) and yet LoxA is a poor catalyst against phosphoester-FAs, suggesting

that LoxA is not involved in membrane decomposition. LoxA also does not react with

5- or 15-HETEs, indicating poor involvement in lipoxin production. A LOX high-

throughput screen of the LOPAC library yielded a variety of low micromolar

inhibitors; however, none selectively targeted LoxA over the human LOX isozymes.

With respect to cellular activity, LoxA expression is increased when *P. aeruginosa*

transitions to a biofilm mode of growth, but LoxA is not required for biofilm growth

on abiotic surfaces. However, LoxA does appear to be required for biofilm growth in

association with the host airway epithelium, suggesting a role for LoxA in mediating

bacterial-host interactions during colonization.

4.3 Introduction

Pseudomonas aeruginosa (*P. aeruginosa*) is the second most prevalent cause of

nosocomial pneumonia infections and a major cause of morbidity and mortality

among cystic fibrosis (CF) patients.[1] Recent studies show that in (CF), the

71

opportunistic pathogen *P. aeruginosa* is a major contributor to respiratory failure; it is the predominant airway pathogen in ~50% of patients, and present in another ~30% of patients.[2–4] Compounding its pathogenicity, *P. aeruginosa* has high intrinsic antibiotic resistance in the planktonic state and infections are often refractory to treatment.[5] During chronic infections, as is the case for a majority of CF patients, *P. aeruginosa* forms biofilms that further increase resistance to the point that they are virtually impossible to clear with existing antibiotics.[6–8] Contributing to the pathology in the CF airway, chronic bacterial infection induces vigorous inflammatory responses in the airways dominated by polymorphonuclear neutrophils and the potent inflammatory mediators that they release when activated.[9–13] This combination of chronic infection and uncontrolled inflammation in the CF airway leads to progressive lung damage, and eventually bronchiectasis, creating an urgent need for the identification of new therapeutic targets to combat chronic *P. aeruginosa* infections.

P. aeruginosa produces and secretes a functional 15-lipoxygenase (15-LOX),[14] whose transcription is up-regulated more than 200-fold during biofilm formation.[15] In addition, *P. aeruginosa* has been shown to activate cytosolic phospholipase A2 during infection, increasing the available pool of cytosolic and extracellular arachidonic acid (AA).[16] These data, coupled with the finding that exogenous 15-LOX can initiate anti-inflammatory signaling, suggest a role for *P. aeruginosa* 15-lipoxygenase (LoxA) in modulation of host-bacterial interactions.[17] Indeed, *P. aeruginosa* is not the only pathogen shown to possess 15-LOX activity.

Toxoplasma gondii also expresses a 15-LOX enzyme that regulates host inflammatory processes during infection.[17] To investigate a potential role of LoxA in *P. aeruginosa* pathogenesis, further characterization of the effects of enzyme expression and function during the interaction of *P. aeruginosa* with the host during infection is needed.

The original characterization of LoxA verified the functionality of the enzyme and the localization to the periplasm and extracellular space, but did not delve into the kinetics or substrate specificity of the enzyme. In addition, the authors were unable to determine conditions that yielded significant native protein expression.[14] Since then, gene expression studies have found significant increases in mRNA levels of *loxA* expression when *P. aeruginosa* initiates biofilm formation.[15] Recombinant expression and purification have also been reported recently, allowing further kinetic characterization including temperature and pH activity profiles and product stereochemistry determination using the substrate linoleic acid (LA).[18] Herein, we performed a number of experiments to further characterize the enzyme activity, assess its reactivity with biologically relevant substrates, discover novel inhibitors, and investigate the role of LoxA in host colonization by *P. aeruginosa*.

4.4 Materials and Methods

Materials. Commercial fatty acids were purchased from Nu Chek Prep, Inc. (MN, USA). Fatty acids used for the secondary products study were made by reacting

73

arachidonic acid (AA) with human 5-LOX or soybean LOX15 to generate their respective HpETE or HETE products. Commercial fatty acids were further re-purified using a Higgins HAISIL column (5 μm, 250 X 10 mm) C-18 column. An isocratic elution of 85% A (99.9% methanol and 0.1% acetic acid): 15% B (99.9% water and 0.1% acetic acid) was used to purify the fatty acids. All HpETEs and HETEs generated for the secondary product study were purified using a Higgins HAISIL column (5 μm, 250 X 10 mm) C-18 column. An isocratic elution of 50% A (99.9% acetonitrile and 0.1% acetic acid): 50% B (99.9% water and 0.1% acetic acid) was used to purify the products. All fatty acids were tested for purity using LC-MS/MS and were found to have greater than 95% purity. Post purification, all fatty acids were stored at either -20 °C or -80 °C. Perdeuterated LA (d31-LA) (98% deuterated, Cambridge Isotope Laboratories) was purified as previously described.[19] All other chemicals were of high quality and were used without further purification.

Lipoxygenase (LOX) products were generated by reacting an individual substrate with LoxA in 500 mL of 25 mM HEPES (pH 7.0) with 50 μM substrate and run to completion. Reactions were quenched with 2.5 mL acetic acid, extracted three times with 30% volume of dichloromethane, evaporated to dryness, and reconstituted in methanol. The products were HPLC purified using an isocratic elution of 75% A (99.9% methanol and 0.1% acetic acid): 25% B (99.9% water and 0.1% acetic acid). The products were tested for their purity using LC-MS/MS and were found to have > 98 % purity. *P. aeruginosa* wild type (PAO1) and knockout (PW3111) strains were obtained from the *P. aeruginosa* Mutant Library at The University of Washington.[20]

Overexpression strain was a generous gift from Matthew Parsek. PA1169 (LoxA) and PA1168 were cloned as an operon with the native ribosomal binding site into the arabinose inducible vector pMJT-1. The resulting plasmid was transformed into PAO1 using 300 μg/mL carbenicillin for selection.

Recombinant Plasmid Construction. Several methods to insert *loxA* into an *E. coli* expression plasmid were tried. First a PCR fragment was generated using Taq polymerase and cleaved with Xho1 and Nco1. pET28-a was treated with the same enzymes, then treated with calf intestinal phosphatase. Ligation between pET28-a and *loxA* gene was unsuccessful. The *loxA* gene was then inserted into pCR-XL-TOPO using the TOPO cloning kit (Life Technologies). Correct insertion was confirmed by PCR. pET28-a was digested with NdeI and XhoI. Insertion of *loxA* gene from TOPO was attempted, but unsuccessful.

loxA with a His$_6$ tag was generated using Invitrogen Platinum PFX DNA Polymerase in combination with the following primers from a Custom Gateway PAO1 Clone set:

pLO151f: c acc gaa ttc atg AAT GAC TCG ATA TTC TTT TCA CCC

pLO151r: gcg ctc gag aag ctt tta tca GAT ATT GGT GCT CGC CGG GAT C

This PCR fragment was reacted with pet151d-TOPO to produce pet151/His$_6$-LoxA. The plasmid was then checked for orientation by restriction digest and the PCR fragment sequenced at the DNA Sequencing Facility of UC Berkeley to confirm the correct sequence and codon alignment.

Protein Expression and Purification. Purification of LoxA was carried out using the N-terminal His$_6$-tag construct described above, with the parent plasmid, pet151d-TOPO (Life Technologies). The His$_6$-LoxA protein was expressed using the pet151d-TOPO plasmid in *E. coli* BL21 (DE3). The host cells were grown to 0.6 OD at 37 ºC, induced by dropping the temperature to 20 ºC and grown overnight (16 hr). The cells were harvested in 2L fractions at a velocity of 5,000 x g, then snap frozen in liquid nitrogen. The cell pellets were re-suspended in buffer A (25 mM HEPES, pH 7.5, containing 150 mM NaCl), and lysed using sonication. The cellular lysate was centrifuged at 40,000 x g for 25 min, and the supernatant was loaded onto an NTA-Ni affinity column. The column was eluted with a gradient of 0-500 mM imidazole in buffer A. LoxA fractions were collected at approximately 200 mM imidazole and pooled together yielding greater than 90% purity. Protein samples were combined with glycerol to 10% (v/v) and then snap frozen under liquid nitrogen.

Protein and Metal Concentration. LoxA was subjected to amino acid analysis to determine protein concentration. Purified protein was concentrated using a Millipore polyethersulfone 30 kD cutoff membrane in an Amicon ultrafiltration cell and analyzed at Davis Molecular Structure Facility (UCD). The same protein sample was also subjected to Bradford assay and absorbance measurement at 280 nm, allowing for calculation of the extinction coefficient. Iron content of LoxA was determined using a Finnegan inductively coupled plasma mass spectrometer (ICP-MS). An internal Co^{3+} standard and external standardized Fe solutions were used for

quantitation. Enzyme concentrations were standardized to Fe content since only iron-loaded enzyme is active.

Recombinant LoxA Cleavage. pET151/D-TOPO vector based construct adds 35 amino acids between start site and beginning of the signal-peptide-cleaved native protein. A vector TEV site was used to remove 26 of those residues, including the N-terminal His_6 tag. Recombinant His_6-TEV enzyme was used as previously described.[21,22] Kinetic properties of cleaved LoxA were compared to un-cleaved enzyme to verify that additional residues do not affect enzyme properties. Metal analysis was performed with cleaved protein as described above.

Steady-State Kinetic pH Profile. Lipoxygenase rates were determined by following the formation of the conjugated diene product at 234 nm ($\varepsilon = 25000$ $M^{-1}cm^{-1}$). All reaction mixtures were 2 mL in volume and constantly stirred using a magnetic stir bar at room temperature (22 ºC), unless otherwise described. Assays were conducted in 25 mM HEPES buffer (pH 6.5, 7.0, 7.5) containing 0.01% TX-100 with substrate concentrations ranging from 1 to 60 μM and were initiated by the addition of enzyme, as described above. Substrate concentrations were quantitatively determined by allowing the enzymatic reaction to go to completion. Kinetic data were obtained by recording initial enzymatic rates at each substrate concentration and were then fitted to the Michaelis-Menten equation using KaleidaGraph (Synergy) to determine K_{cat} and K_{cat}/K_M values.

Steady-State Kinetic Temperature Profile. Initial rates of reaction were measured by the above methods. Temperature control of the reaction was achieved by using temperature-controlled cuvette holders. To account for temperature-induced pH differences in HEPES, buffers were equilibrated to temperatures from 22 to 45 °C and then the pH values were adjusted. Approximately 7 nM LoxA enzyme was added to initiate the reactions. Approximately 10 μM AA was used as substrate and the reactions were performed in 25 mM HEPES pH 7.0 (with no Triton X-100).

Substrate Preference. Substrate preference was determined by comparison of the initial reaction rate by monitoring product formation on a Perkin Elmer Lambda 40 spectrophotometer at 234 nm. Approximately 7 nM LoxA enzyme was added to initiate the reaction. All substrates were at 10 μM concentration and in 25 mM HEPES pH 7.0 (with no Triton X-100).

Product Profile. Products formed by LoxA were determined by reacting 10 μM substrate with LoxA to approximately 75% total turnover, monitored at 234 nm. Reactions were quenched with 1% glacial acetic acid and analyzed by LC-MS on a Thermo-Electron LTQ. Product separation was achieved by using a C18 HAIsil 250 × 4.6 mm analytical column (Higgins Analytical). Solution A was 99.9% acetonitrile and 0.1% acetic acid; solution B was 99.9% H_2O and 0.1% acetic acid. An isocratic gradient of 55% A and 45% B was used to purify products. The identification of

LoxA products was achieved by comparing MS/MS fragments with known standards at www.lipidmaps.org. In cases where MS/MS fragmentation standards were not available, products were identified by comparing fragment masses with predicted fragment masses with cleavage mediated by the hydroxy group near an unsaturated carbon.[23]

Product Stereochemistry. Determining the stereochemistry of the 15-HETE produced by LoxA was achieved by Mosher ester analysis.[24] The HPLC purified LOX product (evaporated in a glass vial) was reacted with 39 equivalents of anhydrous pyridine, 100 μL of anhydrous deuterated chloroform, and 16 equivalents of either (S)-(+)-alpha-methoxy-alpha-trifluoromethylphenylacetyl chloride or (R)-(–)-alpha-methoxy-alpha-trifluoromethylphenylacetyl chloride. Samples were diluted with deuterated chloroform to a final volume of 700 μL, transferred to a 5 mm NMR tube, and then both 1D proton and 2D COSY spectra were taken (Varian 600 MHz NMR). The unmodified LOX product was also analyzed in a similar manner for comparison, and the proton assignments determined. The differences in proton chemical shifts between R and S Mosher esterified products were tabulated. Subtracting the chemical shifts between S and R spectra yields a positive or negative value, which indicates the priority of each side of the alcohol in regards to the Cahn-Ingold-Prelog convention and thus allows the determination of the absolute configuration of the secondary alcohol.[25]

Phosphoester Substrate Activity. Affinity for phosphoester linked substrates was determined for several enzymes by comparing initial rate of phosphoester linked AA to free AA. Phosphatidylcholine with C18 in position 1 and AA in position 2 (PC-C18-AA) and Porcine Brain Phosphatidylserine (Avanti) were mixed in a 3:1 ratio and extruded into liposomes using an Avanti lipid extruder. Activity buffer consisted of 20 μM Tris pH 7.5 with 150 mM NaCl and 0.2 mM EDTA. $CaCl_2$ (4.0 mM) was added directly to the reaction mixture before enzyme addition when required. Total phospholipid concentration was approximately 20 μg/mL in activity buffer. AA reactions were performed at 10 μM substrate. Initial rates were measured as described above. Rates were normalized to enzyme concentration used in each trial.

Kinetic Isotope Effect. The noncompetitive kinetic isotope effect on the K_{cat} $^D(K_{cat}[LA])$ and K_{cat}/K_M $^D(K_{cat}/K_M[LA])$ values was determined by comparing the steady-state kinetic results of protonated linoleic acid with that of perdeuterated linoleic acid, as previously described.[26] Kinetic measurements were performed following product formation at 234 nm, in 25 mM HEPES buffer (pH 7.0). Reactions were initiated using 8 and 160 nM LoxA for protonated and perdeuterated linoleic acid, respectively, with substrate concentrations ranging from 1 to 60 μM. Kinetic parameters were determined as described in steady-state kinetic pH profile. Kinetic isotope effect was also determined competitively as previously described.[19]

Secondary Product Profile. LoxA products and secondary products were generated by reacting LoxA with 10 μM AA, 15-hydroperoxyeicosatetraenoic acid (15-HpETE), 5-hydroperoxyeicosatetraenoic acid (5-HpETE) as well as with their reduced hydroxyl derivatives; 15-HETE and 5-HETE. Each reaction was 2 mL in volume and carried out in 25 mM HEPES, pH 7.0 for 30 minutes using a magnetic stir bar. Once completed, the reactions were quenched with 200 μL acetic acid and extracted three times with 1 mL of dichloromethane (DCM). The DCM was evaporated to dryness under nitrogen, and reconstituted in 100 μL methanol containing a known concentration of 13-HODE as an internal MS standard. The products were analyzed using a Thermo Scientific Velos pro mass spectrometer with an Orbitrap attached, equipped with a Phenomenex Kinetex column (c1.7 μm C18, 100 A, 150 mm x 2.1 mm) using a flow rate of 350 μL/min. Solvent A was 99.9% acetonitrile with 0.1% formic acid and solvent B was 99.9% milli Q water with 0.1% formic acid. First a gradient was used from 40% A to 45% A over 19 minutes, followed by a step to 50% A. Then a gradient was used from 50% A to 75% A over another 19 minutes. Finally, MS retention times and fragmentations were matched with standards bought from Cayman Chemical and quantified using a standard curve of each AA product. The rates of product formation found using MS were compared to rates of product formation using UV absorbance. Rates determined by UV were done using a Perkin Elmer Lambda 45 spectrophotometer by monitoring the formation of the products at their respective wavelengths. All reactions were 2 mL in

volume and carried out in 25 mM HEPES buffer, pH 7.0 and continually stirred at room temperature. All substrate concentrations were 10 ± 1.0 µM.

Tryptophan Fluorescence Measurement. The fluorescence reduction resultant of product binding previously reported for soybean LOX-1 (s15-LOX-1) was checked with LoxA.[27] Fluorescence was measured continuously as 0.5 µM LoxA was added to 2 mL of 25 mM HEPE pH 7.5. 13-HpODE (20 µM) was added to induce fluorescence decrease. s15-LOX-1 was used as a positive control.

LoxA Inhibitor Selectivity against Human LOX Inhibitors. The one-point inhibition percentages were determined for human LOX inhibitors by following the formation of the conjugated diene product at 234 nm ($\varepsilon = 25000$ $M^{-1}cm^{-1}$) at 25 µM inhibitor concentration. All reactions were 2 mL in volume and constantly stirred using a magnetic stir bar at room temperature (22º C) with 7 nM LoxA. Reactions were carried out in 25 mM HEPES buffer (pH 7.0), 0.01% Triton X-100, and 10 µM AA. The concentration of AA was quantitatively determined by allowing the enzymatic reaction to go to completion. Confirmed hits were then screened against the human isozymes 5-LOX, 15-LOX-1, 15-LOX-2, and h12-LOX for specificity. IC_{50} values were determined by measuring percent inhibition at various inhibitor concentrations and fitted to a simple hyperbolic equation using KaleidaGraph (Synergy).

HTP LoxA Inhibitor Screen. The Library of Pharmacologically Active Compounds (LOPAC)[28] were also screened in qHTS format[29] for potential selective LoxA inhibitors using a Xylenol orange high throughput screening (HTS) assay previously developed by our lab. Compounds flagged as inhibitors in the HTS screen were retested in the manual cuvette assay against LoxA for potency.

Prior to screening, enzyme and substrate concentration, in addition to reaction time were optimized with regard to enzyme kinetics, quantity of reagents, and signal window.[30,31] Briefly, 3 μL of enzyme (approximately 20 nM LoxA, final concentration) or buffer (no-enzyme control) were dispensed into 1,536-well Greiner black clear-bottom assay plates using a BioRAPTR Flying Reagent Dispenser (Beckman Coulter, Fullerton, CA). Compounds and controls (broad spectrum LOX inhibitor, nordihydroguaiaretic acid (NDGA), concentration ranging from 3.4 mM to 0.208 μM) were transferred (23 nL or 46 nL) via Kalypsys PinTool, equipped with 1536-pin array, to yield final library compound concentrations ranging from 114 μM to 0.73 nM.[32] The plate was covered and incubated for 15 min at room temperature, followed by an addition of a 1 μL aliquot of substrate solution (40 μM arachidonic acid final concentration; $K_m = 10$ μM) to start the reaction, for a final assay volume of 4 μL. The reaction was stopped after 15 minutes (~90% conversion, data not shown) by the addition of 4 μL FeXO solution (final concentrations of 200 μM XO and 300 μM ferrous ammonium sulfate in 50 mM sulfuric acid). After a short spin (1000 rpm, 15 sec), the assay plate was incubated at room temperature for 30 minutes and the absorbances at 405 and 573 nm were collected using a ViewLux high throughput

CCD imager (Perkin-Elmer, Waltham, MA) using standard absorbance protocol settings. During dispense, enzyme and substrate bottles were kept on ice to minimize degradation. Percent inhibition was computed from the median values of the catalyzed, or neutral control, and the uncatalyzed, or 100% inhibited control, respectively, and plate-based data corrections were applied to filter out background noise.[33] Average Z' was 0.59 across six 1,536-well assay plates, with a signal to background of 1.8. The intraplate control compound NDGA performed extremely well, with an IC_{50} value of 23 μM and MSR[34] of 2.1. The screen and subsequent cheminformatics analysis yielded 94 potential hits, of which 22 compounds were selected using a cheminformatics analysis process previously described.[29] Compound were subsequently retested using the manual cuvette assay.

LoxA Antibody Purification. Polyclonal rabbit antibody was raised to purified recombinant LoxA protein by Pocono Rabbit Farm & Laboratory. Antibody was purified from whole blood by affinity for the purified recombinant LoxA protein, immobilized using a Pierce Aminolonk immobilization kit. Coupling and antibody purification was performed following manufacturers recommendation. Briefly, 3 mL of 2 mg/mL recombinant protein in pH 7.2 phosphate buffer was rocked in column overnight at 20º C. Reaction was quenched and column was washed and stored at 4 ºC. 4 mL rabbit serum was loaded on column and washed with 7 mL PBS, 1 mL 1 M NaCl, 7 mL PBS and eluted with 6 mL glycine. 1.5 mL fractions were collected and subjected to Bradford protein analysis. Eluted fractions with >0.05 mg/mL protein

were combined and 10% glycerol was added. Pooled AB aliquots were frozen in liquid nitrogen and stored at -80 ℃.

***P. aeruginosa* Mutant Strain Growth and LoxA Production Analysis.** LoxA production was determined using immunoprecipitation and western blot analysis. 50 mL liquid cultures of wild type (PAO1), *loxA*::Tn (*loxA* transposon mutant to disrupt *loxA* gene expression), *wspF* mutant (*wspF* gene deletion strain), *loxA* overexpression (both induced and non-induced) strains were grown overnight in Luria broth at 37 ℃, shaking at 225 rpm. To promote biofilm formation wild-type, *loxA*::Tn, and *wspF* mutant strains were also grown at minimal agitation (30 rpm) with a stir bar to facilitate biofilm adhesion. LoxA overexpression was induced by adding 0.5% arabinose 4 hr before harvesting. Cultures were pelleted at 10,000 x G, 4 ℃, resuspended in lysis buffer and sonicated. Cellular debris was removed by centrifuging at 15,000 x G. Immunoprecipitation was performed using Protein A beads (Santa Cruz Biotech) following manufacturer instructions. Briefly, Bradford assay was performed and 2 mg total cellular protein was combined with 20 μL bead slurry. After incubation, 2 μL of crude LoxA antibody sera was added. Beads were incubated and washed. PAGE was performed using Life Technologies NuPAGE 4-12% Bis-Tris gels with MOPS running buffer. A western blot was performed using purified LoxA polyclonal antibody as the primary and Sigma Aldrich goat anti-rabbit IgG HRP as the secondary. Bands were visualized using Pierce ECL western blotting substrate. Bands were detected and quantified using a BioRad ChemiDoc XRS

System. Loading control was performed to verify that Bradford normalization of immunoprecipitation samples was accurate. For this, a western blot was performed with normalized samples using Neoclone RpoA antibody as the primary and Sigma Aldrich goat anti mouse HRP antibody as the secondary. Analysis was performed as above.

Bacterial Cloning. To complement the *loxA* defect in the PW3111 transposon mutant, the *loxA* gene was fused to a constitutive promoter and inserted at a neutral site on the genome. The *nptII* promoter was used for constitutive expression and amplified from pMQ118[35] by PCR using forward primer 5'-GAGCTCCGCTGCCGCAAGCACTCAG-3' and reverse primer 5'-ACTAGTTCCTCATCCTGTCTCTTGATCAGATCTTG-3'. The P$_{nptII}$ fragment was inserted into pUC18-mini-Tn7T-Gm[36] by digestion with SacI and SpeI (NEB) followed by ligation with T4 DNA ligase (NEB) to create pUC18-mini-Tn7T-Gm-P$_{nptII}$. Ligations were transformed into *E. coli* DH5α and transformants were selected on LB agar containing 100 μg/mL ampicillin. The *loxA* gene was amplified from *P. aeruginosa* strain MPAO1 genomic DNA by PCR using forward primer 5'-CCCGGGATGAAACGCAGGAGTGTGCTCTTG-3' and reverse primer 5'-GGTACCTCAGATATTGGTGCTCGCCGG-3'. The *loxA* fragment was inserted into pUC18-mini-Tn7T-Gm-P$_{nptII}$ by digestion with XmaI and KpnI and ligation with T4 DNA ligase to create pUC18-mini-Tn7T-Gm-P$_{nptII}$-*loxA*. Ligations were transformed into *E. coli* DH5α and transformants were selected on LB agar

containing 100 μg/mL ampicillin. Correct construction of the pUC18-mini-Tn7T-Gm-P$_{nptII}$-*loxA* was confirmed by Sanger sequencing with forward primer 5'-GAACTTCAGAGCGCTTTTGAAGCTAATTC-3' and reverse primer 5'-GGGAACTGGGTGTAGCGTCGTAAGC-3'. The pUC18-mini-Tn7T-Gm-P$_{nptII}$-*loxA* plasmid was inserted at the *att*Tn7 site downstream of the *glmS* gene in the PW3111 transposon mutant strain by co-transformation with a pTNS3 helper plasmid constitutively producing the Tn7 transposase.[36] Colonies were isolated on LB agar plates containing 50 μg/mL gentamycin and 50 μg/mL tetracycline to ensure retention of the transposon as well as insertion of the complement plasmid. Insertion of the complement plasmid at the *att*Tn7 site was confirmed by PCR using forward primer 5'-CACAGCATAACTGGACTGATTTC-3' and reverse primer 5'-GCACATCGGCGACGTGCTCTC-3'.

Airway Epithelial Cell Culture. Airway epithelial cells were cultured as previously described.[37] In brief, the human bronchial epithelial cells (16HBE cell line) were seeded at 7.4x10^4 cells per 6.5 mm transwell filter (Corning), before polarization at air-liquid interface for seven days prior to the start of the biotic biofilm/attachment assay.

Biotic Biofilm/Attachment Assay. To examine *P. aeruginosa* biofilm growth in association with airway epithelial cells, we followed previously published methods.[37] Briefly, the airway epithelial cells were rinsed in minimal essential media (MEM) and

the washed bacteria were applied at an MOI between 25 and 30. After one hour, the apical media was removed and replaced with the MEM + 0.4% L-arginine, and the biofilms were allowed to grow for an additional five hours at 37 °C. At the end of the five hour incubation, the cells were washed once with MEM and biofilms were removed with 0.1% Triton-X 100 and serially diluted to determine the colony forming units (CFU). For the attachment assay, the wash steps and determination of colony forming units immediately followed the one-hour incubation on airway epithelial cells. For experiments with recombinant LoxA protein, 1ug protein was added directly to the apical surface of the epithelial cells in MEM media.

Abiotic Biofilm Assay. Microtiter abiotic biofilm assays were performed, as previously published.[38] Bacterial cultures were prepared as described above. The overnight cultures were then diluted 1:30 in minimal essential media and plated in a 96-well dish. The bacteria were grown for 24 hours without agitation at 37 °C. Following incubation, the liquid media was removed, and the biofilm were washed and stained with 41% crystal violet solution in water. Biofilm growth was quantified by reading absorbance in a plate reader at 550 nm.

4.5 Results and Discussion

Sequence Alignment. The sequence of *P. aeruginosa* LoxA was compared to s15-LOX-1 and human 5-LOX, h12-LOX, 15-LOX, and 15-LOX-2 using the

alignment program Clustal Omega, available at http://www.clustal.org/omega/.[39] Alignment statistics are shown in Table 1. Interestingly, the protein with greatest identity and similarity is 5-LOX. LoxA has an asparagine as the fifth coordination ligand (N540), similar to s15-LOX-1, h12-LOX and 5-LOX. However, the highest alignment score goes to 15-LOX-2. Pairwise alignment scores from Clustal Omega are calculated by taking the number of identities between the two sequences, divided by the length of the alignment, and presenting this number as a percentage. The alignment score (and similarity) for s15-LOX-1 is better than 15-LOX-1, but this does not take into account the large sequence gaps that appear in the human and *Pseudomonas* proteins when aligned with the significantly larger plant enzyme.

Protein Expression and Purification Yield. The construction of the LoxA plasmid was difficult to achieve by standard methods, therefore, Life Technologies Champion pET151 directional TOPO expression kit was used. The final recombinant construct of LoxA used in this study contains an N-terminal His_6 tag, followed by 29 residues from the TOPO expression vector that are not present in the wild type LoxA gene (Figure 1). This construct lacks the 19 amino acid predicted signal peptide region, which is present on the N-terminus of the bacterial enzyme, but presumably cleaved before the protein is excreted. The gene in the plasmid was successfully sequenced, however, there was difference from the reported sequence, with Gly 324 being replaced by Asp in our vector. We considered this a normal variant of the gene because the mutation was determined to be in the original Gateway PAO1 Clone set

by sequencing. In addition, it is not a conserved residue in an essential portion of the protein, so we did not change the residue.

Recombinant LoxA was expressed in *E. coli* on 4 L scale at 22 ºC and purified with Probond Ni resin, yielding 48 mg of >90% pure protein based on SDS PAGE gel (data not shown). Pure protein had an approximate molecular weight (MW) of 76 kD based on gel MW markers. The concentration of LoxA in a sample of pure protein was determined by amino acid analysis and used to establish an extinction coefficient of 169000 $M^{-1}cm^{-1}$ at 280 nm. Thus, 1.0 absorbance unit equates to 2.20 mg/mL of LoxA protein. ICPMS was performed and the purified recombinant LoxA was determined to be 67% metalated. This enzyme concentration was subsequently used to determine the K_{cat} and K_m of 15p-LOX. To verify that the additional 26 amino acids added by the expression vector has no effect on enzymatic activity, the enzyme was cleaved with TEV and kinetics were compared at pH 7.0 in the presence and absence of TX-100. Metal content was also compared by ICPMS using cleaved and uncleaved enzyme. No difference in activity or metal content were observed (data not shown).

Enzyme Kinetics, pH and Temperature Dependence. The kinetic parameters, K_{cat} and K_{cat}/K_m were determined as a function of pH using AA as the substrate (Table 2). The greatest kinetic efficiency was observed at pH 6.5. Activity decreased quickly below pH 6.5, as described previously by activity measurements in culture media.[14] This may be related to decreasing substrate solubility at low pH. The

enzymatic activity above pH 7.5 decreases rapidly to almost no observable turnover. Due to the low solubility of the substrate at pH 6.5, all subsequent kinetic measurements in this study were performed at pH 7.0 to balance enzyme activity with substrate solubility. Interestingly, this is shifted slightly from previous observations using KH_2PO_4 buffer and LA substrate.[18] In contrast, human LOX enzymes have maximal activity above pH 7.0, while s15-LOX-1 is most active at pH 9.0. The structural basis for the low pH preference of LoxA is as yet unclear. However, it is interesting to note that the pH of the extra-cellular fluid within the lung is close to pH 7, and becomes lower in patients with cystic fibrosis, where chronic *P. aeruginosa* infections are common.[40]

Kinetic rate measurements for selected 15-LOX isozymes are compared in Table 3. The enzymatic efficiency of LoxA at pH 6.5 far exceeds that of its human homologues,[41] and is similar to the soybean 15-LOX enzyme (s15-LOX-1).[42] The 5 endogenous ligands to the LoxA iron site consist of three histidines (His 353, His 358 and His 536), the C-terminal isoleucine carboxylate and Asn 540, similar to the coordination environments of 5-LOX, h12-LOX and s15-LOX-1. The presence of the asparagine at the 5th coordination site can help to rationalize the high kinetic rate of this enzyme, as the weak Asn ligand has been shown to increase kinetic efficiency by increasing the reduction potential of the iron, thus making the abstraction of the hydrogen more facile.[43]

The enzymatic activity of LoxA as a function of temperature was determined. Little variation was observed in the enzymatic activity over the range of 22 ºC to 35

°C, however, activity decreased significantly above 35 °C (data not shown). This data is in agreement with previous studies indicating an optimum temperature of 25 ºC,[44] and suggests that an *in vivo* activity for LoxA would be more likely in the nasal passages or the skin (with temperatures ranging from 25-33 ºC), as compared to infections of the lower respiratory tract.

Substrate Preference and Product Profile. The substrate preference and product profile differences of the human 15-LOX isozymes may be the basis of their distinct biological activities.[45,46] To investigate the ability of LoxA to produce biologically relevant LOX products, the enzyme activity with a range of possible LOX substrates was determined. Substrates were ranked by initial rate observed at 10 μM using UV absorbance detection (Table 4). Products produced from each substrate were determined by HPLC-MS/MS and shown ranked by percent of total product peak area. The LoxA reaction with AA produces predominantly 15-HETE as previously determined.[14] The most reactive substrates tend to produce predominantly a single product while slower substrates generally produce higher percentages of minor products. Dihomo-gamma-linolenic acid (DGLA) is a notable exception to this trend, with a low catalytic efficiency but only one observed product. Reaction with LA produces predominantly 13-HODE as previously established.[18] Similar to 15-LOX-2, LoxA prefers AA substrate over LA and does not produce significant 12-HETE product.[47] Interestingly, a recent study observed a reduction in 15-LOX-2 expression in cystic fibrosis (CF) patients, which was correlated with lower levels of

the inflammatory resolution mediator, lipoxin A$_4$.[48] Considering *P. aeruginosa* is an important cause of chronic infection for CF patients, the interplay between LoxA product generation and the unique conditions of the CF lung require further investigation.

Product Stereochemistry. To verify that LoxA products will have the same biological effects as those generated from the human 15-LOX enzymes, the stereochemistry of 15-HETE generated from the *P. aeruginosa* enzyme was determined. Mosher analysis was performed on 15-HETE generated from enzymatic reaction with LoxA, as previously described.[24,25] The change in chemical shift for each proton of the R-mosher reacted product can be subtracted from that of the *S*-mosher reacted product, and the resulting shift difference determines the stereochemistry of the original product (Figure 2). Chemical shift values indicate that the 15-(S)-HETE product is generated by LoxA, which is similar to human 15-LOX enzymes. This result is in agreement with the chiral HPLC experiment performed previously using 13-HPOD generated by LoxA.[18]

Phosphoester Substrate Activity. LoxA has been speculated to use phosphoester-linked substrate natively.[49] To test this hypothesis, the ability of LoxA to react with PC-AA was examined (Table 5). For comparison, the human enzymes 15-LOX-1, 15-LOX-2 and h12-LOX were also assayed. Enzymes were compared by normalizing max rate of PC-AA catalysis to the initial rate of AA turnover under

similar conditions. Thus, enzymes are ranked by activity with PC-AA as a percentage of that enzyme's AA rate. Reactions were run in the presence and absence of calcium as it has been shown to aid in membrane binding.[50] Of the enzymes tested, LoxA had the slowest relative rate under both calcium-added and no-calcium conditions. The ability of 15-LOX-1 to oxidize phosphoester-linked substrates is similar to that of LoxA in the absence of calcium, but significantly higher with calcium present. 15-LOX-2 is kinetically the slowest enzyme tested with AA, but its PC-AA is highest relative to its rate with AA. LoxA and 15-LOX-2 both show a small increase in PC-AA reaction rate when calcium is added. h12-LOX lies in between the human 15-LOX isozymes with respect to reaction rate with PC-AA but interestingly is the only enzyme whose peroxidating ability is unaffected by the addition of calcium. Although LoxA is faster than the human 15-LOX enzymes with free fatty acid substrates, the absolute rate of peroxidation of the phosphoester-linked substrate by the bacterial enzyme is comparable to human LOX rates. It should be noted that the pH of this assay (pH 7.5) is not optimal for LoxA, and thus its rate is not significantly greater than human 15-LOX-1. LoxA was also assayed at pH 7.0, but no significant difference in phospholipid peroxidating ability was observed.

Kinetic Isotope Effect. To verify that hydrogen atom abstraction is rate limiting, as it the case with other LOX enzymes,[19,26] the noncompetitive kinetic isotope effect (KIE) was determined for LoxA with LA. The KIE for K_{cat} was 32 +/- 6 and for K_{cat}/K_m the KIE is 450 +/- 70 (Table 6). High error in the K_{cat}/K_m KIE is

due to the large error in K_m, most likely due to the poor solubility of the substrate above 30 µM at pH 7. The competitive method for determination of the KIE was also attempted, however the magnitude of the KIE made detection of the deuterated product difficult via HPLC, adding to its error. The K_{cat}/K_m KIE from the competitive method was estimated at 120 +/- 70, consistent with the large K_{cat}/K_m KIE, seen with the noncompetitive method. The large KIE is consistent with other LOX isozymes and indicates that hydrogen abstraction proceeds through a tunneling mechanism and is a rate-limiting step in the reaction.[19]

Secondary Product Profile. LoxA secondary product profiling was performed to identify any products made by LoxA when reacted with different HpETE and HETEs. 15-HpETE, 15-HETE, 5-HpETE and 5-HETE were chosen as substrates due to their reaction products (5,15-diHpETE and 5,15-diHETE) being potential precursors to the formation of lipoxin (LXB_4). Rates of these reactions were compared to the rates with AA. The K_{cat} for LoxA with its preferred substrate AA was found to be 3.13 sec^{-1} (moles product/sec/moles enz). Relative to the K_{cat} with AA, LoxA reacted 10,000 times slower with 15-HpETE and 100,000 times slower with 15-HETE. The K_{cat} for 5-HpETE and 5-HETE was 100,000 times slower. (Table 7) The small production of 5,15-diHpETE and 5,15-diHETE was confirmed with mass spectrometry. The slow rate of formation of these diHpETE and diHETEs by LoxA brings into question the relevance of this reaction. However, it should be noted that in epithelial lung tissue, human 15-1 lipoxygenase is expressed at high levels[51,52]

and has been shown to convert these diHpETE and diHETE products into LXB4,[53,54] so LoxA could have a similar effect if expressed at high levels.

Tryptophan Fluorescence Measurement. s15-LOX-1 exhibits a unique fluorescence signal which can be quenched with addition of 13-HpODE.[27] To determine if LoxA also has this property, the fluorescence of LoxA was measured with the addition of an excess of 13-HpODE. No decrease in fluorescence was observed. The fluorescence change of s15-LOX-1 arises from decreases in tryptophan fluorescence due to tryptophan residue in the vicinity of the s15-LOX-1 active site. Only tryptophans 480, 618, 624 and 648 of s15-LOX-1 align with tryptophans in the LoxA sequence.

LOX Inhibitor Selectivity. In order to determine the feasibility of specific inhibition of LoxA in a biologically relevant context, the cross reactivity of several high potency, high specificity human lipoxygenase inhibitors for LoxA were assayed. IC_{50} values for these compounds against LoxA are shown in Figure 3. Inhibition of LoxA was determined via one point screen, as described previously.[55] The 15-LOX-1 active compound chosen was a recently reported highly specific, nanomolar potent 15-LOX-1 inhibitor.[56] The potency difference observed when assayed against LoxA was approximately 2000-fold. A selective 15-LOX-2 inhibitor was also assayed and showed the smallest difference in potency from its selective enzyme of all inhibitors tested.[57] However, this may be due to the relatively low potency of this inhibitor

96

compared to the selective inhibitors for other isozymes. The chosen h12-LOX compound was also a recently reported high specificity inhibitor.[58] This compound had no effect on LoxA. The 5-LOX specific inhibitor chosen showed a potency decrease of 100-fold. It is interesting that 5-LOX and 15-LOX-2 inhibitors have the smallest potency difference since they also have the highest degree of sequence similarity to LoxA based on alignment data. The nonspecific reductive inhibitor NDGA was also assayed, and exhibited an IC_{50} value comparable to the values obtained against the human enzymes.[59]

HTP LoxA Inhibitor Screen. To complement our search for LoxA-specific inhibitors, we screened the Library of Pharmacologically Active Compounds (LOPAC) using a high throughput screening assay developed earlier by our lab.[60] Nine of the top compounds that showed the largest inhibition in the screen were further investigated for selectivity to LoxA versus the other human isozymes using single-point screens (Table 8). To confirm their potency to LoxA, IC_{50} studies were performed (Table 9). The IC_{50} studies validated that these compounds were potent towards LoxA, with IC_{50} values ranging from ~4 to ~16 μM. The most potent compound NCGC00015424 had an IC_{50} value of 4.1 ± 1.4 μM with selectivity towards LoxA over h12-LOX and 15-LOX-2 and not the other human isozymes. The second and third potent compounds, NCGC00018102 and NCG00015802 had IC_{50} values of 4.5 ± 0.4 μM and 5.8 ± 1.4 μM respectively, with selectivity towards LoxA

97

over h12-LOX, 15-LOX-1, and 15-LOX-2. See tables 8 and 9 for IC_{50} values and selectivity data for the less potent compounds.

LoxA *in vivo* Production. To probe the production level of LoxA in *P. aeruginosa* during varying growth conditions, western blots were performed. Previous experiments showed that mRNA was increased during abiotic biofilm growth.[60] To test whether this corresponds to a significant protein abundance increase during biofilm growth, a western blot for LoxA was performed with *P. aeruginosa* cultures grown in planktonic and biofilm growth conditions (Figure 4). Under planktonic growth conditions, wild type PAO1 has no detectable production of LoxA. Using biofilm growth conditions, wild type bacteria displays a low level of detectable LoxA protein. Using a *wspF* deletion mutant strain, which forms biofilms more quickly and to a greater extent than wild type PAO1,[61] we observed a low level of LoxA production in planktonic culture, and dramatically increased protein abundance in biofilm conditions for the mutant (Figure 4). In agreement with previously published mRNA data, these data indicate that conditions that favor biofilm growth correspond to higher levels of LoxA production.

Since LoxA production was increased during biofilm growth, we next investigated if LoxA had a role in *P. aeruginosa* biofilm growth. To test this hypothesis, we first examined biofilm growth of wild-type *P. aeruginosa* and a *loxA* transposon mutant in a microtiter dish biofilm assay. We observed no change in biofilm growth of *P. aeruginosa* with the *loxA* mutant (Figure 5). Moreover, in an

abiotic setting of biofilm growth, addition of LoxA protein to complement the mutant or even addition to wild-type bacteria did not alter biofilm growth (Figure 5).

Due to the previously observed interactions of *P. aeruginosa* with host-derived lipids, we also examined if LoxA mediates *P. aeruginosa* biofilm growth in association with the host. To test this hypothesis, we used a unique model system where *P. aeruginosa* biofilms are cultured on the surface of airway epithelial cells, mimicking a colonizing infection in the host. Bacterial biofilms grown in the setting of the host airway epithelium quickly transition to a biofilm mode of growth, as measured by gene expression and acquisition of incredible antibiotic resistance.[62] Using this biotic biofilm model, we observed a decrease in bacterial biofilm growth with the *loxA* transposon mutant, as compared to wild-type *P. aeruginosa* (Figure 6A). This decrease could be complemented by expression *loxA* in the transposon mutant bacteria (Figure 6A) or by delivering recombinant LoxA protein (Figure 6B). We confirmed that the reduction in biotic biofilm growth in the *loxA* mutant bacteria was not due to altered attachment to the airway epithelial cells (Figure 6C). Taken together, these results suggest that LoxA is required for *P. aeruginosa* biofilm growth in association with host tissue, but not in an abiotic setting. Future studies to determine the mechanism by which LoxA alters lipid signaling to promote biofilm formation in the host are of great interest.

4.6 Conclusions.

The current experimental results indicate that LoxA is a highly active enzyme capable of efficiently catalyzing the peroxidation of a broad range of free fatty acid substrates with high positional specificity. Its mechanism is through a hydrogen-atom abstraction and yet LoxA is a poor catalyst against phosphoester-FAs and HETEs, suggesting that LoxA may not be involved in membrane decomposition or lipoxin signaling. In addition, production of LoxA is increased in biofilm growth, and while LoxA is not required for abiotic biofilm growth, it does appear to contribute to biofilm growth in association with host tissue. We are currently utilizing the newly discovered LoxA selective inhibitors to determine if inhibition of LoxA will impact *P. aeruginosa* biofilm growth on host cells, and ultimately serve as a novel therapeutic approach to combat chronic *P. aeruginosa* infections.

Table 4.1- Pairwise sequence alignment statistics for selected LOX enzymes with LoxA.

Protein	Mol Wt (kD)	Identity	Similarity	Gaps	Score
LoxA	74.81	--	--	--	--
s15-LOX-1	94.38	23.9%	37.3%	22.4%	20.00
5-LOX	78.00	27.1%	42.5%	8.5%	23.57
h12-LOX	75.71	23.5%	37.8%	7.8%	20.39
15-LOX	74.82	24.7%	39%	9.9%	19.36
15-LOX-2	75.87	26.2%	40.8%	6.4%	24.77

Table 4.2- Kinetic parameters for LoxA, determined at multiple pH values.

pH	K_{cat} (s^{-1})	K_m (μM)	K_{cat}/K_m $(\mu M^{-1} s^{-1})$
6.5	181(6)	12(1)	16(2)
7.0	157(5)	12(1)	13(1)
7.5	86(2)	13(1)	6.6(0.6)

Table 4.3- Kinetic parameters for LoxA at pH of maximal activity compared to selected 15-LOX enzymes at their maximal activities. Kinetic parameters for s15-LOX-1,[63] 15-LOX-1[41] and 15-LOX-2[41] were published previously.

Enzyme	K_{cat} (s⁻¹)	K_{cat}/K_m ($\mu M^{-1} s^{-1}$)
LoxA	181 (6)	16 (2)
s15-LOX-1	287 (5)	19 (1)
15-LOX-1	5.3 (0.4)	2.0 (0.2)
15-LOX-2	0.74 (0.03)	0.1 (0.01)

Table 4.4- LoxA substrates ordered by maximum turnover rate as a percentage of the fastest substrate (AA). Products made by each substrate were determined with approximate percentage of total product shown. N/D: not determined

Substrate	% AA Rate (10 μM)	Product	Approximate % of total
AA	100	15-HETE	94
		9-HETE	6
		11-HETE	<1
ALA	78(10)	13-HOTrE	91
		N/D	9
LA	72(10)	13-HODE	93
		9-HODE	4
DHA	72(10)	17-HDoHE	93
		4-HDoHE	7
		20-HDoHE	<1
EPA	61(10)	15-HEPE	78
		18-HEPE	14
		11-HEPE	8
DGLA	44(10)	15-HETrE	100
GLA	44(10)	13-HOTrE(ϒ)	78
		N/D	20
		N/D	2
EDA	33(10)	15-HEDE	70
		11-HEDE	30

Table 4.5- Comparison of peroxidating ability of LoxA to selected human LOX enzymes with phosphoester linked substrate, in the presence and absence of calcium.

Enzyme	AA Act/ μg	PC-AA Act/ μg	%PC-AA/AA Ratio - Ca	PC-AA +Ca Act/ μg	%PC-AA/AA Ratio + Ca
15-LOX-1	25	0.08	0.31	0.51	2.1
15-LOX-2	0.86	0.03	4.1	0.05	6.3
h12-LOX	2.5	0.02	0.97	0.02	0.96
LoxA	40	0.09	0.22	0.14	0.35

Table 4.6- Comparison of kinetic parameters for LoxA with LA and perdeuterated LA to determine the KIE.

Substrate	K_{cat} (s^{-1})	K_m (μM^{-1})	K_{cat}/K_m (μM^{-1} s^{-1})
LA	28 (2)	7 (2)	3.8 (0.9)
d31-LA	0.9 (0.1)	100 (24)	0.009 (0.002)
KIE	32 (6)		450 (70)
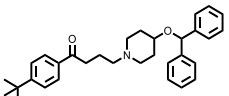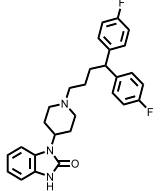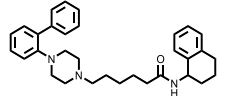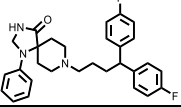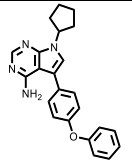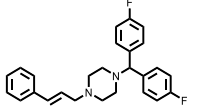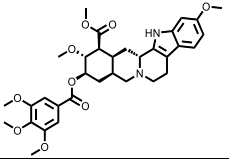
Table 4.7- K_{cat} comparison of secondary products relative to AA. The relative K_{cat} of LoxA with A.A is set to 1. All other K_{cat} values are standardized to this value and are unitless.

Substrate	Relative K_{cat}
AA	1
15-HpETE	$1e^{-4}$
15-HETE	$1e^{-5}$
5-HpETE	$1e^{-5}$
5-HETE	$1e^{-5}$

Table 4.8- LoxA single-point screen inhibition percentages. Compounds are listed relative to their percent potency towards LoxA, with the most potent listed first. Each reaction contained 10 µM of A.A. and 25 mM inhibitor.

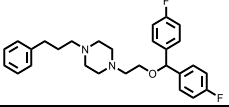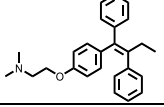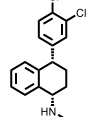| Inhibitor	LoxA	15-LOX-1	h12-LOX	5-LOX	15-LOX-2
NCGC00164603	95%	76%	33%	23%	0%
NCGC00015802	90%	69%	50%	80%	16%
NCGC00186032	87%	57%	36%	78%	5%
NCGC00015424	87%	76%	63%	74%	21%
NCGC00015280	86%	51%	38%	42%	0%
NCGC00018102	86%	65%	25%	96%	0%
NCGC00015300	83%	65%	48%	41%	13%
NCGC00024928	82%	73%	39%	79%	8%
NCGC00092386	76%	51%	26%	83%	5%
NCGC00091250	69%	57%	23%	37%	5%

Table 4.9- LoxA IC$_{50}$ inhibitor values. Compounds are listed relative to their potency towards LoxA, with the most potent listed first.

	Inhibitor	IC$_{50}$ (µM)
	NCGC00164603	10.1 ± 3.3
	NCGC00015802	5.8 ± 1.4
	NCGC00186032	11.4 ± 1.9
	NCGC00015424	4.1 ±1.4
	NCGC00015280	16.2 ± 3.1
	NCGC00018102	4.5 ± 0.4
	NCGC00015300	8.0 ± 1.2
	NCGC00024928	6.7 ± 1.4
	NCGC00092386	13.1 ± 1.7
	NCGC00091250	13.8 ± 4.2

Figure 4.1- Signal peptide and vector added sequences of wild type and recombinant LoxA protein
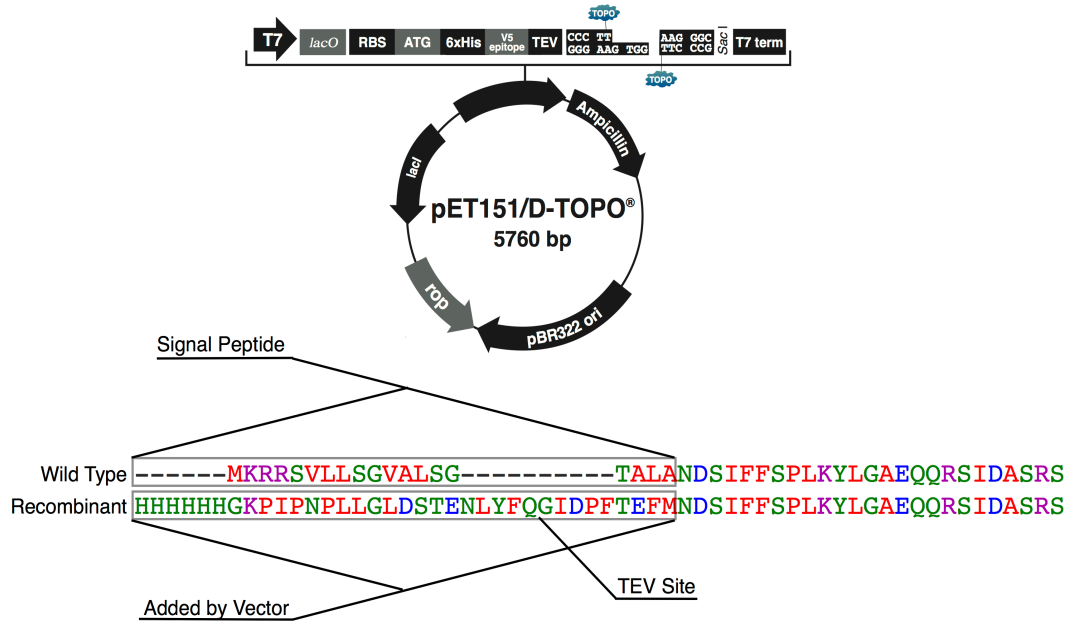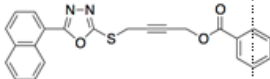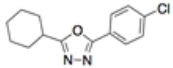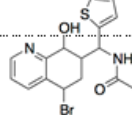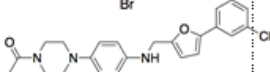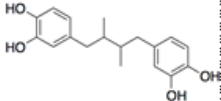
Figure 4.2- Chemical shift values of carbon atoms in 15-HETE, generated by LoxA. Splitting: s; singlet, d; doublet, t; triplet, qa; quartet, qi; quintet, m; multiplet, dd; doublet of doublets. unc: exact position unclear

Label	15-HETE		R-Mosher		S-Mosher		u (S-R)
a	0.89	t	0.81	t	0.84	s	0.038
b	1.30	m	1.19	m	1.26	m	0.063
c	1.55	m	1.58	m	1.62	m	0.047
d	4.27	p	5.51	qa	unc	--	--
e	5.71	dd	5.61	dd	5.50	m	-0.107
f	6.61	dd	6.61	dd	6.53	t	-0.073
g	5.99	m	5.95	t	5.91	t	-0.037
h	5.40	m	5.44	qa	5.41	m	-0.033
i	2.99	m	2.91	t	2.87	t	-0.033
j	5.40	m	5.32	m	5.32	m	-0.002
k	5.40	m	unc	--	unc	--	--
l	2.83	s	2.76	t	2.77	t	0.007
m	5.40	m	unc	--	unc	--	--
n	5.40	m	5.32	m	5.33	m	0.008
o	2.14	m	2.11	qa	2.11	qa	0.003
p	1.69	m	1.70	m	1.71	m	0.008
q	2.34	s	2.42	t	2.43	t	0.004

Figure 4.3- Various specific human LOX inhibitors were assayed against LoxA to determine their potency. Potency difference was calculated using estimated IC_{50} for LoxA divided by previously published IC_{50} for human isozyme.[56–58,64]

Compound	Specificity	Structure	IC_{50} (μM) [± SD (μM)]	% I at 25 μM for LoxA	~IC_{50} (μM) for LoxA	Fold difference In IC_{50}
24	15-LOX-1		0.01 [0.01]	34	20.	2000
MLS000545091	15-LOX-2		2.6[0.4]	11	78	30
5	12-LOX		1.0 [0.2]	1	>100	>100
13	5-LOX		0.52 [0.07]	18	46	100
N/A	N/A (redox)		0.1-10	79	11 [1]	--

Figure 4.4- Western blot for LoxA showing LOX expression in various strains under planktonic and biofilm growth conditions. Strains: WS, WspF knockout of PAO1; WT, PAO1; KO, *loxA* transposon knockout of PAO1; OV, PAO1 carrying pBadLOX, PA1168 and PA1169 overexpression vector; OI, Same as OV, induced with 0.5% arabinose; PP, Purified recombinant LoxA, 100 ng.

Figure 4.5- Abiotic biofilm assay showing P. aeruginosa biofilm growth for *loxA* mutant and reconstitution with recombinant LoxA protein. Using a microtiter biofilm assay, biofilm growth was compared for wild-type PAO1 *P. aeruginosa*, *loxA*::Tn in PAO1, PAO1 + 1μg LoxA protein and *loxA*::Tn + 1 μg LoxA protein to complement. Biofilm growth was normalized to wild-type PAO1 biofilm growth. All experiments were performed at least three times.
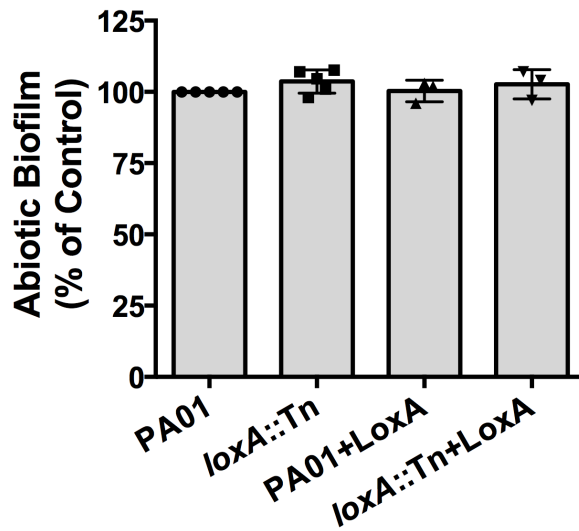
Figure 4.6- Biotic biofilm assays for loxA mutant *P. aeruginosa*. A) P. *aeruginosa* biofilm growth on human airway epithelial cells was compared for wild-type PAO1, *loxA*::Tn mutant and *loxA*::LoxA complemented strains. Bacterial biofilm growth was quantified by enumerating colony-forming units (CFU/ml). Experiments performed four times. *p<0.001. B) P. *aeruginosa* biofilms were grown on human airway epithelial cells for wild-type PAO1 and the *loxA*::Tn mutant and reductions in biofilm growth in the loxA:: Tn mutant were rescued with increasing doses of LoxA protein. Bacterial biofilm growth was quantified by enumerating colony-forming units (CFU/ml). Experiments performed three times. *p<0.01. C) Attachment assays were performed to assess the attachment of wild-type and *loxA*::Tn mutant *P. aeruginosa* to human airway epithelial cells, in the presence and absence of LoxA protein addition. Attached bacteria at one hour post-inoculation were quantified by enumerating colony-forming units (CFU/ml). Experiments were performed four times.

A.
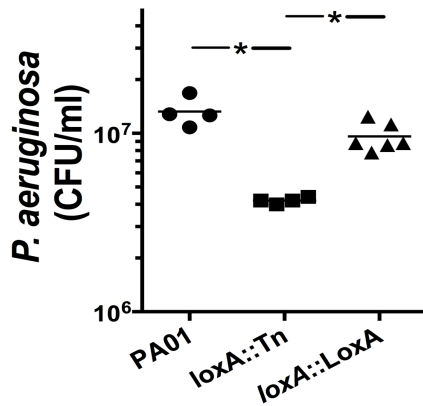
B.
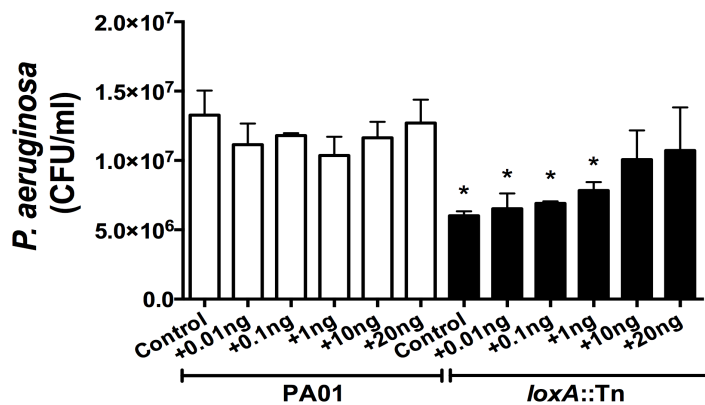
C.
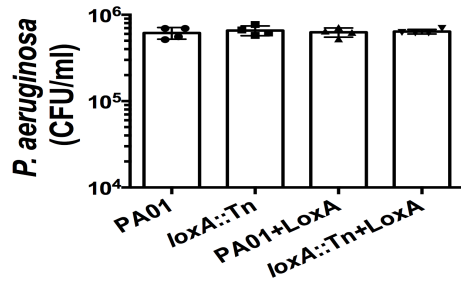
References

[1]   Inweregbu, K., Dave, J., and Pittard, A. (2005) Nosocomial infections. *Contin. Educ. Anaesth. Crit. Care Pain 5*, 14–17.

[2]   George, A. M., Jones, P. M., and Middleton, P. G. (2009) Cystic fibrosis infections: treatment strategies and prospects. *FEMS Microbiol. Lett. 300*, 153–164.

[3]   Donaldson, S. H., and Boucher, R. C. (2003) Update on pathogenesis of cystic fibrosis lung disease. *Curr. Opin. Pulm. Med. 9*, 486–491.

[4]   Filkins, L. M., Hampton, T. H., Gifford, A. H., Gross, M. J., Hogan, D. A., Sogin, M. L., Morrison, H. G., Paster, B. J., and O'Toole, G. A. (2012) Prevalence of Streptococci and Increased Polymicrobial Diversity Associated with Cystic Fibrosis Patient Stability. *J. Bacteriol. 194*, 4709–4717.

[5]   Robertson, D. M., Petroll, W. M., Jester, J. V., and Cavanagh, H. D. (2007) Current concepts: Contact lens related Pseudomonas keratitis. *Contact Lens Anterior Eye 30*, 94–107.

[6]   Costerton, J. W., Stewart, P. S., and Greenberg, E. P. (1999) Bacterial biofilms_a common cause of persistent infections.pdf. *Science 284*, 1318–1322.

[7]   Mah, T.-F. C., and O'Toole, G. A. (2001) Mechanisms of biofilm resistance to antimicrobial agents. *Trends Microbiol. 9*, 34–39.

[8]   Anderson, G. G., Moreau-Marquis, S., Stanton, B. A., and O'Toole, G. A. (2008) In Vitro Analysis of Tobramycin-Treated Pseudomonas aeruginosa Biofilms on Cystic Fibrosis-Derived Airway Epithelial Cells. *Infect. Immun. 76*, 1423–1433.

[9]   Hubeau, C., Lorenzato, M., Couetil, J. P., Hubert, D., Dusser, D., Puchelle, E., and Gaillard, D. (2001) Quantitative analysis of inflammatory cells infiltrating the cystic fibrosis airway mucosa. *Clin. Exp. Immunol. 124*, 69–76.

[10]   Bonfield, T. L., Panuska, J. R., Konstan, M. W., Hilliard, K. A., Hilliard, J. B., Ghnaim, H., and Berger, M. (1995) Inflammatory cytokines in cystic fibrosis lungs. *Am. J. Respir. Crit. Care Med. 152*, 2111–2118.

[11]   Dean, T. P., Dai, Y., Shute, J. K., Church, M. K., and Warner, J. O. (1993) Interleukin-8 concentrations are elevated in bronchoalveolar lavage, sputum, and sera of children with cystic fibrosis. *Pediatr. Res. 34*, 159–161.

[12]   Noah, T. L., Black, H. R., Cheng, P.-W., Wood, R. E., and Leigh, M. W. (1997) Nasal and bronchoalveolar lavage fluid cytokines in early cystic fibrosis. *J. Infect. Dis. 175*, 638–647.

[13]   Schuster, A., Haarmann, A., and Wahn, V. (1995) Cytokines in neutrophil-dominated airway inflammation in patients with cystic fibrosis. *Eur. Arch. Otorhinolaryngol. 252*, S59–S60.

[14]   Vance, R. E., Hong, S., Gronert, K., Serhan, C. N., and Mekalanos, J. J. (2004) The opportunistic pathogen Pseudomonas aeruginosa carries a secretable arachidonate 15-lipoxygenase. *Proc. Natl. Acad. Sci. U. S. A. 101*, 2135–2139.

[15]   Starkey, M., Hickman, J. H., Ma, L., Zhang, N., De Long, S., Hinz, A., Palacios, S., Manoil, C., Kirisits, M. J., Starner, T. D., Wozniak, D. J., Harwood, C. S., and Parsek, M. R. (2009) Pseudomonas aeruginosa Rugose Small-Colony Variants Have Adaptations That Likely Promote Persistence in the Cystic Fibrosis Lung. *J. Bacteriol. 191*, 3492–3503.

[16]   Kirschnek, S., and Gulbins, E. (2006) Phospholipase A2 Functions in Pseudomonas aeruginosa- Induced Apoptosis. *Infect. Immun. 74*, 850–860.

[17]   Bannenberg, G. L., Aliberti, J., Hong, S., Sher, A., and Serhan, C. (2004) Exogenous Pathogen and Plant 15-Lipoxygenase Initiate Endogenous Lipoxin A $_4$ Biosynthesis. *J. Exp. Med. 199*, 515–523.

[18]   Lu, X., Zhang, J., Liu, S., Zhang, D., Xu, Z., Wu, J., Li, J., Du, G., and Chen, J. (2013) Overproduction, purification, and characterization of extracellular lipoxygenase of Pseudomonas aeruginosa in Escherichia coli. *Appl. Microbiol. Biotechnol. 97*, 5793–5800.

[19]   Lewis, E. R., Johansen, E., and Holman, T. R. (1999) Large Competitive Kinetic Isotope Effects in Human 15-Lipoxygenase Catalysis Measured by a Novel HPLC Method. *J. Am. Chem. Soc. 121*, 1395–1396.

[20]   Jacobs, M. A., Alwood, A., Thaipisuttikul, I., Spencer, D., Haugen, E., Ernst, S., Will, O., Kaul, R., Raymond, C., Levy, R., and others. (2003) Comprehensive transposon mutant library of Pseudomonas aeruginosa. *Proc. Natl. Acad. Sci. 100*, 14339–14344.

[21]   Joshi, N., Hoobler, E. K., Perry, S., Diaz, G., Fox, B., and Holman, T. R. (2013) Kinetic and Structural Investigations into the Allosteric and pH Effect on the Substrate Specificity of Human Epithelial 15-Lipoxygenase-2. *Biochemistry (Mosc.) 52*, 8026–8035.

[22]   Blommel, P. G., and Fox, B. G. (2007) A combined approach to improving large-scale production of tobacco etch virus protease. *Protein Expr. Purif. 55*, 53–68.

[23]   Murphy, R. C., Barkley, R. M., Zemski Berry, K., Hankin, J., Harrison, K., Johnson, C., Krank, J., McAnoy, A., Uhlson, C., and Zarini, S. (2005) Electrospray ionization and tandem mass spectrometry of eicosanoids. *Anal. Biochem. 346*, 1–42.

[24]   Hoye, T. R., Jeffrey, C. S., and Shao, F. (2007) Mosher ester analysis for the determination of absolute configuration of stereogenic (chiral) carbinol carbons. *Nat. Protoc. 2*, 2451–2458.

[25]   Ikei, K. N., Yeung, J., Apopa, P. L., Ceja, J., Vesci, J., Holman, T. R., and Holinstat, M. (2012) Investigations of human platelet-type 12-lipoxygenase: role of lipoxygenase products in platelet activation. *J. Lipid Res. 53*, 2546–2559.

[26]   Glickman, M. H., and Klinman, J. P. (1995) Nature of rate-limiting steps in the soybean lipoxygenase-1 reaction. *Biochemistry (Mosc.) 34*, 14077–14092.

[27]   Ruddat, V. C., Mogul, R., Chorny, I., Chen, C., Perrin, N., Whitman, S., Kenyon, V., Jacobson, M. P., Bernasconi, C. F., and Holman, T. R. (2004) Tryptophan 500 and Arginine 707 Define Product and Substrate Active Site Binding in Soybean Lipoxygenase-1 [†]. *Biochemistry (Mosc.) 43*, 13063–13071.Library of Pharmacologically Active Compounds.pdf.

[28]   Inglese, J., Auld, D. S., Jadhav, A., Johnson, R. L., Simeonov, A., Yasgar, A., Zheng, W., and Austin, C. P. (2006) Quantitative high-throughput screening: a titration-based approach that efficiently identifies biological activities in large chemical libraries. *Proc. Natl. Acad. Sci. 103*, 11473–11478.

[29]   Geeganage, S., Kahl, S. D., Montrose, C., Sittampalam, S., Smith, M. C., and Weidner, J. R. (2012) Basics of Enzymatic Assays for HTS.pdf.

[30]   Jameson, J. B., Kantz, A., Schultz, L., Kalyanaraman, C., Jacobson, M. P., Maloney, D. J., Jadhav, A., Simeonov, A., and Holman, T. R. (2014) A

High Throughput Screen Identifies Potent and Selective Inhibitors to Human Epithelial 15-Lipoxygenase-2. *PLoS ONE* (Jung, M., Ed.) *9*, e104094.

[31]   Yasgar, A. (2008) Compound Management for Quantitative High-Throughput Screening. *J. Assoc. Lab. Autom. 13*, 79–89.

[32]   Southall, N. T., Jadhav, A., Huang, R., Nguyen, T., and Wang, Y. (2009) Enabling the Large-Scale Analysis of Quantitative High-Throughput Screening Data, in *Handbook of Drug Screening* 2nd ed., pp 442–464.

[33]   Haas, J. V., Eastwood, B. J., Iversen, P. W., and Weidner, J. R. (2013) Minimum Significant Ratio–A Statistic to Asses Assay Variability.

[34]   Shanks, R. M. Q., Kadouri, D. E., MacEachran, D. P., and O'Toole, G. A. (2009) New yeast recombineering tools for bacteria. *Plasmid 62*, 88–97.

[35]   Choi, K.-H., and Schweizer, H. P. (2006) mini-Tn7 insertion in bacteria with single attTn7 sites: example Pseudomonas aeruginosa. *Nat. Protoc. 1*, 153–161.

[36]   Zemke, A. C., Shiva, S., Burns, J. L., Moskowitz, S. M., Pilewski, J. M., Gladwin, M. T., and Bomberger, J. M. (2014) Nitrite modulates bacterial antibiotic susceptibility and biofilm formation in association with airway epithelial cells. *Free Radic. Biol. Med. 77*, 307–316.

[37]   Hendricks, M. R., Lashua, L. P., Fischer, D. K., Flitter, B. A., Eichinger, K. M., Durbin, J. E., Sarkar, S. N., Coyne, C. B., Empey, K. M., and Bomberger, J. M.

[38]   A et al. (2016) Respiratory syncytial virus infection enhances *Pseudomonas aeruginosa* biofilm growth through dysregulation of nutritional immunity. *Proc. Natl. Acad. Sci. 113*, 1642–1647.

[39]   Sievers, F., Wilm, A., Dineen, D., Gibson, T. J., Karplus, K., Li, W., Lopez, R., McWilliam, H., Remmert, M., Soding, J., Thompson, J. D., and Higgins, D. G. (2014) Fast, scalable generation of high-quality protein multiple sequence alignments using Clustal Omega. *Mol. Syst. Biol. 7*, 539–539.

[40]   Song, Y. (2005) Hyperacidity of secreted fluid from submucosal glands in early cystic fibrosis. *AJP Cell Physiol. 290*, C741–C749.

[41]   Wecksler, A. T., Kenyon, V., Deschamps, J. D., and Holman, T. R. (2008) Substrate Specificity Changes for Human Reticulocyte and Epithelial 15-Lipoxygenases Reveal Allosteric Product Regulation [†]. *Biochemistry (Mosc.) 47*, 7364–7375.

[42]   Schenk, G., Neidig, M. L., Zhou, J., Holman, T. R., and Solomon, E. I. (2003) Spectroscopic Characterization of Soybean Lipoxygenase-1 Mutants: the Role of Second Coordination Sphere Residues in the Regulation of Enzyme Activity [†]. *Biochemistry (Mosc.) 42*, 7294–7302.

[43]   Segraves, E. N., Chruszcz, M., Neidig, M. L., Ruddat, V., Zhou, J., Wecksler, A. T., Minor, W., Solomon, E. I., and Holman, T. R. (2006) Kinetic, Spectroscopic, and Structural Investigations of the Soybean Lipoxygenase-1 First-Coordination Sphere Mutant, Asω-694Gly [†] , [‡]. *Biochemistry (Mosc.) 45*, 10233–10242.

[44]   Lu, X., Liu, S., Feng, Y., Rao, S., Zhou, X., Wang, M., Du, G., and Chen, J. (2014) Enhanced thermal stability of Pseudomonas aeruginosa lipoxygenase through modification of two highly flexible regions. *Appl. Microbiol. Biotechnol. 98*, 1663–1669.

[45]   Hsi, L. C., Wilson, L. C., and Eling, T. E. (2002) Opposing Effects of 15-Lipoxygenase-1 and -2 Metabolites on MAPK Signaling in Prostate: ALTERATION IN PEROXISOME PROLIFERATOR-ACTIVATED RECEPTOR. *J. Biol. Chem. 277*, 40549–40556.

[46]   O'Flaherty, J. T., Hu, Y., Wooten, R. E., Horita, D. A., Samuel, M. P., Thomas, M. J., Sun, H., and Edwards, I. J. (2012) 15-Lipoxygenase Metabolites of Docosahexaenoic Acid Inhibit Prostate Cancer Cell Proliferation and Survival. *PLoS ONE* (Maya-Monteiro, C. M., Ed.) *7*, e45480.

[47]   Brash, A. R., Boeglin, W. E., and Chang, M. S. (1997) Discovery of a second 15S-lipoxygenase in humans. *Proc. Natl. Acad. Sci. 94*, 6148–6152.

[48]   Ringholz, F. C., Buchanan, P. J., Clarke, D. T., Millar, R. G., McDermott, M., Linnane, B., Harvey, B. J., McNally, P., and Urbach, V. (2014) Reduced 15-lipoxygenase 2 and lipoxin A4/leukotriene B4 ratio in children with cystic fibrosis. *Eur. Respir. J. 44*, 394–404.

[49]   Garreta, A., Val-Moraes, S. P., Garcia-Fernandez, Q., Busquets, M., Juan, C., Oliver, A., Ortiz, A., Gaffney, B. J., Fita, I., Manresa, A., and Carpena, X. (2013) Structure and interaction with phospholipids of a

prokaryotic lipoxygenase from Pseudomonas aeruginosa. *FASEB J. 27*, 4811–4821.

[50]   Brinckmann, R., Schnurr, K., Heydeck, D., Rosenbach, T., Kolde, G., and Kühn, H. (1998) Membrane translocation of 15-lipoxygenase in hematopoietic cells is calcium-dependent and activates the oxygenase activity of the enzyme. *Blood 91*, 64–74.

[51]   Hunter, J. A., Finkbeiner, W. E., Nadel, J. A., Goetzl, E. J., and Holtzman, M. J. (1985) Predominant generation of 15-lipoxygenase metabolites of arachidonic acid by epithelial cells from human trachea. *Proc. Natl. Acad. Sci. 82*, 4633–4637.

[52]   Nadel, J. A., Conrad, D. J., Ueki, I. F., Schuster, A., and Sigal, E. (1991) Immunocytochemical localization of arachidonate 15-lipoxygenase in erythrocytes, leukocytes, and airway cells. *J. Clin. Invest. 87*, 1139–1145.

[53]   Kuhn, H., Wiesner, R., Alder, L., Fitzsimmons, B. J., Rokach, J., and Brash, A. R. (1987) Formation of lipoxin B by the pure reticulocyte lipoxygenase via sequential oxygenation of the substrate. *Eur. J. Biochem. 169*, 593–601.

[54]   Levy, B. D., Romano, M., Chapman, H. A., Reilly, J. J., Drazen, J., and Serhan, C. N. (1993) Human alveolar macrophages have 15-lipoxygenase and generate 15(S)-hydroxy-5,8,11-cis-13-trans-eicosatetraenoic acid and lipoxins. *J. Clin. Invest. 92*, 1572–1579.

[55]   Deschamps, J. D., Gautschi, J. T., Whitman, S., Johnson, T. A., Gassner, N. C., Crews, P., and Holman, T. R. (2007) Discovery of platelet-type 12-human lipoxygenase selective inhibitors by high-throughput screening of structurally diverse libraries. *Bioorg. Med. Chem. 15*, 6900–6908.

[56]   Rai, G., Kenyon, V., Jadhav, A., Schultz, L., Armstrong, M., Jameson, J. B., Hoobler, E., Leister, W., Simeonov, A., Holman, T. R., and Maloney, D. J. (2010) Discovery of Potent and Selective Inhibitors of Human Reticulocyte 15-Lipoxygenase-1. *J. Med. Chem. 53*, 7392–7404.

[57]   Jameson, J. B., Kantz, A., Schultz, L., Kalyanaraman, C., Jacobson, M. P., Maloney, D. J., Jadhav, A., Simeonov, A., and Holman, T. R. (2014) A High Throughput Screen Identifies Potent and Selective Inhibitors to Human Epithelial 15-Lipoxygenase-2. *PLoS ONE* (Jung, M., Ed.) *9*, e104094.

[58]   Luci, D. K., Jameson, J. B., Yasgar, A., Diaz, G., Joshi, N., Kantz, A., Markham, K., Perry, S., Kuhn, N., Yeung, J., Kerns, E. H., Schultz, L., Holinstat, M., Nadler, J. L., Taylor-Fishwick, D. A., Jadhav, A., Simeonov, A., Holman, T. R., and Maloney, D. J. (2014) Synthesis and Structure–Activity Relationship Studies of 4-((2-Hydroxy-3-methoxybenzyl)amino)benzenesulfonamide Derivatives as Potent and Selective Inhibitors of 12-Lipoxygenase. *J. Med. Chem. 57*, 495–506.

[59]   Vasquez-Martinez, Y., Ohri, R. V., Kenyon, V., Holman, T. R., and Sepúlveda-Boza, S. (2007) Structure–activity relationship studies of flavonoids as potent inhibitors of human platelet 12-hLO, reticulocyte 15-hLO-1, and prostate epithelial 15-hLO-2. *Bioorg. Med. Chem. 15*, 7408–7425.

[60]   Starkey, M., Hickman, J. H., Ma, L., Zhang, N., De Long, S., Hinz, A., Palacios, S., Manoil, C., Kirisits, M. J., Starner, T. D., Wozniak, D. J., Harwood, C. S., and Parsek, M. R. (2009) Pseudomonas aeruginosa Rugose Small-Colony Variants Have Adaptations That Likely Promote Persistence in the Cystic Fibrosis Lung. *J. Bacteriol. 191*, 3492–3503.

[61]   Hickman, J. W., Tifrea, D. F., and Harwood, C. S. (2005) A chemosensory system that regulates biofilm formation through modulation of cyclic diguanylate levels. *Proc. Natl. Acad. Sci. U. S. A. 102*, 14422–14427.

[62]   Moreau-Marquis, S., Bomberger, J. M., Anderson, G. G., Swiatecka-Urban, A., Ye, S., O'Toole, G. A., and Stanton, B. A. (2008) The F508-CFTR mutation results in increased biofilm formation by Pseudomonas aeruginosa by increasing iron availability. *AJP Lung Cell. Mol. Physiol. 295*, L25–L37.

[63]   Neidig, M. L., Wecksler, A. T., Schenk, G., Holman, T. R., and Solomon, E. I. (2007) Kinetic and Spectroscopic Studies of Ω-694C Lipoxygenase: A Probe of the Substrate Activation Mechanism of a Nonheme Ferric Enzyme. *J. Am. Chem. Soc. 129*, 7531–7537.

[64]   Hoobler, E. K., Rai, G., Warrilow, A. G. S., Perry, S. C., Smyrniotis, C. J., Jadhav, A., Simeonov, A., Parker, J. E., Kelly, D. E., Maloney, D. J., Kelly, S. L., and Holman, T. R. (2013) Discovery of a Novel Dual Fungal CYP51/Human 5-Lipoxygenase Inhibitor: Implications for Anti-Fungal Therapy. *PLoS ONE* (Nie, D., Ed.) *8*, e65928.

Chapter 5

BIOSYNTHESIS OF THE MARESIN INTERMEDIATE, 13S,14S-EPOXY-

DHA, BY HUMAN 15-LIPOXYGENASE AND 12-LIPOXYGENASE AND ITS

REGULATION THROUGH NEGATIVE ALLOSTERIC MODULATORS

5.1 Abbreviations

AA, arachidonic acid; DHA, docosahexaenoic acid; SPM, specialized pro-resolving mediator; 12S-HETE, 12S-hydroxy-5Z,8Z,10E,14Z-eicosatetraenoic acid;

15S-HETE, 15S-hydroxy-5Z,8Z,11Z,13E-eicosatetraenoic acid;

14S-HDHA, 14S-hydroxy-4Z,7Z,10Z,12E,16Z,19Z-docosahexaenoic acid;

14S-HpDHA, 14S-hydroperoxy-4Z,7Z,10Z,12E,16Z,19Z-docosahexaenoic acid;

17S-HpDHA, 17S-Hydroperoxy-4Z,7Z,10Z,13Z,15E,19Z-docosahexaenoic acid;

17S-HDHA, 17S-Hydroxy-4Z,7Z,10Z,13Z,15E,19Z-docosahexaenoic acid;

11S-HpDHA, 11S-Hydroperoxy-4Z,7Z,9E,13E,15E,19Z-docosahexaenoic acid;

11S-HDHA, 11S-Hydroxy-4Z,7Z,9E,13E,15E,19Z-docosahexaenoic acid;

14S-HDPA$_{n-3}$, 14S-hydroxy-7Z,10Z,12E,16Z,19Z-docosapentaenoic acid,

13S,14S-epoxy-DHA, 13S,14S-epoxy-4Z,7Z,9E,11E,16Z,19Z-docosahexaenoic acid

Maresin 1 (MaR1), 7R,14S-dihydroxy -4Z,8E,10E,12Z,16Z,19Z docosahexaenoic acid,

Maresin 2 (MaR2), 13R,14S-dihydroxy-4Z,7Z,9E,11Z,16Z,19Z-docosahexaenoic acid,

7S,14S-EZE-diHDHA,7S,14S-dihydroxy-4Z,8E,10Z,12E,16Z,19Z-docosahexaenoic acid;

7R/S,14S-EEE-diHDHA, 7R/S,14S-dihydroxy-4Z,8E,10E,12E,16Z,19Z-docosahexaenoic acid;

7S,14S-diHpDHA, 7S,14S-dihydroperoxy-4Z,8E,10Z,12E,16Z,19Z-docosahexaenoic

acid; 14S,20S-diHpDHA, 14S-hydroperoxy,20S-hydroperoxy-

4Z,8Z,10Z,12E,16Z,19E-docosahexaenoic acid;

14S,20S-diHDHA, 14S-hydroxy, 20S-hydroxy-4Z,8Z,10Z,12E,16Z,19E-

docosahexaenoic acid; h15-LOX-1, human 15-lipoxygenase-1;

h12-LOX, human platelet 12-lipoxygenase

5.2 Abstract

Human reticulocyte 15-lipoxygenase-1 (h15-LOX-1) and platelet 12-lipoxygenase (h12-LOX) catalysis of DHA and the maresin precursor 14S-HpDHA was investigated to determine their product profiles and relative rates in the biosynthesis of the key intermediates of maresins, 14S-HpDHA and 13S,14S-epoxy-DHA. Both enzymes were shown to be efficient at converting DHA to the 14S-HpDHA product with h12-LOX being 79 times faster than h15-LOX-1 respective to their k_{cat}/K_M values and product percentages, 14.0 +/- 0.8 $s^{-1}\mu M^{-1}$ (81%) and 0.36 +/- 0.08 $s^{-1}\mu M^{-1}$ (46%), respectively. However, h12-LOX was shown to be markedly less effective at creating 13S,14S-epoxy-DHA compared to h15-LOX-1, which was 43 times more efficient with similar product profile and respective k_{cat}/K_M values, 0.0024 +/- 0.0002 $s^{-1}\mu M^{-1}$ and 0.11 +/- 0.006 $s^{-1}\mu M^{-1}$, respectively. This is the first evidence of h15-LOX-1 ability to catalyze this reaction and reveals a novel and more effective *in vitro* pathway for maresin biosynthesis. In addition, it was observed that the epoxidation of 14S-HpDHA is negatively regulated through allosteric oxylipin

126

binding to h15-LOX-1 and h12-LOX. The oxylipins, 14S-HpDHA (K_d = 6.0 μM), 12S-HETE (K_d = 3.5 μM), and 14S-HDPA$_{\omega-3}$ (K_d = 4.0 μM) were shown to decrease 13S,14S-epoxy-DHA production for h15-LOX-1, adding to the biological properties of the previously reported allosteric site. h12-LOX was also shown to be negatively regulated by 14S-HpDHA (K_d = 3.5 μM) and 14S-HDPA$_{\omega-3}$ (K_d = 4.0 μM), however, 12S-HETE was inactive, indicating for the first time an allosteric site for h12-LOX. These biosynthetic pathways and novel alloteric regulators of maresins may help our understanding of in vivo production of maresins and possibly how therapeutic interventions of inflammation affect maresin production.

5.3 Introduction

Acute inflammation is a beneficial response to injury and infection but can develop into chronic inflammation, which leads to disease if not properly regulated [1]. Specifically, resident immune cells initiate a pro-inflammatory response, which is amplified by neutrophils, eosinophils, and M1 polarized macrophages by producing bioactive molecules, such as leukotrienes and prostaglandins [2]. Most inflammatory therapeutics have so far focused on inhibiting the formation of these pro-inflammatory molecules, such as the non-steroidal anti-inflammatory drugs (NSAIDS), however, these molecules have limited effect on chronic inflammatory disease. Subsequently, this pro-inflammatory defensive process eventually transitions to the pro-resolution phase by cell types, such as M2 polarized macrophages, producing potent molecules, such as maresins, resolvins, and neuroprotectins,

otherewise know as specialized pro-resolving mediators (SPMs) [3,4]. This transition from inflammation to resolution is now recognized as being critical for correcting chronic inflammatory diseases, such as cardiovascular disease, alzhiemers disease, atherosclerosis, and cancer, to name a few [5]. The challenge in inhibiting inflammation while simultaneously stimulating resolution is that the biocatalysts that produce the pro-inflammatory molecules, lipoxygenase (LOX) and cyclooxygenase (COX) isozymes, are the same biocatalysts that produce the pro-resolution molecules [6,7]. Therefore, to develop the most effective LOX or COX therapeutics, it is imperative that the biosynthetic pathways for SPMs are characterized in order to determine the specific roles of LOX and COX in their production.

Maresins are a class of SPM made from docosahexaenoic acid (DHA) and were first discovered in macrophage exudates and subsequently characterized by total synthesis [8,9]. They are extremely potent oxylipins that decrease the inflammatory response, as well as promote healing and homeostasis. maresins have nanomolar potency in reducing polymorphonuclear cell infiltration, increasing macrophage phagocytosis of cellular debris, and increasing tissue regeneration in a planaria model [8,17]. They also inhibit TRPV1 currents in neurons and reduce neuropathic pain in mice [10,13]. The first maresin discovered was maresin 1 (MaR1, 7R,14S-dihydroxy-4Z,8E,10E,12Z,16Z,19Z-docosahexaenoic acid), followed by Maresin 2 (MaR2, 13R,14S-dihydroxy-4Z,7Z,9E,11Z,16Z,19Z-docosahexaenoic acid), and then the MaR-peptide derivatives, maresin conjugates in tissue regeneration (MCTR) [10,24].

These maresins are proposed to be synthesized by LOX isozymes, however, which specific LOX isozymes are not well characterized.

There are six human LOX isozymes, whose primary reactivity is to abstract a hydrogen atom from a bis-allylic methylene on a polyunsaturated fatty acid or oxylipin and insert molecular oxygen, generating a hydroperoxide product. The naming of specific LOX isozymes is dependent on the carbon number of arachidonic acid (AA) that becomes oxidized. For example, human platelet 12-lipoxygenase (h12-LOX) produces 12S-HpETE from AA, while human reticulocyte 15-lipoxygenase-1 (h15-LOX-1) produces 15S-HpETE. However, if DHA is the substrate then the numbering of the oxygenated carbon changes. This is due to the fact that the fatty acid substrate enters into the active site methyl-end first, and therefore the oxygenation registry starts from the omega end of the molecule. h12-LOX principally oxygenates on the w-9 carbon (i.e. 12-HpETE or 14S-HpDHA), while h15-LOX-1 principally oxygenates at w-6 (i.e. 15-HpETE or 17S-HpDHA).

In addition to oxygenation reactions, LOX isozymes can also perform dehydration reactions, which is similar to the oxygenation reaction, however an epoxide is the product, not a hydroperoxide. Specifically, LOX isozymes react with their own hydrogen peroxide oxylipin product and abstract a hydrogen atom from an adjacent bis-allylic methylene carbon, generating a septa-dienyl radical, similar to the oxygenation reaction. However, instead of oxygen attacking the septa-dienyl radical intermediate, the hydroperoxide moiety dehydrates to form an epoxide. The most

129

characterized example of this mechanism is the reaction of 5S-HpETE and h5-LOX, to generate the 5,6-epoxide, leukotriene A4 (LTA$_4$).

The biosynthetic pathway for maresin biosynthesis takes into account both of these LOX reactions and is proposed to involve h12-LOX. First, DHA reacts with h12-LOX to generate the w-9 oxylipin (14S-HpDHA). Then h12-LOX reacts with 14S-HpDHA to form 13S,14S-epoxy-4Z,7Z,9E,11E,16Z,19Z-docosahexaenoic acid (13S,14S-epoxy-DHA), a key intermediate to Maresins [15], which is then enzymatically hydrolyzed to form the final maresin product [4]. While h12-LOX is the proposed biocatalyst for maresin production due to its known AA reactivity, it is theoretically possible that h15-LOX-1 is also capable of performing the same set of enzymatic reactions. While h15-LOX-1 generates primarily the w-6 product (i.e. 15-HpETE or 17S-HpDHA), it can also generate the w-9 product in appreciable amounts (i.e. 12-HpETE or 14S-HpDHA) [26]. These two hypothetical biosynthetic pathways have biological ramifications because protein levels of h12-LOX and h15-LOX-1 depend on the inflammatory stimuli and the cellular type involved in the inflammatory response. For example, isolated macrophages have been shown to make MaR1 and MaR2, however, h15-LOX-1 has a 300-fold induction while h12-LOX has no change, during the polarization of macrophages into a pro-resolving M2 phenotype [5,16]. In contrast, h12-LOX is highly expressed in platelets and has been shown to produce 13S,14S-epoxy-DHA in a pro-inflammation state, but a hydrolase from neutrophils was required to make appreciable levels of MaR1 in neutrophil-platelet aggregates [12]. Given these two possible biosynthetic pathways for producing

maresins, the current work investigated the reactivities and kinetics of h12-LOX and h15-LOX-1 with the goal of determining their relative *in vitro* biosynthetic properties. By understanding which LOX enzyme is involved in the *in vitro* biosynthesis of maresins, these results may be extrapolated to their *in vivo* biosynthetic pathways which would help predict the cellular consequences of specific LOX inhibition.

5.4 Materials and Methods

Chemicals: OxyLipin mass spectrometry standards, Maresin 1 (7R,14S-dihydroxy-4Z,8E,10E,12Z,16Z,19Z-docosahexaenoic acid) and d5-Maresin 1 were purchased from Cayman Chemical. DHA, docosapentaenoic acid (DPA$_{\omega-3}$), and AA were purchased from Nu Chek Prep, Inc. at +99% purity. Reagent and HPLC grade chemicals were used (Fisher Scientific, Pittsburgh, PA, USA).

Expression and Purification of h15-LOX-1 and h12-LOX: Recombinant expression and purification of wild-type h15-LOX-1 and h12-LOX were performed as previously described [20,21,22]. The purities of the enzymes were assessed with a sodium dodecyl sulfate polyacrylamide gel to be >95%. The metal content was assessed on a Finnigan inductively coupled plasma mass spectrometer (ICP-MS), using an iron standard solution and curve along with Cobalt-EDTA as an internal standard.

Synthesis and Purification of Oxylipins: 14S-hydroperoxy-4Z,7Z,10Z,12E,16Z,19Z-docosahexaenoic acid (14S-HpDHA), 14S-hydroxy-7Z,10Z,12E,16Z,19Z-docosapentaenoic acid (14S-HDPA$_{\omega-3}$), and 12S-hydroxy-5Z,8Z,10E,14Z-eicosatetraenoic acid (12S-HETE) were synthesized in 200 mL 25 mM HEPES buffer at pH 7.5 for h15-LOX-1 and pH 8.0 for h12-LOX. Absorbance increase at 234 nm was monitored until it reached completion and quenched with 0.4% (v/v) glacial acetic acid. The solution was extracted 3 times with 100 mL Dichloromethane and evaporated to dryness. For the reduction of 12S-hydroperoxy-5Z,8Z,10E,14Z-eicosatetraenoic acid (12S-HpETE) to 12S-HETE, as well as other hydroperoxides, trimethyl phosphite was added in molar excess. The HETE products were then purified on HPLC with a reverse phase Higgins Haisil Semi preparative C18 column (5 μm, 250 mm × 10 mm) and an isocratic 55:45 mixture of 99.9% acetonitrile with 0.1% acetic acid and 99.9% water with 0.1% acetic acid. However, the docosanoid products were purified more effectively with a normal phase Phenomonex silica column (5 μm, 250 mm x 10 mm) and an isocratic mixture of 99% hexane, 1% isopropanol and 0.1% trifluoroacetic acid. The purity was checked by LC-MS/MS to be greater than 95%.

Product Analysis of LOX Enzymes Reacting with DHA, 14S-HpDHA, and 14S-HDHA: h15-LOX-1 (0.125 μM) and h12-LOX (0.300 μM) were reacted in 2 mL of 25 mM HEPES (pH 7.5 for h15-LOX-1, pH 8.0 for h12-LOX) at room temperature. For fatty acids, 10 μM of AA or DHA were reacted for 1 minute while turnover was

monitored by absorbance at 234 nm. For the oxylipin , 1 μM of 14S-HpDHA or 14S-HDHA were reacted for 20 minutes with h15-LOX-1 or 1 h with h12-LOX while monitoring at 270 nm. The reaction was quenched with 0.4% glacial acetic acid and d5-Maresin-1 was added as an extraction/ionization standard. After quenching, the reaction was extracted 3 times with 2 mL of DCM. This reaction was done in parallel with a no enzyme control for background subtraction. In addition, hydroperoxide determination was established by split samples, in which one was reduced with trimethyl phosphite, while the other was left unreduced. A shift in retention time indicated peroxide reduction to the alcohols. The samples were blown down under N_2 to dryness, reconstituted in 50 μL of acetonitrile and 50 μL water with 0.1% formic acid and 90 μL was injected for LC–MS/MS analysis. Structual characterization was performed on a Sciex ExcionLC, using a C_{18} column (Phenomenex Kinetex, 4 μm, 150 mm × 2.0 mm). Mobile phase A consisted of water with 0.1% (v/v) formic acid, and mobile phase B was acetonitrile with 0.1% formic acid. The flow rate was 0.400 mL/min with initial conditions (15% B) maintained for 0.75 min. Mobile phase B was held at 15% over 1 min, and then ramped to 30% over 0.75 min, to 47% over 2 min, to 54% over 1.5 min, to 60% over 4.5 min, to 70% over 4.5 min, to 80% over 1 min, to 100% over 1 min, held at 100% for 2 min, and finally returned to 15% to equilibrate for 2 min [36]. The chromatography system was coupled to a Sciex PDA and x500B qTOF. Analytes were ionized through electrospray ionization with a −4.0 kV spray voltage and 50, 50, and 20 PSI for ion source gas 1, 2, and curtain gas respectively. The CAD gas was set to 7 while the

133

probe temperature was 550 °C, respectively. DP was -60 V and CE was set to -10V with a 5 V spread. MS^2 acquisition was performed using SWATH and m/z ratios ± 0.5: 343.2 (HDHA's) and 359.2 (diHDHA's) were used. All analyses were performed in negative ionization mode at the normal resolution setting. Matching retention times, UV spectra, and fragmentation patterns to known standards with at least 6 common fragments identified the products. In the cases in which MS standards were not available, structures were deduced from comparison to known and theoretical fragments while double bond geometry was determined through UV spectra. In the case of 7S,14S-diHDHA, a previously established standard in our lab was used as a control (REF Steve paper).

Steady State Kinetics of h15-LOX-1 and h12-LOX: Reactions of h15-LOX-1 were performed in a 1-cm^2-quartz cuvette containing 2 mL of RT, 25 mM HEPES buffer (pH 7.5), while h12-LOX reactions had the same conditions but at pH 8.0. DHA and AA concentrations were varied from 0 to 20 μM and product formation was monitored by measuring absorbance at 234 nm using $\varepsilon_{234} = 25{,}000$ M^{-1} cm^{-1} for conjugated diene formation in buffer. Reactions were initiated by the addition of h15-LOX-1 (25 nM) or h12-LOX (18 pM) and were monitored on a PerkinElmer Lambda 45 UV–vis spectrophotometer. The stock concentration of 14S-HpDHA was determined by the absorbance at 234 nm in methanol using $\varepsilon_{234} = 27{,}000$ M^{-1} cm^{-1}. 14S-HpDHA concentrations ranged from 1 to 200 μM for h15-LOX-1 and 5 to 200 μM for h12-LOX. Enyzmes concentrations for oxylipin turnover were 200 nM for

h15-LOX-1 and 1 µM for h12-LOX. The amount of h12-LOX is high due to its low reactivity with 14S-HpDHA. Product formation was measured by the change in absorbance at 270 nm for 7S,14S-EZE-diHDHA, 13S,14S-epoxy-DHA, and the hydrolysis product, 7S,14S-EEE-diHDHA using the extinction coefficient for a conjugated triene in buffer $\varepsilon_{270} = 37,000$ M^{-1} cm^{-1}. Concentrations of the purified secondary products were assessed in methanol with a extinction coefficient of $\varepsilon_{270} = 40,000$ M^{-1} cm^{-1}. KaleidaGraph (Synergy) was used to fit initial rates and the second-order derivatives (k_{cat} /K_M) to the Michaelis–Menten equation for the calculation of kinetic parameters.

Allosteric Modulation of Epoxidation of h15-LOX-1 and h12-LOX: The allosteric effects were investigated using a constant 14S-HpDHA concentration (1 µM) and varying 12S-HETE or 14S-HDPA$_{\omega-3}$ (1-100 µM). H15-LOX-1 (0.125 µM) or h12-LOX (0.3 µM) were used and reacted for 20 min or 1 hour, respectively. 14S-HpDHA was also varied alone (1-50 µM) and products percentages calculated. Products were reduced and analyzed via LC/MS as described above (*vide supra*).

Effect of 14S-HpDHA on Human Platelet Aggregation and Lipidomics.: The University of Michigan Institutional Review Board approved all research involving human volunteers. Platelets were isolated from whole blood through serial centrifugation and resuspended in Tyrode's buffer as previously published [20]. For aggregation assays , 250 µL of washed human platelets (3×10^8/mL) were incubated

with 1-10 μM 14S-HpDHA, 7S,14S-EZE-diHDHA, maresin-1, or control oxylipin 12S-HETrE for 10 minutes at 37 °C in a glass cuvette. The oxylipin metabolite treated platelets were stimulated with 0.25 μg/mL collagen while stirring at 1100 rpm in a Chrono-log model 700 aggregometer and aggregation was analyzed via a decrease in light transmittance. For lipidomics, 1×10^9 platelets resuspended in a mL of Tyrode's buffer were incubated with 10 μM DHA or 17.5 μM 14(S)-HpDHA for 10 minutes and stimulated with collagen. Supernatants from washed platelets were extracted by C18 cartridge using published methods [12]. The products were resuspended in 50/50 acetonitrile and 0.1% formic acid water and analyzed by LC/MS. The m/z transitions used for 14S-HDHA was 343.2 →205.2, 11S-HDHA 343.2 → 165.2, and 7,14 diDHA isomers 359.2→177.2.

5.5 Results

h15-LOX-1 Steady-State Kinetics and Product Distribution With DHA

The efficiency of h15-LOX-1 in converting DHA into the peroxide MaR1 intermediate, 14S-HpDHA, was examined in order to determine its relevancy in maresin biosynthesis. First, the product profile for this reaction revealed dual product specificity with almost equal amounts of 14S-HpDHA (40%) and 17S-Hydroperoxy-4Z,7Z,10Z,13Z,15E,19Z-docosahexaenoic acid (17S-HpDHA) (46%) being produced, with a small amount of 11S-Hydroperoxy-4Z,7Z,9E,13E,15E,19Z-docosahexaenoic acid (11S-HpDHA) (12%) (**Table 5.1**), consistent with previous

work [26]. This is indicative of the ability of h15-LOX-1 to produce both the ω-6 and ω-9 oxylipins, comparable to its production of 12S-HETE and 15S-HETE from AA. However, the increased percentage of the ω-6 oxylipin with DHA (40% 14S-HpDHA versus 10% 12S-HETE) supports the hypothesis that the increased chain length and desaturation of DHA allows for a deeper active site insertion of DHA, as previously seen (Steve Ref). The production of 11S-HpDHA supports this hypothesis and indicates that DHA inserts into the active site even deeper than for 14S-HpDHA production, producing the ω-12 oxylipin product (11S-HpDHA).

With respect to kinetics, the rate of substrate capture (k_{cat}/K_M) for the reaction of h15-LOX-1 with DHA was 0.36 +/- 0.1 $s^{-1}\mu M^{-1}$, only 6 times slower than that of AA, its preferred substrate, indicating DHA is a competent substrate (**Table 5.2**) [32]. The lower k_{cat}/K_M is explained by a k_{cat} value being half and a K_M value being almost 3-fold greater for DHA than that for AA.

h12-LOX Steady-State Kinetics and Product Distribution With DHA: The reaction of h12-LOX with DHA also revealed the production of 14S-HpDHA, however for h12-LOX, it was the major product at 81%, with only 19% of the 11S-HpDHA product being made (**Table 1**). This result is in agreement with the literature, indicating that h12-LOX primarily produces the ω-9 oxylipin (14S-HpDHA) [26]. However; the production of the ω-12 oxylipin from DHA (11S-HpDHA) contrasts the fact that the ω-12 product of AA (9S-HpDHA) is not produced with h12-LOX and AA [18,22]. This result supports the hypothesis that the longer length and higher

137

degree of unsaturation of DHA allows for a deeper insertion into the active site, as was observed for 15-LOX-1 (*vide supra*). For kinetics, the k_{cat}/K_M for this reaction was determined to be 14 +/- 0.8 $s^{-1}\mu M^{-1}$, which is comparable to that with AA [23]. The k_{cat} was also similar to that of AA (k_{cat} = 13 +/- 0.2 s^{-1}), indicating similar rates of substrate capture (k_{cat}/K_M) and product release (k_{cat}) between DHA and AA (**Table 2**).

When comparing the kinetics and product profiles of h15-LOX-1 and h12-LOX, the data revealed that h12-LOX is approximately 80-fold more efficient at producing the maresin intermediate, 14S-HpDHA, than h15-LOX-1 (39-fold from k_{cat}/K_M times 2-fold from product profile percentages equals the 80-fold biosynthetic flux (B.F.)) (**Table 5.3**). This result is consistent with the biological role of h12-LOX considering that its primary reactivity is abstraction from the ω-11 carbon, with oxygen insertion at the ω-9 position (14S-HpDHA for DHA and 12-HpETE for AA).

Enzyme + DHA	14S-HpDHA	17S-HpDHA	11S-HpDHA
h15-LOX-1	40 +/. 1%	46 +/. 1%	12 +/. 1%
h12-LOX	81 +/. 3%	<1.0%	19 +/. 3%

Table 5.1 –Product profile of h12-LOX and h15-LOX-1 reacting with 10 μM of DHA for 1 minute.

Enzyme + Substrate	k_{cat} (s^{-1})	K_M (µM)	k_{cat}/K_M (s^{-1}µM^{-1})	Relative k_{cat}/K_M*
h15-LOX-1				
AA	5.3 $^+$/. 0.4	2.7 $^+$/. 0.3	2.0 $^+$/. 0.2	1.0
DHA	2.4 $^+$/. 0.6	6.7 $^+$/. 3	0.36 $^+$/. 0.1	0.18
h12-LOX				
AA	18 $^+$/. 0.8	0.95 $^+$/. 0.1	19 $^+$/. 2	9.5
DHA	13 $^+$/. 0.2	0.90 $^+$/. 0.06	14 $^+$/. 0.8	7.0

Table 5.2. Steady-state kinetics of h12-LOX and h15-LOX-1 with AA and DHA. The h15-LOX with AA data from were obtained previously [21] *The relative k_{cat}/K_M for h15-LOX-1 and AA is set to 1.

Enzyme + DHA	14S-HpDHA Biosynthetic Flux	Fold Change
h15-LOX-1	0.14	79
h12-LOX	11	0

Table 5.3 -Biosynthetic flux (B.F.) of 14S-HpDHA of h15-LOX-1 and h12-LOX reactions with DHA. (B.F. = k_{cat}/K_M * % Product).

h15-LOX-1 Steady-State Kinetics and Product Distribution With 14S-HpDHA and 14S-HDHA: The kinetics and product profile of h15-LOX-1 reacting with 14S-HpDHA was examined to characterize the efficiency of h15-LOX-1 in synthesizing the key 13,14-epoxide intermediate in the biosynthesis of maresins. The major product formed was the dehydration product, 7R/S,14S-dihydroxy-4Z,EEE,16Z,19Z-docosahexaenoic acid (7S/R,14S-EEE-diHDHA, 71%) (**Table 5.4**), which is formed by the nucleophilic attack of 13S,14S-epoxy-docosa-4Z,7Z,9E,11E,16Z-hexaenoic acid (13S,14S-epoxy-DHA) by water. This degradation epoxide product is characterized by its reduced nature (di-alcohol) in non-reducing conditions and it

139

being the only product made when O_2 concentrations are reduced to near zero (below 10 μM) compared to atmospheric conditions (~250 μM) (**Figure S1, Supplemental**) as well as equal UV absorbance maximum peak shoulder height, indicative of E,E,E conjugation (**Figure S2(B), Supplemental**). The production of 13S,14S-epoxy-DHA is consistent with a hydrogen abstraction from C10 (ω-14) by h15-LOX-1 and a subsequent dehydration to form the epoxide. The abstraction of the hydrogen atom from the ω-14 carbon is similar to the mechanism already observed in the production of 11S-HpDHA by h15-LOX-1 and DHA.

The production of the minor product, 7S,14S-dihydroperoxy-4Z,EZE,16Z,19Z-docosahexaenoic acid (7S,14S-EZE-diHpDHA) (29%), is less easily explained (**Table 5.4**). The diHpDHA nature of this molecule was characterized by its shift in HPLC retention time when the di-hydroperoxide is reduced to the di-alcohol. In addition, its UV spectra at 270 nm revealed the appropriate shoulders for an E,Z,E conjugation motif between the hydroxyls (**Figure S2(A), Supplemental**) [34]. The characterization of 7S,14S-EZE-diHpDHA indicates oxygenation and is best explained by a reverse entry of the substrate, carboxylic acid first, into the active site. This hypothesis is supported by the 7-fold loss in 7S,14S-EZE-diHpDHA production at increased pH (**Figure S3, Supplemental**). The increased pH deprotonates the carboxylic acid of 14S-HpDHA (pKa ≈ 7.4 [31]), and thus its active site binding may be inhibited by repulsion of the charged carboxylate in the hydrophobic cavity.

Regarding the kinetics of h15-LOX-1 and 14S-HpDHA, its efficiency and turnover was found to be comparable to that of DHA, with k_{cat}/K_M being 0.11 +/- 0.006 $s^{-1} \mu M^{-1}$ and k_{cat} being 2.0 +/- 0.04 $s^{-1} \mu M^{-1}$ (**Table 5.5A**). This is a significant result since for 14S-HpDHA, the only available proton for abstraction is on C9, which is the minor reaction mechanism with DHA as the substrate. Consistent with this dehydration reaction being the primary reaction mechanism, the kinetic parameters of 14S-HDHA were markedly reduced relative to 14S-HpDHA. The lack of the hydroperoxide moiety prohibits dehydration and thus only the minor oxygenation product is observed, 7S-hydroxy,14S-hydroperoxy-EZE-HDHA.

h12-LOX Steady-State Kinetics and Product Distribution With 14S-HpDHA and 14S-HDHA: In comparison, the kinetics and product profile were also investigated with h12-LOX and 14S-HpDHA. With respect to its product profile, the major product was the dehydration product, 13S,14S-epoxy-DHA, observed as the non-enzymatic hydrolysis product (7S/R,14S-EEE-diHDHA, 76%), similar to the major product of h15-LOX-1. Two minor products were also observed, the oxygenation product previously seen with h15-LOX-1, 7S,14S-EZE-diHpDHA (12%) and a new product, 14S,20S-dihydroperoxy-4Z,8Z,10Z,12E,16Z,19E-docosahexaenoic (14S,20S-diHpDHA) (13%) (**Table 5.4**). The characterization of 14S,20S-diHpDHA was determined by its MS fragmentation and its absorption of 245 nm light, indicative of two un-conjugated dienes (**Figure S2(C), Supplemental Data**) [31].

The production of 14S,20S-diHpDHA is most likely due to a methyl-end first entry into the active site, however with a restricted entry, thus allowing for C20 oxygenation. Interestingly, this product was also produced by h15-LOX-1 at a pH of 8 or greater, indicating this compound is less relevant at the physiological pH in which the epoxide is favored (pH 7.4). In support of these conclusions, the reduced oxylipin 14S-HDHA, which chemically can not form the epoxide product, only produced the oxygenation product 7S-hydroxy,14S-hydroperoxy-EZE-HDHA, similar to that seen for h15-LOX-1 (*vide supra*). It should be noted that there are no commercially available standards for these two minor products, however, 7S,14S-diHpDHA was stereochemically characterized as previously described (REF). 14S,20S-diHpDHA was not stereochemically characterized due the constraints of the Mosher procedure, so its stereochemistry was predicted due to the common lipoxygenase catalysis mechanism.

The kinetics of h12-LOX with 14S-HpDHA were dramatically reduced, relative to AA. The k_{cat}/K_M was found to be 0.0024 +/- 0.0002 $s^{-1}\mu M^{-1}$ and the k_{cat} to be 0.22 +/- 0.02 $s^{-1}\mu M^{-1}$ (**Table 5.5B**), which corresponds to a 5800-fold and 60-fold reduction, respectively, and indicates that 14S-HpDHA is a poor substrate, relative to DHA. The kinetic rates of the alcohol, 14S-HDHA, were also examined, and found to be about a third as efficient as 14S-HpDHA, consistent with a loss of the epoxide generating pathway (**Table 5.5B**).

When comparing the biosynthesis of 13S,14S-epoxy-DHA by both h15-LOX-1 and h12-LOX, it is observed that the k_{cat} value of h15LO-1 is almost 10-fold greater

than that of h12-LOX and its k_{cat}/K_M, is over 45-fold greater. When taking into account the percent production of 13S,14S-epoxy-DHA, the biosynthetic flux of h15-LOX-1 is over 40 times greater than h12-LOX (h15-LOX-1 k_{cat}/K_M *% = 0.078 and h12-LOX k_{cat}/K_M *% = 0.0018) (**Table 5.6**), indicating that h15-LOX-1 is a better catalyst in making the maresin intermediate, 13S,14S-epoxy-DHA, than h12-LOX and suggests that h15-LOX-1 could contribute significantly to maresin formation (*vida infra*).

Enzyme + 14S-HpDHA	13S,14S-epoxy-DHA*	7S,14S-diHDHA	14S,20S-diHDHA
h15-LOX-1	71 $^+/_-$ 6%	29 $^+/_-$ 6%	<1%
h12-LOX	76 $^+/_-$ 11%	12 $^+/_-$ 2%	13 $^+/_-$ 9%

Table 5.4- h15-LOX-1 and h12-LOX product profile with 1 μM 14S-HpDHA incubated for 20 minutes (pH = 7.5) and 60 minutes (pH = 8.0) respectively. *7S/R,14S- EEE- diHDHA is the detected product from non-enzymatic hydrolysis of 13S,14S-epoxy-DHA.

(A)

Substrate With h15-LOX-1	k_{cat} (s^{-1})	K_M (μM)	k_{cat}/K_M s^{-1} μM^{-1}	Relative k_{cat}/K_{M*}	*Fold Change
DHA	2.4 $^+/.$ 0.6	6.7 $^+/.$ 3	0.36 $^+/.$ 0.08	1.0	-1.0
14S-HpDHA	2.0 $^+/.$ 0.04	18 $^+/.$ 1	0.11 $^+/.$ 0.006	0.31	-3.2
14S-HDHA	0.57 $^+/.$ 0.01	18 $^+/.$ 4	0.03 $^+/.$ 0.002	0.080	-13

(B)

Substrate With h12-LOX	k_{cat} (s^{-1})	K_M (μM)	k_{cat}/K_M s^{-1} μM^{-1}	Relative k_{cat}/K_{M*}	*Fold Change
DHA	13 $^+/.$ 0.2	0.90 $^+/.$ 0.06	14 $^+/.$ 0.8	1.0	-1.0
14S-HpDHA	0.22 $^+/.$ 0.02	88 $^+/.$ 16	0.0024 $^+/.$ 0.0002	0.00017	-5880
14S-HDHA	0.17 $^+/.$ 0.03	210 $^+/.$ 70	0.00080 $^+/.$ 0.00003	0.00006	-16,700

Table 5.5 -Kinetics of DHA, 14S-HpDHA, and 14S-HDHA with (A) h15-LOX-1 and (B) h12-LOX. *Relative and fold change of k_{cat}/K_M of enzyme with DHA set to 1 and 0 respectively.

Enzyme + 14S-HpDHA	13S,14S-epoxy-DHA Biosynthetic Flux	Fold Change
h15-LOX-1	0.078	43
h12-LOX	0.0018	1

Table 5.6 -Biosynthetic flux (B.F.) of 13S,14S-epoxy-DHA of h15-LOX-1 and h12-LOX reactions with 14S-HpDHA. (B.F. = k_{cat}/K_M * % Product).

h15-LOX-1 Allosteric Regulation of 14S-HpDHA epoxidation : It was observed that when h15-LOX-1 reacted with 14S-HpDHA at low concentration (1 μM), dehydration and the subsequent epoxide formation was the favored mechanism, resulting in mostly 7R/S,14S-EEE-diHDHA being formed (71 +/- 11%). However, it was observed that at high concentration of 14S-HpDHA (50 μM), oxygenation was favored, producing mostly 7S,14S-EZE-diHDHA (76 +/- 0.5%) (**Figure 2A**). This was a substantial change in the reaction mechanism, with an approximately 80% increase in oxygenation products, indicating a possible allosteric interaction, as

previously seen for h15-LOX-1 reacting with AA and linoleic acid (LA) [21]. In fact, when this response was titrated and fit to a hyperbolic curve, it resulted in a K_D value of 6.0 +/- 3 μM, comparable in magnitude to previous allosteric regulators of h15-LOX-1 [21].

To investigate this hypothesis further, a previously reported allosteric modulator 12S-HETE and a similar LOX product to 14S-HDHA, 14S-hydroxy-7Z,10Z,12E,16Z,19Z-docosapentaenoic acid (14S-HDPA$_{ω-3}$), were titrated into the reaction mixture and the epoxidation/oxygenation product percentages recorded. With a constant concentration of 14S-HpDHA (1 μM) and a titration of 12S-HETE from 0 to 100 μM, h15-LOX-1 produced almost 80% less epoxidation product, changing from 73% to 20% and resulting in a K_D of 3.5 +/- 0.7 μM (**Figure 5.1A**). Repeating the same experiment with 14S-HDPA$_{ω-3}$ as the titrant, the epoxidation product was reduced almost 100% from 71% to 2.6%, with a K_D of 4.0 +/- 0.6 μM (**Figure 5.1A**). These data indicate that these three oxylipins, 14S-HpDHA, 14S-HDPA$_{ω-3}$, and 12S-HETE, bind to an allosteric site in h15-LOX-1 and regulate the product profile of 14S-HpDHA as the substrate and could potentially affect maresin formation (*vide infra*).

h12-LOX Allosteric Regulation of 14S-HpDHA epoxidation : Considering the allosteric effect observed for h15-LOX-1, the same experiments were performed to determine if an allosteric site was also present in h12-LOX and if it regulated the production of the maresin epoxide intermediate. A titration of h12-LOX with 14S-

HpDHA (1 to 50 μM) decreased the epoxidation product from 76 % to 19 %, similar to the change seen for h15-LOX-1. In addition, the data were fit to a hyperbolic saturation curve, yielding a K_D of 3.5 +/- 2 μM (**Figure 5.1B**), which supports the hypothesis that h12-LOX also has an allosteric site. This conclusion was confirmed with the titration of h12-LOX with 14S-HDPA$_{\omega-3}$, which manifested a decrease in epoxidation of almost 100%, from 72.0% to 5.0%, with a K_D of 4.6 +/- 0.7 μM (**Figure** 5.**1B**). In contrast, 12S-HETE was subsequently titrated into the h12-LOX reaction but no allosteric effect was observed (**Figure** 5.**1B**). These data indicate for the first time that h12-LOX also has an allosteric site, however it is more selective than that observed with h15-LOX-1, responding to only 14S-HpDHA and 14S-HDPA$_{\omega-3}$, but not 12S-HETE.

(A)
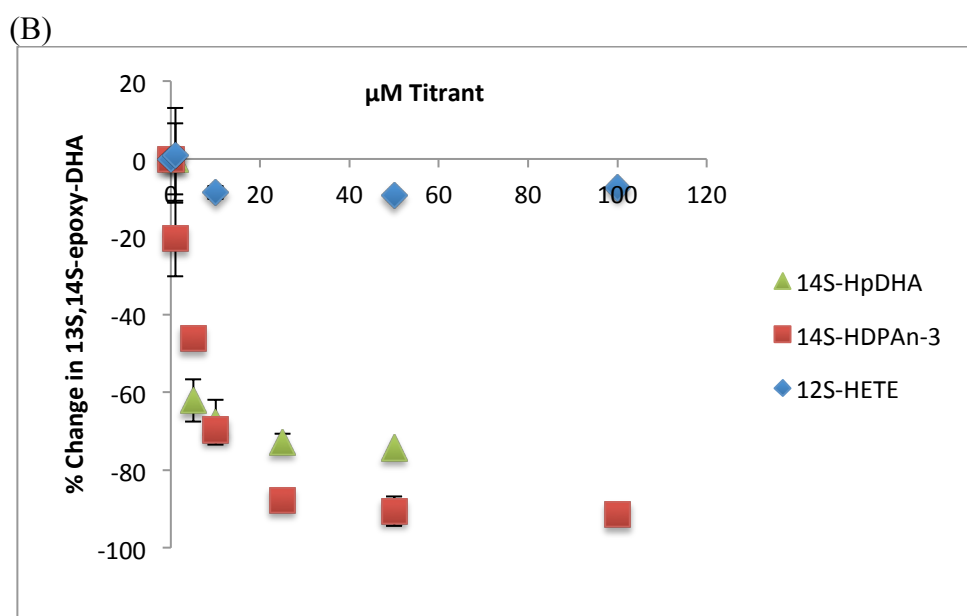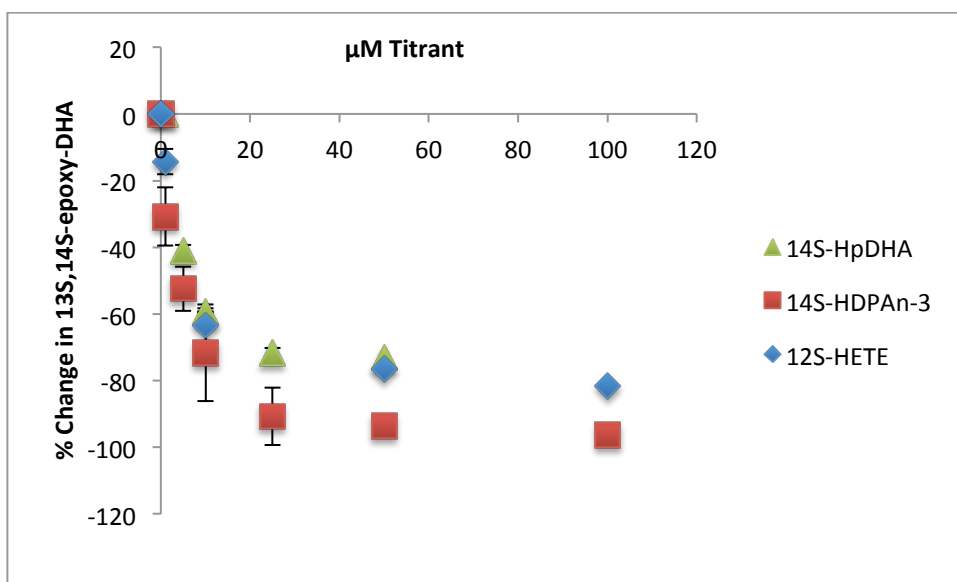
Figure 5.1. Percent 13S,14S-epoxy-DHA (dehydration) vs. 7S,14S-EZE-diHDHA/14S,20S-diHpDHA (oxygenation). (A) h15-LOX-1 reaction with 1 μM 14S-HpDHA and increasing 14S-HpDHA (green triangles), increasing 14S-HDPA$_{\omega-3}$ (red squares), and increasing 12S-HETE (blue diamonds) concentration. (B) h12-LOX reaction with 1 μM 14S-HpDHA and increasing 14S-HpDHA (green triangles), increasing 14S-HDPA$_{\omega-3}$ (red squares), and increasing 12S-HETE (blue diamonds) concentration.

***Ex vivo* Incubations of Human Platelets and DHA and 14S-HpDHA:** Considering that h12-LOX produced a mixture of 14S-HpDHA (81%) and 11S-HpDHA (19%) when reacted with DHA *in vitro*, DHA was administered to human platelets to determine if the *ex vivo* metabolites were of comparable ratios. Consistently, platelets produced the same oxylipins, however, their ratio was slightly different, with 14S-HDHA manifesting 94 +/- 5% and 11S-HDHA 6% +/- 1% (**Figure 5.2A**). The percentage of 11S-HDHA produced by platelets is less than that observed *in vitro* and could represent a cellular allosteric effect favoring the maresin pathway. Furthermore, these two oxylipins were reduced around 70% with selective h12-LOX inhibitor ML355 was added (data not shown).
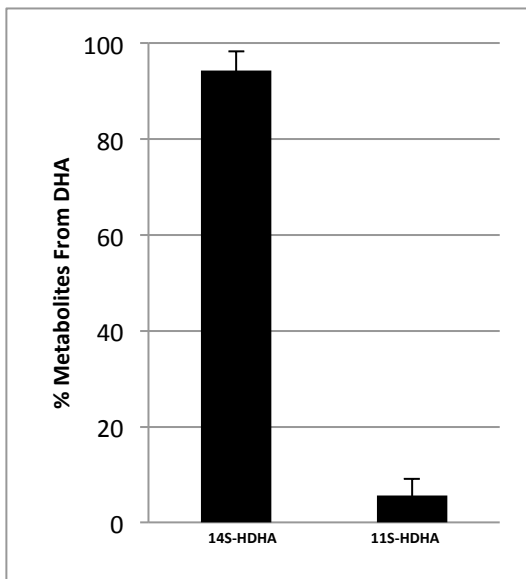
(A)   (B)
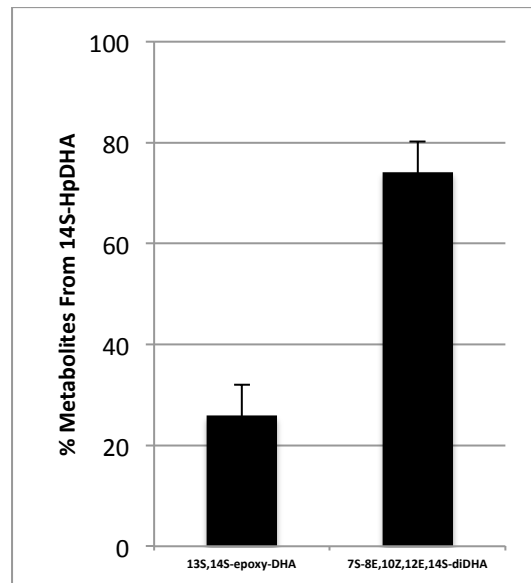
Figure 5.2- Percent metabolites of human platelets N=3 (3 x10^8 Platelets/mL) reacting with (A) 10 μM DHA, (B) percent metabolites with 1 x 10^9 platelets reacting with 17.5 μM 14S-HpDHA.

The *in vitro* kinetic data of h12-LOX also indicated that 14S-HpDHA was a poor substrate, however, this may not be the case *ex vivo* with human platelets. Therefore, human platelets were incubated with 14S-HpDHA (17.5 μM) to determine the quantity of oxylpins produced and the cellular product profile. The primary metabolite of 14S-HpDHA was the oxygenation product, 7S,14S-EZE-diHDHA (34.3 ngs/ 1 x 10^9 platelets, 76 +/- 6%), while the minor metabolite was the epoxidation product, 7R/S,14S-EEE-diHDHA (11.8 ngs/1 x 10^9 platelets, 24 +/- 6%) (**Figure 5.2B**). This percentage of products is similar to the percentage of epoxidation and oxygenation when using recombinant h12-LOX at 20 μM 14S-HpDHA concentration (20% 13S,14S-epoxy-DHA), highlighting the fact that at lower substrate concentrations, more of the epoxide would be favored in platelets as well. The amount of oxylipin products is considerably less than that seen when AA is used as a substrate (6000 ngs/ 1 x 10^9 platelets,), indicating that 14S-HpDHA is a poor substrate for h12-LOX *ex vivo*, similar to its *in vitro* activity.
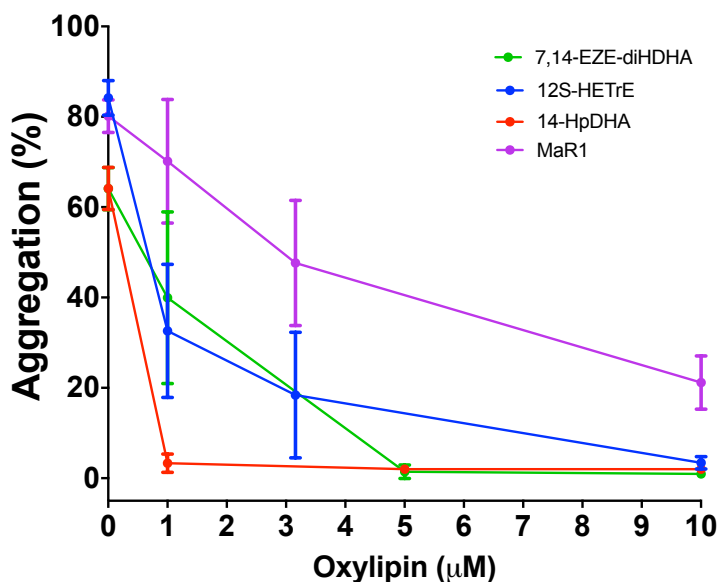
Figure 5.3: 14S-HpDHA inhibits platelet aggregation. Human platelets were incubated with 14HpDHA, 12S-HETrE, 7,14-EZE-diHDHA or MaR1 at concentrations ranging from 1 to 10 μM, and then stimulated with collagen (0.25 μg/mL) in a Chrono-log aggregometer. Data represent mean ± S.E.M of the maximum aggregation of 3-5 independent experiments. Statistical analysis was performed using one-way ANOVA with Dunnett's test comparing the aggregation of platelets treated with each concentration of oxylipin to the aggregation of vehicle-treated platelets. **P<0.01, ***P<0.001

14S-HpDHA Inhibits Platelet Aggregation: The ability of platelet-derived oxylipins to activate or inhibit platelet function depends at least in part on the metabolizing enzyme and starting PUFA. Our lab previously demonstrated h12-LOX-derived oxylipins of DHA and DGLA, including 7S,14S-EZE-diHDHA, 12S-HETrE, and MaR1, inhibit platelet activation. Therefore, isolated human platelets were treated with 14S-HpDHA for ten minutes and then stimulated with collagen (0.25 μg/mL) in an aggregometer to determine the effect of 14S-HpDHA on platelet activation (Figure 2). Platelets treated with ≥ 1 μM of 14S-HpDHA had over a 90%

reduction in aggregation compared to vehicle control. 14S-HpDHA was slightly more potent relative to the previously reported h12-LOX-derived antiplatelet oxylipins tested 7S,14S-EZE-diHDHA, MaR-1 and 12S-HETrE, which all required 5-10 µM to completely inhibit platelet aggregation.

5.6 Discussion

Maresins are critical bioactive molecules that turn off inflammation and promote healing by reducing polymorphonuclear cell infiltration, increasing macrophage phagocytosis of cellular debris and tissue regeneration [1,17]. It has been proposed that h12-LOX is the primary LOX isozyme in its *in vivo* biosynthesis [16]. In an attempt to understand the *in vivo* biosynthesis of MaR1, *in vitro* investigations have been performed to determine potential routes of biosynthesis.

In the current work, h12-LOX has been shown to be much more efficient in producing the maresin intermediate, 14S-HpDHA, than h15-LOX-1. This result is expected since hydrogen atom abstraction from the ω-11 carbon with oxygenation at the ω-9 carbon is the canonical biosynthetic mechanism for h12-LOX (i.e. 12S-HpETE production from AA and 14S-HpDHA from DHA). For h15-LOX-1, the canonical mechanism is hydrogen atom abstraction from the ω-8 carbon, with oxygenation at the ω-6 carbon (i.e. 15S-HpETE production from AA and 17S-HpDHA from DHA), and indeed 17S-HpDHA is the majority product from DHA (46%). However, h15-LOX-1 also makes a significant amount of the non-canonical

product, 14S-HpDHA (40%), which is substantially more than that seen with AA (10% 12S-HpETE). This shift in reactivity to the oxygenation of the ω-9 carbon is most likely due to the change in the nature of the substrate, with DHA having increased length and unsaturation relative to AA (Steve REF). This hypothesis is supported by the fact that h15-LOX-1 also produces 12% 11S-HpDHA, which implies an even deeper fatty acid insertion into the active site and a subsequent hydrogen atom abstraction from the ω-14 carbon. This expanded reactivity of h15-LOX-1, led us to consider h15-LOX-1 as a possible partner in the next step of maresin biosynthesis, the dehydration of 14S-HpDHA to form 13S,14S-epoxy-DHA.

Utilizing 14S-HpDHA as the substrate, the present work confirmed that 13S,14S-epoxy-DHA, the maresin intermediate, was the major product from the reaction with h12-LOX [15]. In this reaction, a hydrogen atom is abstracted from the ω-14 carbon, with dehydration of the hydroperoxide on the ω-9 carbon to form the ω-8,9 epoxide. However, in addition to this expected result, the data indicates that h15-LOX-1 can also produce 13S,14S-epoxy-DHA from 14S-HpDHA as the major product. This result demonstrates that both h12-LOX and h15-LOX-1 can abstract a hydrogen atom from the ω-14 carbon of 14S-HpDHA, enabling dehydration of the hydroperoxide to form the epoxide. For both h12-LOX and 15-LOX-1, this is a non-canonical reaction however it is not an un-expected outcome, as seen by the production of 11S-HpDHA for both h12-LOX (19%) and h15-LOX-1 (12%), indicating oxygenation of the ω-12 carbon of DHA. It should be noted that the ability of both h12-LOX and 15-LOX-1 to abstract from the ω-14 carbon is unique to the

C22:6 oxylipins. Neither h12-LOX nor 15-LOX-1 react with AA to produce the corresponding 9S-HpETE, even though the ω-14 carbon of AA is also an activated methylene carbon in the middle of a 1,4-diene moiety. Clearly, the longer length and higher degree of unsaturation of the C22:6 oxylipins allow for a productive binding event in the active sites of both isozymes.

However, even though both h12-LOX and 15-LOX-1 react with 14S-HpDHA and produce a majority of 13S,14S-epoxy-DHA, their rates are not comparable. H15-LOX-1 produces 13S,14S-epoxy-DHA with a k_{cat}/K_m value over 40-times faster than that for h12-LOX, implicating h15-LOX-1 as a possible source of maresins *in vivo*. For example, it has been established that M2 polarized macrophages and platelet-neutrophil aggregates produce substantial amounts of Maresin [12,16]. When M2 polarized macrophages are challenged by the h15-LOX-1 inhibitor BLX-3887 , the production of maresin and 14S-HDHA are decreased by 70% and 45%, respectively [27]. This pro-resolution polarization of macrophages also coincides with very high h15-LOX-1 expression compared to h12-LOX [17] and therefore, it is possible that the maresins in this cell type are synthesized primarily by h15-LOX-1, similar to our *in vitro* data. However, h12-LOX may also be involved in the biosynthesis of maresisn since high levels of h12-LOX are found in platelets, along with high neutrophil hydrolase expression, which could allow for maresin trans-cellular biosynthesis during aggregation. A plausible scheme is presented for maresin formation below indicating both enzymes in the biosynthesis (**Scheme 5.1**).
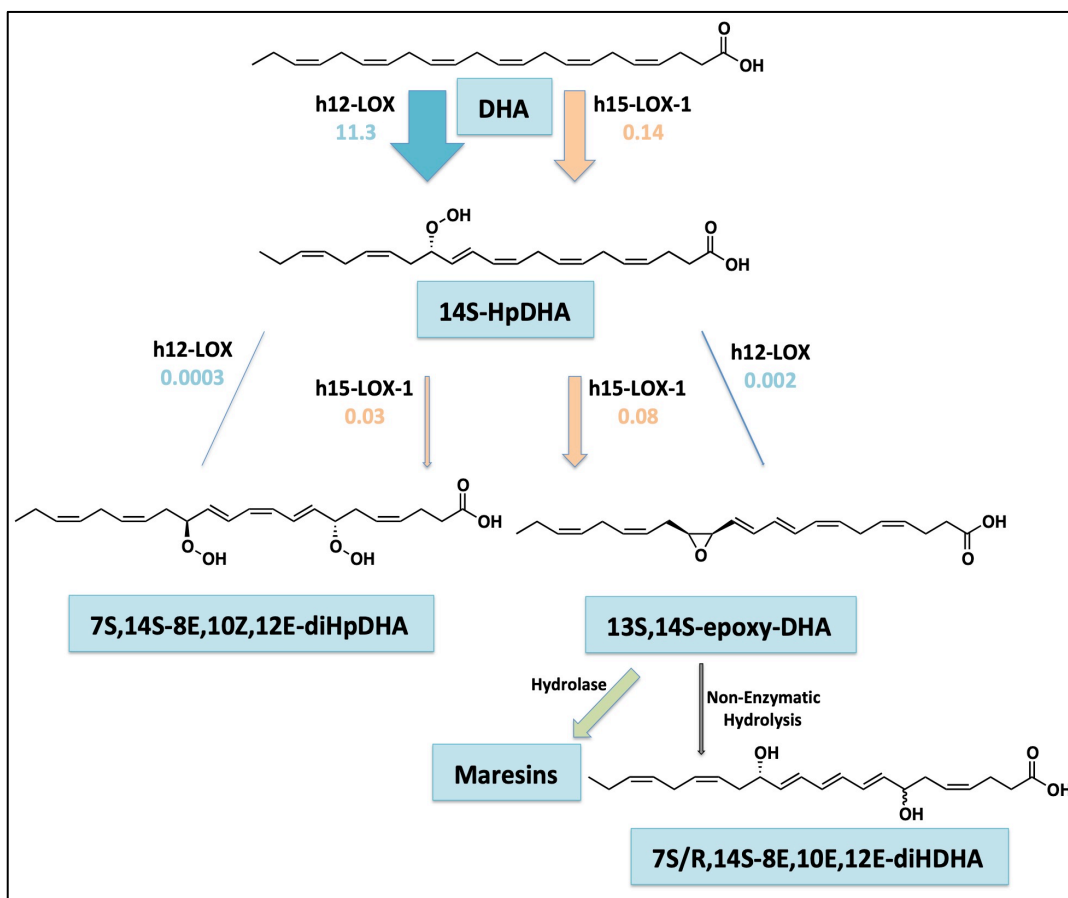
Scheme 5.1- A proposed biosynthetic scheme of maresins with lipoxygenase kinetic parameter k_{cat}/K_M represented as biosynthetic flux (B.F.) (B.F. = k_{cat}/K_M x % Product).

Nevertheless, translation of *in vitro* results into *in vivo* systems should be considered cautiously. Often in biochemistry, enzymes behave differently in buffer as compared to the cellular milieu, which contains high concentrations of proteins and small molecules. This is especially true for LOX isozymes due to the presence of an allosteric site in h15-LOX-1, which was previously shown to affect its ability to react with AA and LA [21]. Therefore the role of an allosteric site for both h12-LOX and h15-LOX-1 was investigated in order to determine if the generation of maresin

intermediates (i.e. 13S,14S-epoxy-DHA) was affected. The data indicated that 14S-HpDHA did decrease 13S,14S-epoxy-DHA production and increase oxygenation products, thus suggesting a negative product feedback effect for maresin formation. The molecular mechanism for this allosteric effect is more challenging to explain. The oxygenation product, 7S,14S-EZE-diHDHA, which increases as allosteric effector increases appears to be due to a reverse entry into the active site (i.e. carboxylate first). This result could be explained if the allosteric effector increases the size of the active site, then the oxygenation mechanism could be enhanced by lowering the energetic cost of burying the partially negative charged carboxylic acid to enter first, as see for h5-LOX catalysis [35].

In conclusion, we have demonstrated that while h12-LOX is a viable biocatalyst for the production of the key maresin intermediate, 13S,14S-epoxy-DHA, h15-LOX-1 may be a more efficient pathway to maresin biosynthesis. In addition, we have identified allosteric regulation of maresin biosynthesis for both h12-LOX and h15-LOX-1 by oxylipins. Given that 14S-HpDHA has micromolar potency for affecting maresin formation, it is biologically feasible that maresin formation is negatively regulated by oxylipin concentrations in the cell. This fact, coupled with the high potency of maresins and the slow rate in which h12-LOX and 15-LOX-1 make the necessary epoxide intermediate, 13S,14S-epoxy-DHA, suggest that there may be multiple biosynthetic pathways to help control inflammation resolution with maresins. These new insights into the biochemistry of maresin biosynthesis will allow for a better understanding of the biological consequences of LOX inhibitors, as well

as provide a novel target for therapeutic investigations in accelerating resolution of

acute inflammation.

*Unpublished as of now (Winter, 2019)

References

[1] Tabas I, Glass CK (2013) Anti-inflammatory therapy in chronic disease: challenges and opportunities. *Science* 339: 166–172.

[2] Chen, L.; Deng, H.; Cui, H.; Fang, J.; Zuo, Z.; Deng, J.; Li, Y.; Wang, X.; Zhao, L. Inflammatory responses and inflammation-associated diseases in organs. *Oncotarget* 2018, *9*, 7204–7218

[3] Serhan, C. N., Chiang, N., and Van Dyke, T. E. (2008) Resolving 646 inflammation: dual anti-inflammatory and pro-resolution lipid 647 mediators. *Nat. Rev. Immunol.* 8, 349−361.

[4] Wongrakpanich, S.; Wongrakpanich, A.; Melhado, K.; Rangaswami, J. A comprehensive review of non-steroidal anti-inflammatory drug use in the elderly. *Aging   Dis.* 2018, *9*,   143–150.

[5] Su Sugimoto MA, Sousa LP, Pinho V, Perretti M, Teixeira MM. Resolution of Inflammation: What Controls Its Onset? *Front Immunol.* 2016; *7*:160. doi: 10.3389/fimmu.2016.00160.

[6] R. Wisastra, F.J. DekkerInflammation, cancer and oxidative lipoxygenase activity are intimately linked Cancers. *Basel.* 6 (3) (2014), pp. 1500-1521

[7] Serhan, C. N., Chiang, N. & Van Dyke, T. E. Resolving inflammation: dual anti-inflammatory and pro-resolution lipid mediators. *Nature Rev. Immunol.* 8, 349–361 (2008).

[8] Serhan, C.N., Yang, R., Martinod, K., et al., 2009. Maresins: novel macrophage mediators with potent anti-inflammatory and proresolving actions, *J Exp Med.* 206(1):15-23.

[9] Rodriguez, A.R., Spur B.W., 2012. Total synthesis of the macrophage derived anti-inflammatory lipid mediator Maresin 1, *Tetrahedron Lett.*, 53, pp. 4169-4172

[10] Dalli, J., Vlasakov, I., Riley, I.R., Rodriguez, A.R., Spur, B. W., Petasis, N.A., Chiang, N., Serhan, C.N., 2016. Maresin conjugates in tissue regeneration biosynthesis enzymes in human macrophages. *Proc. Natl. Acad. Sci. USA* 113, 12232-12237

[11] Serhan C.N., Yang R., Martinod K., Kasuga K., Pillai P.S., Porter T.F., Oh S.F., Spite M., 2009. Maresins: novel macrophage mediators with potent anti-inflammatory and pro-resolving actions. *J Exp Med* 206:15-23. Doi:10.1084/jem.20081880.

[12] Abdulnour, R. E. et al. 2016. Maresin 1 biosynthesis during platelet-neutrophil interactions is organ-protective. *Proc. Natl Acad. Sci. USA* 111, 16526–16531.

[13] Y.Y. Jo, J.Y. Lee, C.K. Park 2016. Resolvin E1 inhibits substance P-Induced potentiation of TRPV1 in primary sensory neurons, *Mediat. Inflamm.*, p. 5259321

[14] B. Deng, C.W. Wang, H.H. Arnardottir, Y. Li, C.Y. Cheng, J. Dalli, et al., 2014. Maresin biosynthesis and identification of maresin 2, a new anti-inflammatory and pro-resolving mediator from human macrophages *PLOS ONE*, 9, p. e102362

[15] Dalli, J. et al., 2013. The novel 13S,14S-epoxy-maresin is converted by human macrophages to maresin1 (MaR1), inhibits leukotriene A4 hydrolase (LTA4H), and shifts macrophage phenotype. *FASEB J.* 27, 2573–2583.

[16] Dalli J., Serhan C.N., 2012. Specific lipid mediator signatures of human phagocytes: microparticles stimulate macrophage efferocytosis and pro-resolving mediators. *Blood*, 120(15):e60-72.

[17] Wuest SJ, Crucet M, Gemperle C, Loretz C, Hersberger M, 2012. Expression and regulation of 12/15-lipoxygenases in human primary macrophages. *Atherosclerosis* 225: 121–127.

[18] Wang, CW, Colas, RA, Dalli, J, Arnardottir, HH, Nguyen, D, Hasturk, H, Chiang, N,Van Dyke, TE, Serhan, CN. 2016. Maresin 1 biosynthesis and proresolving anti-infective functions with human-localized aggressive periodontitis leukocytes. *Infect Immun*: 84: 658– 665.

[19] Coffa G., Imber A.N., Maguire B.C., Laxmikanthan G., Schneider C., Gaffney B.J., Brash A.R. 2005. On the relationships of substrate orientation, hydrogen abstraction and product stereochemistry in single and double dioxygenations by soybean lipoxygenase-1 and its Ala542Gly mutant. *J. Biol. Chem.*, 280 pp. 38756-38766

[20] Smyrniotis, C. J., Barbour, S. R., Xia, Z., Hixon, M. S., and Holman, T. R. 2014. ATP Allosterically Activates the Human 5-Lipoxygenase Molecular Mechanism of Arachidonic Acid and 5S-Hydroperoxy-6(E),8(Z),11(Z),14(Z)-eicosatetraenoic Acid. *Biochemistry 53*, 4407– 4419, DOI: 10.1021/bi401621d

[21] A.T. Wecksler, V. Kenyon, J.D. Deschamps, T.R. Holman 2008. Substrate specificity changes for human reticulocyte and epithelial 15-lipoxygenases reveal allosteric product regulation *Biochemistry*, 47, pp. 7364-75

[22] Wecksler, A. T., Kenyon, V., Garcia, N. K., Deschamps, J. D., van der Donk, W. A., and Holman, T. R. 2009. Kinetic and structural investigations of the allosteric site in human epithelial 15-lipoxygenase-2. *Biochemistry 48*,8721– 8730, DOI: 10.1021/bi9009242

[23] Ikei, K. N., Yeung, J., Apopa, P. L., Ceja, J., Vesci, J., Holman, T. R., and Holinstat, M. 2012. Investigations of human platelet-type 12-lipoxygenase: role of lipoxygenase products in platelet activation. *J. Lipid Res. 53*, 2546–2559, DOI: 10.1194/jlr.M026385

[24] Deng B., Wang C. W., Arnardottir H. H., et al. 2014. Maresin biosynthesis and identification of maresin 2, a new anti-inflammatory and pro-resolving mediator from human macrophages. *PLoS One*;9(7, article e102362) doi: 10.1371/journal.pone.0102362.

[25] S. Tang, et al. 2018. Maresins: specialized proresolving lipid mediators and their potential role in inflammatory-related diseases *Mediators Inflamm*. p. 2380319

[26]Kutzner, K. Goloshchapova, D. Heydeck, S. Stehling, H. Kuhn, N.H. Schebb 2017. Mammalian ALOX15 orthologs exhibit pronounced dual positional specificity with docosahexaenoic acid *Biochim Biophys Acta*, 1862 pp. 666-675

[27] Werner, M., Jordan, P. M., Romp, E., Czapka, A., Rao, Z., Kretzer, C., … Gerstmeier, J. 2019. Targeting biosynthetic networks of the proinflammatory and proresolving lipid metabolome., *FASEB J* fj.201802509R

[28] Green, A.R.; Freedman, C.; Tena, J.; Tourdot, B.E.; Liu, B.; Holinstat, M.; Holman, T.R. 2018. 5 S,15 S-Dihydroperoxyeicosatetraenoic Acid (5,15-diHpETE) as a Lipoxin Intermediate: Reactivity and Kinetics with Human Leukocyte 5-Lipoxygenase, Platelet 12-Lipoxygenase, and Reticulocyte 15-Lipoxygenase-1. *Biochemistry*, 57, 6726–6734

[29] C.N. Serhan, J. Dalli, S. Karamnov, A. Choi, C.K. Park, Z.Z. Xu, R.R. Ji, M. Zhu, N.A. Petasis 2012. Macrophage proresolving mediator maresin 1 stimulates tissue regeneration and controls pain *FASEB J.*, 26 pp. 1755-1765

[30] R. G. Snodgrass, B. Brune 2019. Regulation and functions of 15-Lipoxygenase in Human Macrophages, *Front. Pharmacol.*, pp. 719., doi:10.3389/fphar.2019.00719

[31] Dobson EP, Barrow CJ, Kralovec JA, Adcock JL. 2013. Controlled formation of mono- and dihydroxy-resolvins from EPA and DHA using soybean 15-lipoxygenase. *J Lipid Res* **54**(5): 1439- 47.

[32] D.B. Northrop 1998. So what is V/K, anyway? *Journal of Chemical Education.Vol 75 No 9.* 1153- 57.

[33] Yang J, Schmelzer K, Georgi K, Hammock BD 2009. Quantitative profiling method for oxylipin metabolome by liquid chromatography electrospray ionization tandem mass spectrometry. *Anal Chem* 81(19):8085–8093.

[34]P. Chen, B. Fenet, S. Michaud, N. Tomczyk, E. Véricel, M. Lagarde, M. Guichar dant 2009. Full characterization of PDX, a neuroprotectin/protectin D1 isomer, which inhibits blood platelet aggregation. *FEBS Lett.*, 583, pp. 3478-3484

[35] M. Browner, S.A. Gillmor, R. Fletterick 1998. Burying a charge. *Nature Struct. Biol.*, p 179.
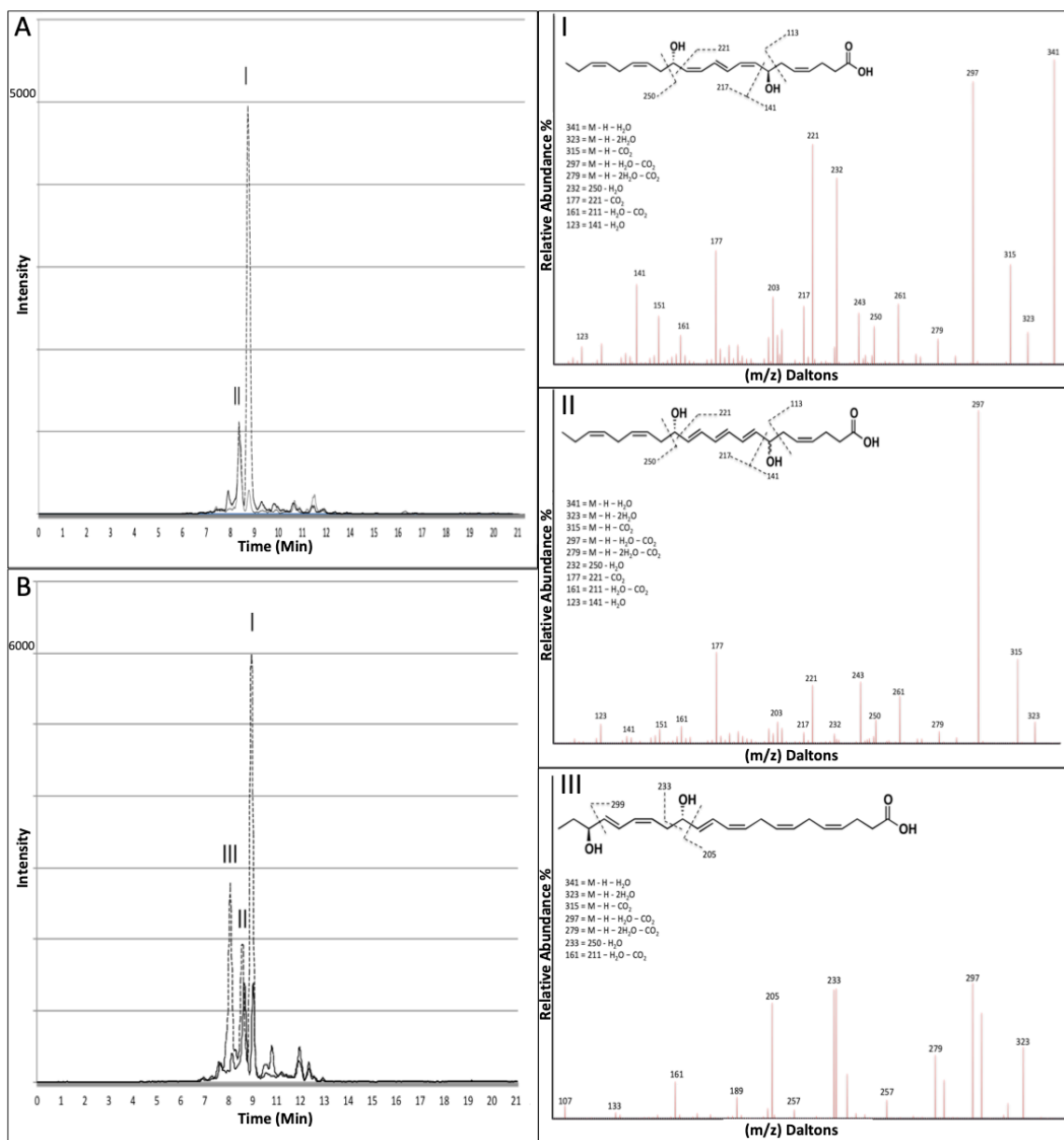
Figure S5.1 - (A) LC/MS trace at 359.2 (m/z) of enzyme incubations with 14S-HpDHA (10μM) for 20 minutes with h15-LOX-1 (0.125 μM). Reduced reaction is dashed line, unreduced is solid line. Molecule I is oxygenation product 7S,14S-EZE-diHDHA RT-9.4 min with corresponding fragments. Molecule II is epoxidation product 7R/S,14S-EEE-diHDHA RT-8.9 min found in reduced and unreduced samples (B) LC/MS trace at 359.2 (m/z) of enzyme incubations with 14S-HpDHA (10μM) for 60 minutes with h12-LOX (1.2 μM). Reduced reaction is dashed line,

160

unreduced is solid line. Molecule I is oxygenation product 7S,14S-EZE-diHDHA RT-9.4 min with corresponding fragments. Molecule II is non-enzymatic hydrolysis epoxidation product 7R/S,14S-EEE-diHDHA RT-8.9 min found in reduced and unreduced samples. Molecule III is another oxygenation product 14S,20S-diHDHA with corresponding fragments.
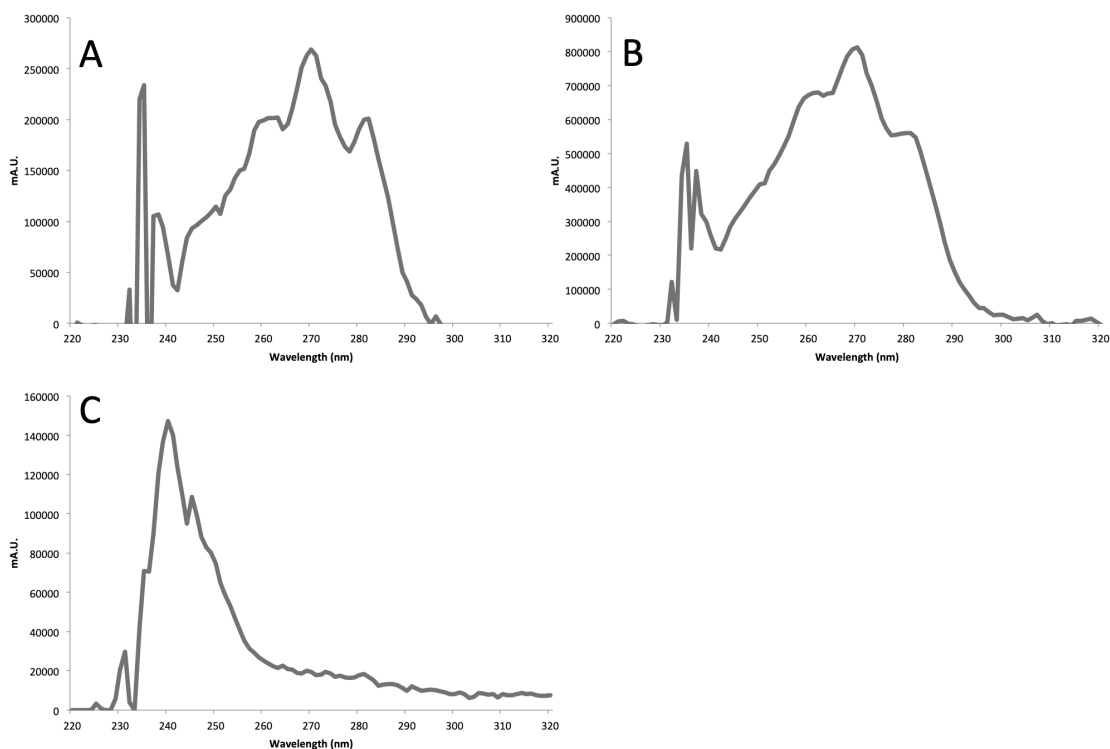
Figure S5.2- PDA spectrum showing absorbance maxima and shoulder peak heights for (A) 7S,14S-EZE-diHDHA, (B) 7R/S,14S-EEE-diHDHA, and (C) 14S,20S-diHDHA.
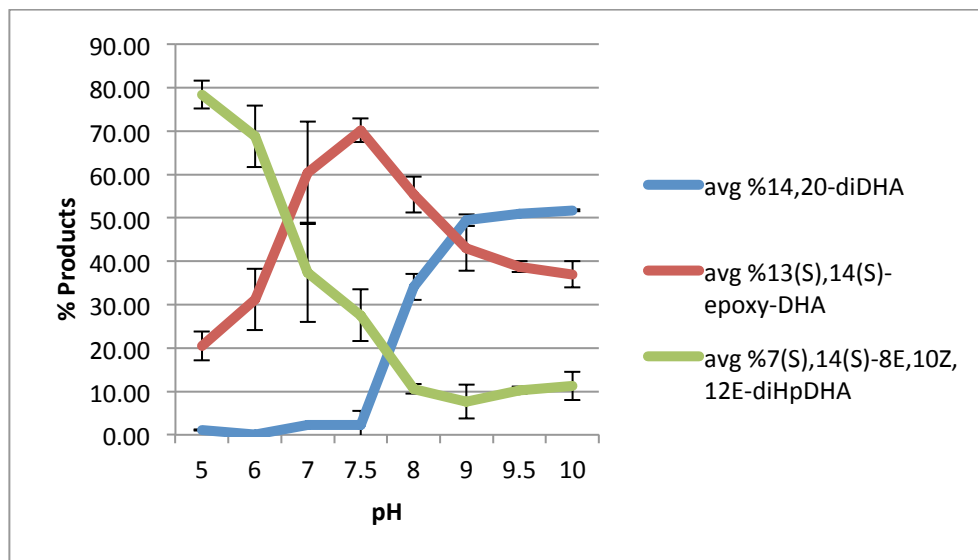
Figure S5.3- Percent products made from h15-LOX-1 with 4 μM 14S-HpDHA at various pH conditions. Loss of 7S,14S-EZE-diHpDHA at high pH is consistent with reverse binding (carboxylic acid first).